

8-1-2015

## Feasibility Study of Custom Manufacturing of Ionic Polymer-Metal Composite Sensors

Shelby E. Nelson

University of Nevada, Las Vegas, shelby.e.nelson@gmail.com

Follow this and additional works at: <https://digitalscholarship.unlv.edu/thesesdissertations>



Part of the [Engineering Science and Materials Commons](#), [Materials Science and Engineering Commons](#), and the [Mechanical Engineering Commons](#)

---

### Repository Citation

Nelson, Shelby E., "Feasibility Study of Custom Manufacturing of Ionic Polymer-Metal Composite Sensors" (2015). *UNLV Theses, Dissertations, Professional Papers, and Capstones*. 2493.  
<https://digitalscholarship.unlv.edu/thesesdissertations/2493>

This Thesis is protected by copyright and/or related rights. It has been brought to you by Digital Scholarship@UNLV with permission from the rights-holder(s). You are free to use this Thesis in any way that is permitted by the copyright and related rights legislation that applies to your use. For other uses you need to obtain permission from the rights-holder(s) directly, unless additional rights are indicated by a Creative Commons license in the record and/or on the work itself.

This Thesis has been accepted for inclusion in UNLV Theses, Dissertations, Professional Papers, and Capstones by an authorized administrator of Digital Scholarship@UNLV. For more information, please contact [digitalscholarship@unlv.edu](mailto:digitalscholarship@unlv.edu).

FEASIBILITY STUDY OF CUSTOM MANUFACTURING METHODS OF  
IONIC POLYMER-METAL COMPOSITE SENSORS

By

Shelby E Nelson

Bachelor of Science Degree in Engineering – Mechanical Engineering  
University of Nevada, Las Vegas  
2013

A thesis submitted in partial fulfillment  
of the requirements for the

Master of Science in Engineering – Mechanical Engineering

Department of Mechanical Engineering  
Howard R. Hughes College of Engineering  
The Graduate College

University of Nevada, Las Vegas  
August 2015



## **Thesis Approval**

The Graduate College  
The University of Nevada, Las Vegas

June 15, 2015

This thesis prepared by

Shelby E. Nelson

entitled

Feasibility Study of Custom Manufacturing of Ionic Polymer-Metal Composite Sensors

is approved in partial fulfillment of the requirements for the degree of

Master of Science in Engineering – Mechanical Engineering  
Department of Mechanical Engineering

Kwan J. Kim, Ph.D.  
*Examination Committee Chair*

Kathryn Hausbeck Korgan, Ph.D.  
*Graduate College Interim Dean*

Brendan O'Toole, Ph.D.  
*Examination Committee Member*

Woosoon Yim, Ph.D.  
*Examination Committee Member*

Dong-Chan Lee, Ph.D.  
*Graduate College Faculty Representative*

## **ABSTRACT**

### **Feasibility Study of Custom Manufacturing of Ionic Polymer-Metal Composite Sensors**

By

Shelby E Nelson

Dr. Kwang J. Kim, Committee Chair  
Southwest Gas Professor of Energy & Matter  
Department of Mechanical Engineering  
University of Nevada, Las Vegas (UNLV)

The ability to create an ion exchange membrane with any shape or thickness through custom manufacturing techniques is highly desirable in ionic polymer-metal composite (IPMC) research. This is caused by the poor selection and limited availability of certain thicknesses of commercial ion exchange membranes. The objective of this study is to determine the feasibility of manufacturing custom ion exchange membranes for IPMC sensors. The manufacturing methods used in this study are extrusion, injection molding, and hot pressing. A commercial membrane from Golden Energy Fuel Cells (GEFC) is used as a comparison. After the membranes are fabricated, certain properties of the membranes are tested throughout each processing stage to determine if they are suitable to be developed into IPMCs. The three processing stages are pre-activation, activation (hydrated and dehydrated), and IPMC. It was observed that the stiffness of the membranes increased from pre-activation to activation and decreased from activation to IPMC. A more flexible membrane in an IPMC allows for larger cation displacement within the membrane. The extruded and injection molded membranes showed the most potential with having the lowest stiffness of all the samples; however, they were not able to be made into

IPMCs due to repeated membrane failures in the primary plating process. Gas accumulated between the layers that formed in the membranes due to the extrusion and injection molding cooling process during manufacturing. The hot pressed membrane was the only custom manufactured membrane to be fully processed into an IPMC. The hot pressed and GEFC IPMC sensors were operated at 1 Hz, 5 Hz, and 10 Hz frequencies with the GEFC IPMC producing the strongest output voltage signal. While the extruded and injection molded membranes showed potential to become IPMCs with their high water uptake percentage, high ion exchange capacity, and low stiffness, more development is needed within the manufacturing process to make a uniform sample that does not fail during chemical processing.

## ACKNOWLEDGEMENTS

This work was in part supported by the U.S. Office of Naval Research (N00014-13-1-0274).

I would like to thank my advisor, Dr. Kwang J. Kim, for his support throughout this research and my graduate studies. Also, thank you to my committee members for their guidance throughout this work to help me understand the tough concepts and to get my work done.

I would like to thank all the members of my research group during my graduate studies at UNLV, especially Dr. Viljar Palmre and Dr. Taeseon Hwang for sharing their knowledge and their help in learning lab equipment and procedures. Your willingness to help is much appreciated.

I would like to thank my boyfriend, Jarrett Plies, who revitalized my interest in engineering and who gave me that last push of motivation that I needed to complete this project.

Most importantly, I would like to thank my family, especially my mom and dad, for their constant support throughout my entire education from grade school to graduate school. They have always been there inspiring me to persevere through the challenging times in getting my degree. I couldn't have done it without you!

# TABLE OF CONTENTS

## ABSTRACT

ACKNOWLEDGEMENTS .....v

LIST OF TABLES ..... viii

LIST OF FIGURES .....x

NOMECLATURE..... xiv

CHAPTER 1: Introduction and Objectives .....1

1.1 Ionic Polymer Metal Composite Fundamentals .....1

1.1.1 IPMC Sensor Applications ..... 4

1.2 Ion Exchange Membrane.....5

1.2.1 Commercially Available Nafion® Membranes ..... 5

1.2.2 Custom Fabricated Membranes ..... 7

1.2.2.1 Typical Methods ..... 7

1.2.3 Characterization ..... 8

1.3 Research Objectives and Thesis Structure .....8

CHAPTER 2: Custom Membrane Fabrication and Processing Techniques .....10

2.1 Custom Membrane Fabrication.....10

2.1.1 Extrusion ..... 10

2.1.1.1 Process Design and Set-Up ..... 10

2.1.1.2 Die and Adapter Design ..... 15

2.1.1.3 Process Procedure ..... 16

2.1.1.4 Results ..... 18

2.1.2 Injection Molding ..... 19

2.1.2.1 Process Design and Set-Up ..... 19

2.1.2.2 Injection Mold Design and Fabrication ..... 20

2.1.2.3 Processing Procedure ..... 22

2.1.2.4 Results ..... 23

2.1.3 Hot Pressing ..... 24

2.1.3.1 Mold Design ..... 24

2.1.3.2 Processing Procedure ..... 25

2.1.3.3 Results ..... 26

2.2 IPMC Processing .....27

2.2.1 Membrane Activation (Base Hydrolysis) ..... 27

2.2.2 Primary Plating ..... 28

2.2.3 Secondary Plating .....	29
2.2.4 Ion Exchange .....	30
2.2.5 Results.....	30
<b>CHAPTER 3: Characterization, Results, and Discussion.....</b>	<b>32</b>
<b>3.1 Water Uptake.....</b>	<b>32</b>
<b>3.3 Contact Angle .....</b>	<b>38</b>
<b>3.4 Thermal Degradation.....</b>	<b>45</b>
<b>3.5 Tensile Properties.....</b>	<b>50</b>
<b>3.6 Dynamic Mechanical Analysis .....</b>	<b>59</b>
3.6.1 Pre-activated Membrane Results .....	60
3.6.2 Activated, Dehydrated Membrane Results .....	62
3.6.3 Activated, Hydrated Membrane Results.....	66
3.6.4 Hot Pressed and GEFC IPMC Results .....	70
<b>3.7 Surface and Cross-sectional Quality .....</b>	<b>72</b>
<b>3.8 Platinum Layer Thickness.....</b>	<b>76</b>
<b>3.9 Surface Electrode Resistance .....</b>	<b>77</b>
<b>CHAPTER 4: IPMC Performance Sensor Test.....</b>	<b>80</b>
<b>CHAPTER 5: Conclusion and Recommendations for Future Study .....</b>	<b>89</b>
<b>5.1 Recommendation for Future Work .....</b>	<b>90</b>
<b>APPENDIX A: Error Discussion for the Tensile Tests .....</b>	<b>93</b>
<b>APPENDIX B: Extrusion and Injection Molding Challenges .....</b>	<b>95</b>
<b>REFERENCES.....</b>	<b>101</b>
<b>CURRICULUM VITAE.....</b>	<b>106</b>



## LIST OF TABLES

Table 1.1: Commercially available Nafion® sheets that can be purchased from Ion Power, Inc [20].....	6
Table 3.1: Summary table for average water uptake % measurements taken of activated membranes with the % change from GEFC*, a value taken from Park [4].....	33
Table 3.2: Summary of ion exchange capacity of activated membrane and % change from GEFC membrane.....	36
Table 3.3: Degree of wetting of contact angle measurements. This table was taken from Wikipedia [37]. .....	39
Table 3.4: Contact angle and degree of wetting summary table for all membranes.....	40
Table 3.5: Pre-activated membrane contact angle summary and comparison to extruded membrane.....	41
Table 3.6: Summary table of activated, hydrated membrane contact angles and comparison to GEFC with % difference.....	42
Table 3.7: Summary table of activated, dehydrated membrane contact angle measurements and comparison to GEFC.....	43
Table 3.8: Summary of IPMC contact angle measurements and comparison to GEFC IPMC .....	44
Table 3.9: Summary table of thermal degradation temperature of pre-activated membranes and comparison to extruded membrane .....	47
Table 3.10: Summary table of activated, dehydrated membrane thermal degradation temperature and % change from GEFC membrane .....	48
Table 3.11: Summary table of activated, dehydrated membrane second thermal degradation temperature and % change from GEFC membrane .....	48
Table 3.12: Summary of thermal degradation temperature of IPMCs and % difference to GEFC IPMC.....	50
Table 3.13: Modulus of elasticity of pre-activated membranes and % change from extruded membrane.....	55
Table 3.14: Summary of modulus of elasticity of activated, hydrated membrane and % change from GEFC membrane.....	56

Table 3.15: Summary of modulus of elasticity of activated, dehydrated membrane and % change from GEFC membrane.....	57
Table 3.16: Summary of modulus of elasticity of IPMC and % change from GEFC membrane .	58
Table 3.17: Summary table of DMA results of pre-activated membranes and percent change from extruded membrane.....	60
Table 3.18: Summary of DMA results of activated, dehydrated membranes and percent change from GEFC membrane.....	64
Table 3.19: Summary of DMA results of activated, hydrated membranes and percent change from GEFC membrane.....	67
Table 3.20: Hot Pressed and GEFC IPMC DMA results summary and % Change from GEFC IPMC.....	70
Table 3.21: Summary of the measured platinum layer thicknesses and the percentage of platinum to membrane.....	77
Table 3.22: Surface resistance measurement of each side of the membrane and percent change from GEFC membrane.....	79
Table 4.1: Summary of the average absolute value of the maximum voltage and % change from the GEFC IPMC.....	88
Table 5.1: Storage modulus vs. elastic modulus and a % difference calculation .....	92

## LIST OF FIGURES

Figure 1.1: Nafion® chemical structure in acid form. Diagram inspired by [5] .....	2
Figure 1.2: Cation migration in IPMC sensing .....	4
Figure 2.1: Galomb Model E benchtop injection molder machine with labeled parts. The machine was modified to use in the extrusion of samples. This machine has a maximum processing temperature of 315°C, a dual display temperature controller, and a 17g plastic capacity.....	11
Figure 2.2: Force body diagram of plunger handle. The user applies the force, $F_a$ , on the cantilevered end. The force applied is multiplied by a factor of 4.2 directly into the axis of the plunger. ....	12
Figure 2.3: Die swell diagram. The polymer remembers its shape before the orifice due to viscoelastic effects. Diagram inspired by [34]. ....	14
Figure 2.4: SolidWorks rendering of the extruder die adapter. This part replaced the injection molder nozzle and outfitted the injection molder machine to an extruder. ....	15
Figure 2.5: (a) SolidWorks sketch with dimensions of the extruder die, (b) fabricated extruder die made out of brass.....	16
Figure 2.6: Extruded die orifice zoomed to 1000X using the optical microscope .....	16
Figure 2.7: Extruded membranes .....	19
Figure 2.8: SolidWorks rendering of the mold designed with labeled parts. ....	21
Figure 2.9: Injection mold fabricated out of aluminum; (a) mold half containing the mold cavity, (b) opposite mold half with runner.....	22
Figure 2.10: (a) injection mold containing molded membrane right after injection, (b) molded membrane removed from mold .....	24
Figure 2.11: Stainless steel hot press mold with spacer (both halves pictured) .....	25
Figure 2.12: Carver heated press used to press the mold halves together .....	26
Figure 2.13: Hot pressed membranes from Nafion® N1110. Resulting average thickness is 0.48 mm.....	27
Figure 2.14: IPMC samples cut to 5 mm x 25 mm strips. (a) hot pressed IPMC strips (b) GEFC IPMC strips.....	31

Figure 3.1: Average measured water uptake % of all activated membranes .....	35
Figure 3.2: Ion exchange capacity found from activated membranes. GEFC* is the value taken from the GEFC website [36]. .....	38
Figure 3.3: Contact angle definition. The contact angle of a water droplet is measured from the inside of the droplet outwards. ....	38
Figure 3.4: Pre-activated membrane contact angle photograph and measurements; (a) Extruded pre-activated membrane, (b) injection molded pre-activated membrane .....	41
Figure 3.5: Activated, hydrated membrane contact angle photographs and measurements; (a) extruded membrane, (b) injection molded membrane, (c) hot pressed membrane, (d) GEFC membrane .....	42
Figure 3.6: Activated, dehydrated membrane contact angle photographs and measurements; (a) extruded membrane, (b) injection molded membrane, (c) hot pressed membrane, (d) GEFC membrane .....	44
Figure 3.7: IPMC contact angle photographs and measurements; (a) hot pressed IPMC, (b) GEFC IPMC .....	45
Figure 3.8: Thermal gravimetric analysis of pre-activated membranes. ....	47
Figure 3.9: Thermal gravimetric analysis of activated, dehydrated membranes .....	49
Figure 3.10: Thermal gravimetric analysis of IPMCs .....	50
Figure 3.11: (a) Tensile sample with dimensions: $t = 0.38 \text{ mm} - 0.79 \text{ mm}$ , $W_G = 2.5 \text{ mm}$ , $R = 15$ $\text{mm}$ , $W_T = 10 \text{ mm}$ , $L_G = 10 \text{ mm}$ , $L_T = 60 \text{ mm}$ ; (b) all activated, dehydrated tensile samples cut from tensile die. Membranes from left to right: extruded, injection molded, hot pressed, and GEFC. Note that the injection molded sample is shorter than the other three samples. This is due to the slightly smaller injection molding size. ....	51
Figure 3.12: Tensile fixture with tensile specimen clamped in and ready to start the test. The load cell is a 100 N load cell and is not pictured in this photograph. ....	52
Figure 3.13: Pre-activated membrane stress-strain curve with a zoomed section of the initial curve .....	55
Figure 3.14: Activated, hydrated membrane stress-strain curve with a zoomed section of the initial curve .....	56

Figure 3.15: Activated, dehydrated membrane stress-strain curve with a zoomed section of the initial curve.....	57
Figure 3.16: Hot pressed and GEFC IPMC stress-strain curve with a zoomed section of the initial curve. Extruded and injection molded are not pictured because they were not able to be processed into IPMCs.....	58
Figure 3.17: Pre-activated membrane - storage modulus, $E'$ .....	61
Figure 3.18: Pre-activated membranes - loss modulus, $E''$ .....	61
Figure 3.19: Pre-activated membranes - damping, $\tan(\delta)$ .....	62
Figure 3.20: Activated, dehydrated membrane – storage modulus, $E'$ .....	65
Figure 3.21: Activated, dehydrated - loss modulus, $E''$ .....	65
Figure 3.22: Activated, dehydrated - damping, $\tan(\delta)$ .....	66
Figure 3.23: Activated, hydrated membrane - storage modulus, $E'$ .....	68
Figure 3.24: Activated, hydrated membranes - loss modulus, $E''$ .....	68
Figure 3.25: Activated, hydrated membranes - damping, $\tan(\delta)$ .....	69
Figure 3.26: IPMC - storage modulus, $E'$ .....	71
Figure 3.27: IPMC - loss modulus, $E''$ .....	71
Figure 3.28: IPMC - damping, $\tan(\delta)$ .....	72
Figure 3.29: Optical microscope photographs of the surfaces of IPMCs; (a) GEFC at 100X, (b) GEFC at 1000X, (c) hot pressed at 100X, (d) hot pressed at 1000X.....	73
Figure 3.30: Optical microscope photographs of the surface and cross-section of activated, dehydrated membranes all at 100X; (a) extruded surface, (b) extruded cross-section, (c) injection molded surface, (d) injection molded cross-section, (e) hot pressed surface, (f) hot pressed cross-section, (g) GEFC surface, (h) GEFC cross-section ...	75
Figure 3.31: SEM photographs of the cross-section of IPMCs showing the platinum layer; (a) GEFC cross-section at 150X, (b) GEFC cross-section at 1000X, (c) hot-pressed cross-section at 200X, (d) hot pressed cross-section at 1000X.....	77
Figure 3.32: Surface resistance bar graph of the GEFC and hot pressed IPMCs. Each bar represents the front and back sides of the membrane.....	79

Figure 4.1: Experimental set up for IPMC sensor; (a) IPMC clamped in electrode contact clamp and shaker submerged in deionized water, (b) complete experimental set-up of IPMC sensor test .....81

Figure 4.2: GEFC IPMC sensor data at 1 Hz and 3 mm peak to peak displacement .....83

Figure 4.3: GEFC IPMC sensor data at 5 Hz and 3 mm peak to peak displacement .....84

Figure 4.4: GEFC IPMC sensor data at 10 Hz and 3 mm peak to peak displacement .....85

Figure 4.5: Hot pressed IPMC sensor data at 1 Hz and 3 mm peak to peak displacement .....86

Figure 4.6: Hot pressed IPMC sensor data at 5 Hz and 3 mm peak to peak displacement .....87

Figure 4.7: Hot pressed IPMC sensor data at 10 Hz and 3 mm peak to peak displacement .....87

## NOMECLATURE

IPMC	Ionic polymer-metal composite
GEFC	Global Energy Fuel Cells
$F_p$	Plunger force, N
$F_a$	Applied force, N
P	Pressure, MPa
$A_p$	Area of the plunger, $m^2$
$D_{do}$	Thickness of the die orifice, mm
$D_x$	Thickness of the extruded cross-section, mm
$r_s$	Die swell
$M_{hydrated}$	Mass of the hydrated membrane, g
$M_{dehydrated}$	Mass of the dehydrated membrane, g
V	Volume, ml
C	Molar concentration
TGA	Thermogravimetric analysis
$T_d$	Degradation temperature, °C
$W_G$	Width of the gauge section, mm
R	Radius of curvature, mm
$W_T$	Total width of clamp section, mm
$L_G$	Gauge length, mm
$L_T$	Total length, mm
$\sigma_t$	Tensile stress, MPa
$F_I$	Force recorded by the Instron machine, N

$A_0$	Initial area, mm <sup>2</sup>
$\epsilon_t$	Tensile strain, mm/mm
$D_I$	Displacement recorded by the Instron machine, mm
$E$	Modulus of elasticity, MPa
$E'$	Storage modulus, MPa
$E''$	Loss modulus, MPa
SEM	Scanning electron microscope

#### Greek Letters

$\theta$	Contact angle, °
$\delta$	Phase angle, radians

#### Subscripts

p	plunger
a	applied
do	Die orifice
x	Cross-section
s	Swell
hydrated	Hydrated membrane
dehydrated	Dehydrated membrane
d	Degradation



## **CHAPTER 1: Introduction and Objectives**

This chapter explains the fundamentals of ionic polymer-metal composites (IPMC). The metal electrode and polymer membrane are the two main components of the IPMC. The structure of both is explained as well as how they function together as an IPMC sensor. The commercial availability of the ion exchange membrane is also explored, as well as the typical manufacturing methods of the membrane when a commercially available option is not suitable. Finally, research objectives and thesis organization is explained at the end of the chapter.

### **1.1 Ionic Polymer Metal Composite Fundamentals**

Ionic polymer-metal composites (IPMC) are a type of electroactive polymer smart material which can be controlled as either a soft actuator or sensor device. Unlike their piezoelectric ceramic counterparts, IPMCs are known for their low operating voltage ( $< 4$  V), high strain rate, and the ability to operate in water [1]. These qualities give IPMCs a high potential for use in biomimetic applications such as in artificial muscles as well as in fluid flow sensor applications.

The main component of an IPMC is the electroactive polymer membrane. Although there are several different ion exchange membranes available, such as Flemion<sup>®</sup>, the most common membrane used in IPMCs is Nafion<sup>®</sup>, a perfluorinated polymer, which will be used in this thesis project. The hydrophobic backbone structure of Nafion<sup>®</sup> is similar to Teflon<sup>®</sup> giving the polymer its mechanical strength. However, its hydrophilic side chains are short and are terminated by sulfonic acid groups [2, 3]. A diagram of the Nafion<sup>®</sup> chemical structure can be seen in Figure 1.1. The positively charged hydrogen ion attached to the sulfonic acid group is mobile within the membrane

and is balanced by the fixed anionic side chains. This hydrogen cation within the membrane can be exchanged with other common cations used in IPMC membranes such as lithium, sodium, and potassium [4].

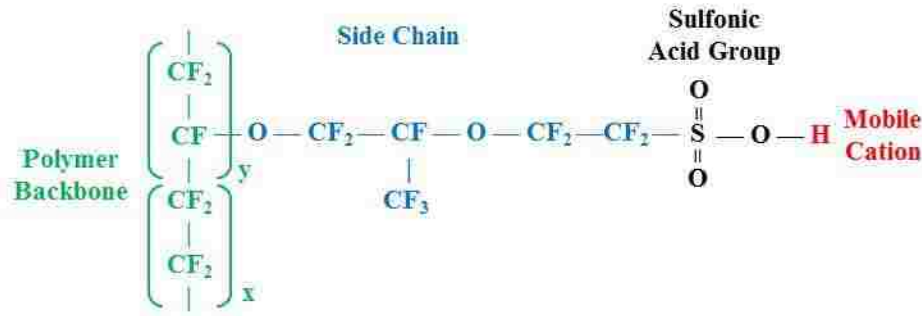


**Figure 1.1: Nafion<sup>®</sup> chemical structure in acid form. Diagram inspired by [5]**

Along with an electroactive polymer membrane, an IPMC also consists of metal electrodes electrochemically plated on the surface of the membrane. Although palladium and other conductive metals [6, 7] as well as nonmetals [8, 9] have been used as the IPMC electrodes, research points towards platinum or gold as being the best electrode for IPMC performance due to the higher surface conductivity and electrochemical stability [1, 10]. Due to this finding, platinum is used as the electrode for the IPMC for this thesis project.

The highly conductive platinum electrode and the hydrated Nafion<sup>®</sup> membrane work together allowing an IPMC to function. When an electric potential is applied to the electrodes plated on the surface of the Nafion<sup>®</sup>, the hydrated mobile cations inside the membrane are pulled toward the cathode due to its negative charge. They travel through the stationary anionic tunnels created by the polymer side chains. As the cations migrate to one side of the membrane, the water molecules attached to them are also dragged along with them. Due to the cation concentration and swelling from the water molecules at one side of the membrane, the membrane swells causing the IPMC to bend towards the anode

[11, 12]. This voltage can be controlled and reversed to make the IPMC bend in the opposite direction. This is the principle of IPMC actuation.

IPMCs are unique in that they can also function as sensors. If one end of the IPMC is fixed and a force is applied to the other end, the cations inside the membrane are forced to move from one side to the other which produces a charge that can be sensed on the electrode. This charge can be read as voltage and amplified to produce a readable signal. Figure 1.2 illustrates the main principle of IPMC sensing motion. Figure 1.2(a) shows the side view of the IPMC membrane. The platinum layers are represented by the thick gray lines on the top and the bottom. The polymer matrix is represented by the green lines. The polymer matrix consists of the polymer backbone and side chains. The anions represented by the black circles are fixed throughout the polymer matrix. The hydrated mobile cations represented by the blue circles are scattered randomly throughout the polymer. They are not attached to anything.

Figure 1.2(b) illustrates the IPMC sensor in motion. A displacement is applied to one end of the IPMC sensor which causes a bending deformation. The cations are forced to move from where they were originally. They do not move as much as they do during actuation, but they do move a certain distance that is dependent upon the frequency of the applied displacement. At a lower frequency, the larger the distance the cations move. When the frequency is high, the cations do not move as much, and the anions, which are fixed to the backbone of the polymer, are now the dominant force in the charge.

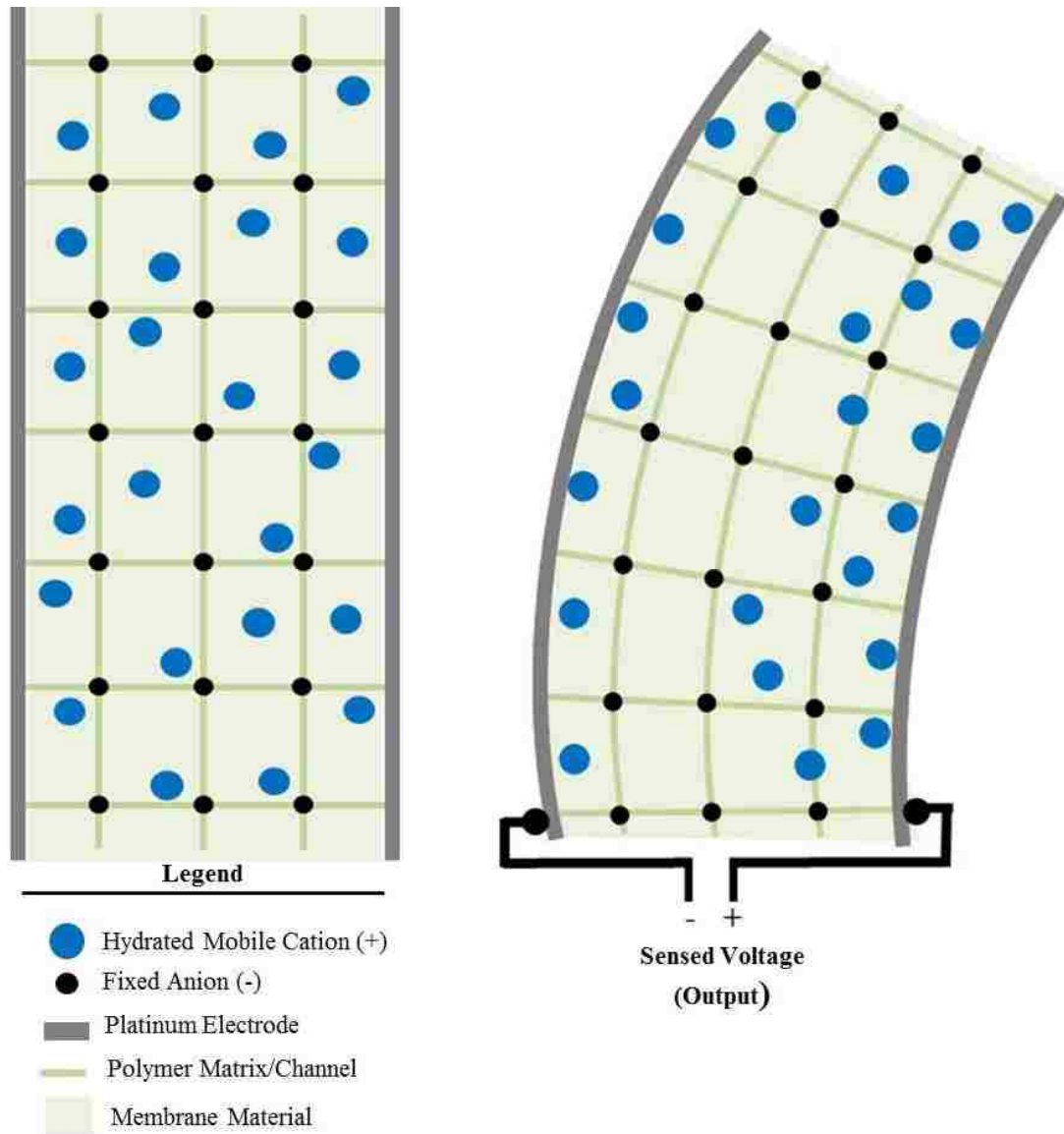


**Figure 1.2: Cation migration in IPMC sensing**

### 1.1.1 IPMC Sensor Applications

Most of the IPMC sensor applications are used in flow displacement sensing. Lei and coworkers have researched small IPMC beams to be used as cilia for flow sensing [13]. Dominik and others have researched the ability of IPMC sensors to sense displacement when oriented in a sensor array [14]. Zhong and others have also researched IPMCs as sensors in pulsing flow applications [15].

Another interesting application of IPMC sensors is in the research carried out by Griffiths [16] where an IPMC was used as a bio-acoustic sensor to sense cardiac sounds and vibrations in the body, similar to a stethoscope. Also IPMC was used in a seismic sensor application prototyped by Ando and coworkers [17]. A cantilever IPMC sensor was immersed in ferrofluid. When the viscosity of the ferrofluid is increased by an applied magnetic field, the response of the IPMC sensor and its resonance frequency decreases. The goal of this research was to use this device as a tunable sensor in seismic applications.

## **1.2 Ion Exchange Membrane**

An ion exchange membrane is a polymer membrane that allows the transport of ions when the membrane is hydrated. The ion exchange membrane is the base material of an IPMC. There are many different types of ion exchange membranes. Nafion<sup>®</sup> and Flemion<sup>®</sup> are two popular choices for the ion exchange membrane used in IPMCs. There are also other variations of these polymers that can be used. In this thesis, Nafion<sup>®</sup> will be used because of its ease of availability to this lab.

### **1.2.1 Commercially Available Nafion<sup>®</sup> Membranes**

DuPont<sup>™</sup> is the leading supplier of Nafion<sup>®</sup> products. DuPont<sup>™</sup> offers prefabricated Nafion<sup>®</sup> ion exchange membranes of various thicknesses. These membranes are typically used in the fuel cell industry [18]; however, they are still very well suited for IPMCs. DuPont<sup>™</sup> also offers Nafion<sup>®</sup> precursor pellets and liquid Nafion<sup>®</sup> dispersions of various concentrations.

DuPont<sup>™</sup> Nafion<sup>®</sup> precursor pellets can be purchased from Ion Power, Inc, an official DuPont<sup>™</sup> distributor. Since these pellets are in the sulfonyl fluoride (SO<sub>2</sub>F) form,

they can be used to melt and form into different geometries through manufacturing processes such as extrusion for example. In order for these pellets to have cation exchange properties, they must be chemically altered [19]. More methods of using Nafion<sup>®</sup> precursor pellets in custom manufacturing membranes will be discussed in the next section.

Prefabricated Nafion<sup>®</sup> membranes are limited to certain geometries. Ion Power, Inc offers extrusion-cast non-reinforced and reinforced dispersion-cast Nafion<sup>®</sup> sheets ranging in thicknesses from 0.025 mm to 0.254 mm. A summary of the available DuPont<sup>™</sup> Nafion<sup>®</sup> sheets that can be purchased from Ion Power are shown in Table 1.1 [20]. Dispersion-cast Nafion<sup>®</sup> membranes are manufactured from a liquid polymer dispersion while the extruded Nafion<sup>®</sup> is extruded through a die.

**Table 1.1: Commercially available Nafion<sup>®</sup> sheets that can be purchased from Ion Power, Inc [20]**

<b>DuPont<sup>™</sup> Nafion<sup>®</sup> Sheet (Ion Power, Inc)</b>		
<b>Model Number</b>	<b>Dry Thickness (mm)</b>	<b>Manufacturing Process</b>
NR-211	0.025	Dispersion-Cast
NR-212	0.051	Dispersion-Cast
N 115	0.127	Extrusion
N 117	0.183	Extrusion
N 1110	0.254	Extrusion

Another ion exchange membrane similar to Nafion<sup>®</sup> that was readily available in the lab is available for purchase from Golden Energy Fuel Cells (GEFC). GEFC produces a variety of membranes on the thicker range from about 0.5 mm to 0.7 mm. The

thicknesses in one single sheet varied 0.2 mm due to the casting method used. For this thesis, GEFC was chosen as the commercial membrane due to its large thickness.

### **1.2.2 Custom Fabricated Membranes**

Some applications require membranes with different geometries (i.e. thickness) than what is available commercially. Custom manufacturing of Nafion<sup>®</sup> membranes allows more options and flexibility when trying to produce a more complicated shape. Depending on the fabrication process and the desired shape, existing Nafion<sup>®</sup> membranes or Nafion<sup>®</sup> precursor pellets can be used to produce a custom membrane.

#### **1.2.2.1 Typical Methods**

Several researchers have been using solution casting to fabricate custom Nafion<sup>®</sup> thin sheets [23–27]. Solution casting involves using a commercially available Nafion<sup>®</sup> liquid dispersion, pouring it into a mold, and allowing it to dry under a controlled environment. The result is a very thin sheet membrane. The downside to this method is that it takes a significant amount of Nafion<sup>®</sup> liquid dispersion and several repeats of the process to get a thick membrane. It is also difficult to control the resulting thickness of the membrane. Because of these downsides, solution casting was not attempted in this thesis.

Another custom sheet membrane fabrication process used by researchers is hot pressing [26, 27]. Hot pressing involves taking existing membranes and placing them in a heated mold while applying pressure to laminate them together creating a thicker membrane. Researchers are attracted to hot pressing to make custom membranes because it allows more control in the resulting membrane thickness.

Extrusion is another fabrication process used mainly to manufacture Nafion<sup>®</sup> tubes [28, 29]. Nafion<sup>®</sup> precursor pellets are heated up in a cylinder and a piston forces the molten pellets through a die. The result is a continuous Nafion<sup>®</sup> strand with a uniform cross-section. The strand will require additional chemical processing to convert it into an ion exchange membrane.

### **1.2.3 Characterization**

Understanding the properties of the membranes used in IPMCs as well as knowing the properties of the membranes after they have been processed into IPMCs is important. Some research has been done in characterizing membranes after they have been processed into IPMCs [30–32]. There has also been work done to find the mechanical, thermal, chemical and other properties of different commercial membranes [33] as well as custom manufactured membranes before they have been processed into IPMCs [32]. There is also data available the DuPont<sup>™</sup> website outlining the different properties of their extruded-cast membranes. With all these properties available, there is still lack of properties known between the processing stages, especially for the Nafion<sup>®</sup> precursor (pre-activated) stage.

### **1.3 Research Objectives and Thesis Structure**

The main objective of this thesis is to fabricate custom Nafion<sup>®</sup> sheet membranes by extrusion, injection molding, and hot pressing. The custom fabricated membranes will undergo a series of property tests throughout each processing stage with the final stage being an IPMC. This thesis will provide mechanical, thermal, chemical, electrical and surface properties throughout each processing step. The resulting properties from the



custom manufactured membranes will be compared to a commercial membrane (GEFC) that will undergo similar processing and testing.

This thesis is organized into five chapters with the first being an introduction to the fundamental concepts. The second chapter discusses in detail the custom manufacturing methods used to create membranes for this thesis. The third chapter discusses the procedures of the tests used to determine the membrane properties. The results are also discussed. The fourth chapter discusses the procedure and results of the samples undergoing IPMC sensing. The fifth and final chapter concludes this thesis and discusses the suggested future work for the next researcher involved.

## **CHAPTER 2: Custom Membrane Fabrication and Processing Techniques**

### **2.1 Custom Membrane Fabrication**

The following section explains the custom membrane fabrication techniques used in this thesis. A membrane thickness of 0.5 mm was the thickness chosen for the membranes of this thesis because it is easier to injection mold a thicker membrane. The thickness was limited by the injection molding process because it would require a large amount of pressure to injection a very thin sheet. A mathematical model is provided for each method to explain the underlying physics occurring during the processes. The custom fabrication processes chosen for investigation for this thesis are extrusion, injection molding, and hot pressing. Solution casting was not chosen due to material cost to produce a large enough sample to be tested.

#### **2.1.1 Extrusion**

The extrusion process involves forcing a molten polymer, the extrudate, through a die to form a continuous piece of a constant cross-section that is determined by the shape of the die. The following sections describe the process developed to successfully extrude Nafion<sup>®</sup> strips.

##### **2.1.1.1 Process Design and Set-Up**

The machine used to extrude the samples is the Galomb Model E benchtop injection molder shown in Figure 2.1. This injection molder was modified from its original injection molding set up to extrude samples as well. The injection molder provides a convenient way to extrude polymer at a controlled temperature.

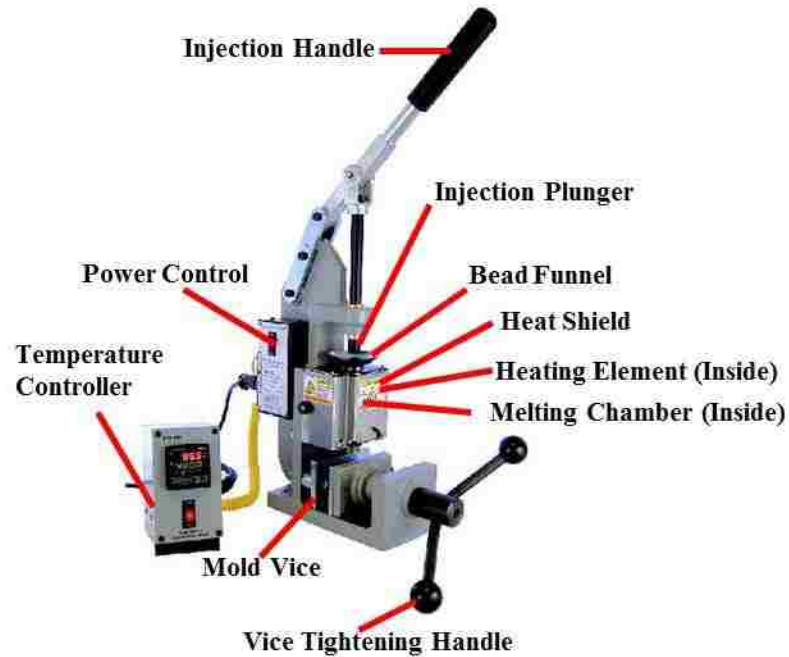


**Figure 2.1: Galomb Model E benchtop injection molder machine with labeled parts. The machine was modified to use in the extrusion of samples. This machine has a maximum processing temperature of 315°C, a dual display temperature controller, and a 17g plastic capacity.**

A couple of major factors in the extrusion process are the pressure inside the extrusion chamber and the die swell. The pressure in the extrusion chamber can be determined by finding the cross-sectional area of the plunger. A free body diagram was drawn to figure out the force going into the plunger. This diagram is shown in Figure 2.2. The force applied to the plunger,  $F_p$ , is found by the sum of moments around point O. The resulting equation is a multiplication of the force applied at the end of the lever.

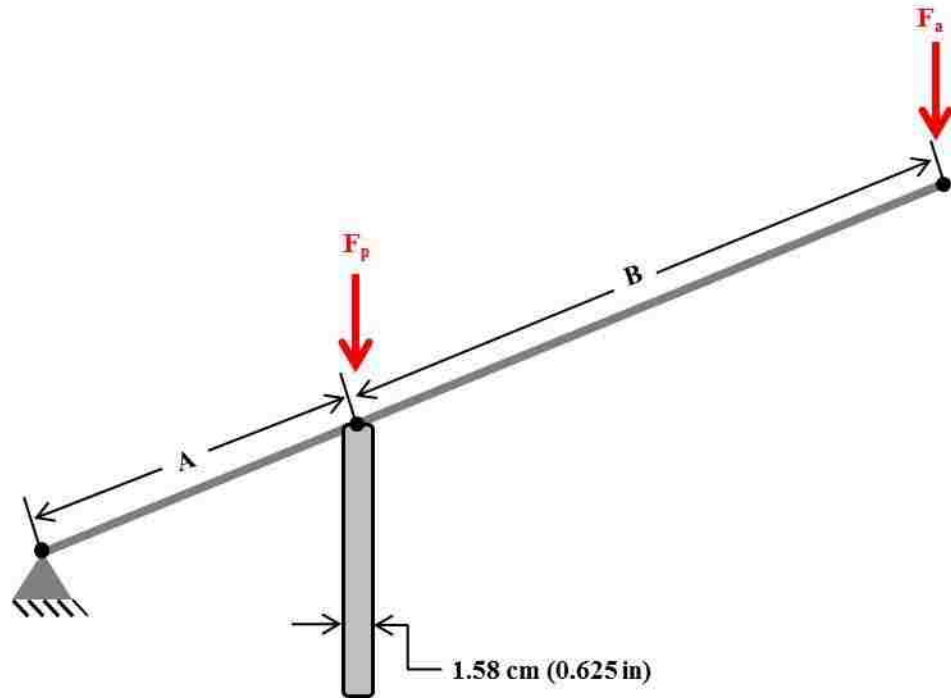


**Figure 2.2: Force body diagram of plunger handle. The use applies the force,  $F_a$ , on the cantilevered end. The force applied is multiplied by a factor of 4.2 directly into the axis of the plunger.**

$$\sum M_O = F_a(A + B) - F_p A = 0 \quad (2.1)$$

$$F_p = \frac{A + B}{A} F_a \quad (2.2)$$

where,

$$F_a = 22.25 \text{ N} (5 \text{ lb})$$

$$A = 0.075 \text{ m} (2.95 \text{ in})$$

$$B = 0.240 \text{ m} (9.45 \text{ in})$$

$$\begin{aligned} F_p &= 4.2 F_a & (2.3) \\ &= 93.45 \text{ N} (21.0 \text{ lb}) \end{aligned}$$

A force of about 22.25 N (5 lb) applied at the end of the lever,  $F_a$ , was required to start the flow of polymer melt through the orifice. This force was determined by trial and error. A weight was hung on the end of the lever handle until the polymer was pushed through the die at a constant rate. Through lever multiplication, the force at the plunger is 4.2 times greater than at the end of the lever. Using the force calculated,  $F_p$ , with the area of the piston,  $A_p$ , the pressure in the extrusion chamber required to extrude the polymer can be calculated

$$P = \frac{F_p}{A_p} \quad (2.4)$$
$$= 0.472 \text{ MPa (68.5 psi)}$$

where,

$$A_p = 1.98e^{-4}m^2 (0.307 \text{ in}^2)$$

Another factor to consider in the design of the extruder die is die swell. Die swell is when the polymer expands to a larger cross-section after it is forced through a smaller orifice. This is due to viscoelastic nature of the polymer. The extruding chamber is a much larger cross-sectional area than the die orifice. As the polymer is forced into the much smaller orifice, it still maintains the compressive stresses after it is extruded through the orifice. That is why the polymer expands after it is extruded [34]. Figure 2.3 illustrates the die swell concept.

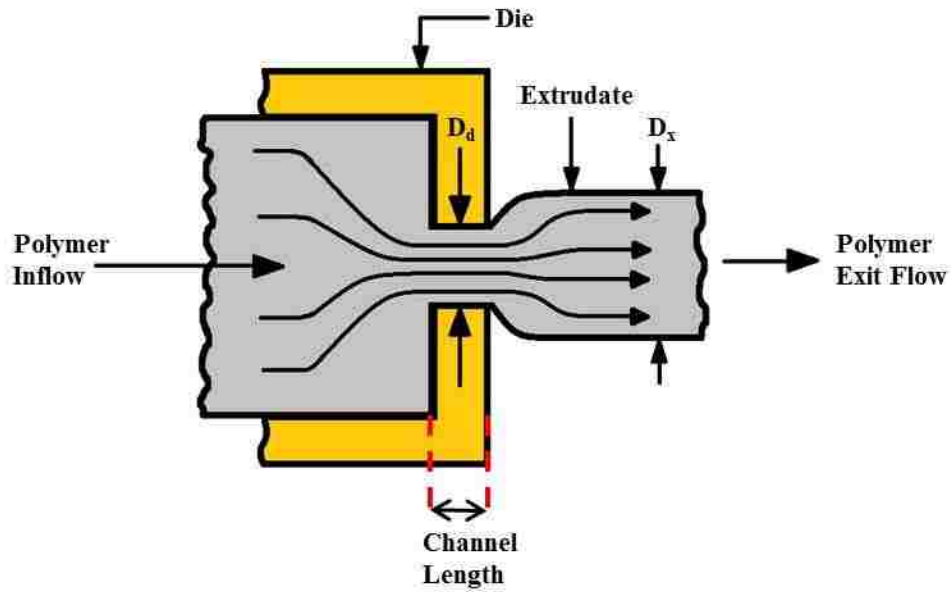


**Figure 2.3: Die swell diagram. The polymer remembers its shape before the orifice due to viscoelastic effects. Diagram inspired by [34].**

The intended thickness of the final extrudate was 0.50 mm. That means that the die orifice needs to be smaller than the final desired extrudate. The thickness of the die orifice used in this study was found by trial and error to result in a membrane that is 0.5 mm thick. Die swell can be expressed with the following equation.

$$r_s = \frac{D_x}{D_{do}} \quad (2.5)$$

Where  $r_s$  is the swell ratio,  $D_x$  is the diameter or thickness of the extruded cross-section, and  $D_{do}$  is the diameter or thickness of the die orifice. The die swell is hard to predict and is calculated after the polymer is extruded. The amount of die swell is also affected by the length of the channel that the polymer travels through. A short channel will increase the die swell because the polymer does not have enough time in the channel to reduce the unrelaxed stresses in the cross-section [34].

An average membrane thickness was taken to be 0.60 mm and was substituted for  $D_x$  in the equation. The thickness of the slot was 0.35 mm and was substituted in for  $D_d$  in the equation. The resulting die swell ratio for the extruded sample is 1.71. The extrudate expands 1.71 times greater than the thickness of the die orifice.

### 2.1.1.2 Die and Adapter Design

As mentioned above, the injection molder was modified to be an extruder. This was done by replacing the injection molder nozzle with a custom adapter that fits the extruder die. A SolidWorks rendering of the adapter can be seen in Figure 2.4. The total length of the adapter was about 31.75 mm (1.25 in). Section A fits into the injection molding chamber and is sealed with an O-ring. The extruder die fits over section B and is held in place with a set screw.

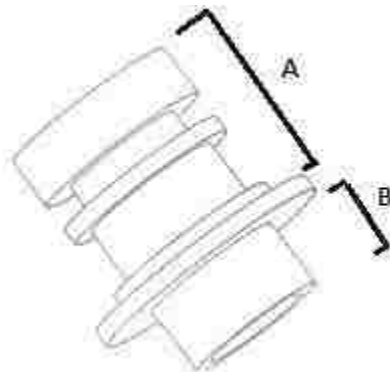


**Figure 2.4: SolidWorks rendering of the extruder die adapter. This part replaced the injection molder nozzle and outfitted the injection molder machine to an extruder.**

The extruder die was designed to extrude the polymer with a rectangular cross-section. Since the slot was so small (0.35 mm), machining the slot was a challenge. An end mill that small is expensive and difficult to use without breaking it. A 0.014 in thick jeweler's slitting saw purchased from McMaster-Carr Supply Company was used to cut the slot.

A sketch of the final design with dimensions is depicted in Figure 2.5 (a) and (b). The final product was made out of brass for its machinability and its ability to maintain heat. Figure 2.6 is an optical microscope photograph of the die orifice. The die orifice has a rough surface that will affect the surface structure of the extruded membranes.

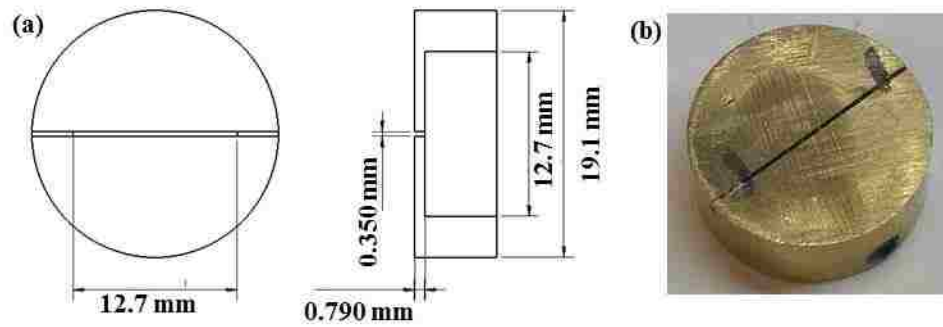


**Figure 2.5: (a) SolidWorks sketch with dimensions of the extruder die, (b) fabricated extruder die made out of brass**

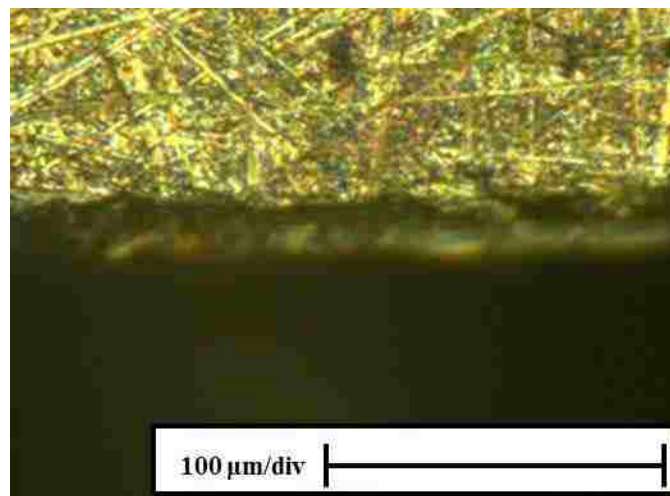


**Figure 2.6: Extruded die orifice zoomed to 1000X using the optical microscope**

### 2.1.1.3 Process Procedure

The brass extruder die slips over the end of the injection molder-extruder die adapter. A set screw in the extruder die tightens the die onto the adapter. The stock injection molder nozzle must be switched with the custom brass extruder nozzle adapter



assembly. This is an easy switch that requires an hex key. Once the appropriate equipment is installed on the injection molder, the machine may now be allowed to warm up.

With both the temperature control unit and the injection molder being turned on, the temperature is set to 220°C. This temperature was determined by trial and error. This was found to be the best temperature where the Nafion<sup>®</sup> precursor beads were able to easily flow, yet it is still low enough for them to not degrade. The injection molder chamber is allowed 10 minutes for it to be fully up to temperature. Once the temperature in the injection molder chamber has reached a steady state, the Nafion<sup>®</sup> precursor pellets are poured into the open end of the injection molder chamber. Apply a small force on the added pellets with the plunger to ensure that they are packed firmly in the bottom of the chamber.

The Nafion<sup>®</sup> precursor pellets will start to become soft and gooey after about 10-15 minutes. Once this occurs, the plunger applies another small force to the polymer melt in the chamber in order to fill the empty spaces in the extruder adapter and die. More pellets should be added to compensate for the filling of the extruder adapter and die. A small force was applied incrementally to the polymer melt with the plunger until the Nafion<sup>®</sup> was seen to extrude from the outside of the extruder die. Tweezers were used to snip off the excess polymer that flowed from the die.

Once the Nafion<sup>®</sup> precursor pellet melt begins to flow out of the die easily, the plunger was pressed onto the polymer melt with a small force until the polymer started flowing from the extruder die. This force was firm and constant, and it was about the force of a hand resting on the plunger handle. Tweezers were used to grab the beginning

of the polymer as it started flowing from the extruder die. The tweezers were used to gently guide the extrudate as it was extruded from the die at a constant pace relative to the speed of the extrudate exiting the die.

Once the desired length of the extrudate was reached (about 50 mm), the force was let off the plunger to stop the flow. The tweezers were used to pinch off the extrudate resulting in a strip of Nafion<sup>®</sup> pre-activated membrane about 15 mm wide, 0.48 mm - 0.70 mm (depending upon the sample and pulling rate from the tweezer guides), and about 50 mm long.

The duration of the Nafion<sup>®</sup> precursor pellet extrusion must be done all at one time and quickly. If the Nafion<sup>®</sup> precursor pellet melt sits in the extrusion chamber at temperature for too long, it will start to turn brown and start to degrade which could leave contaminants in the membrane.

#### **2.1.1.4 Results**

The resulting membranes that were extruded can be seen in the photograph in Figure 2.7. The thicknesses of the membrane ranged from 0.48 mm to 0.69 mm. This range was due to the rate at which the extrudate was guided out of the orifice with the tweezers. Human error contributed to the range in thicknesses. The bottom is noticeably thicker than the top. Both are within the range mentioned above. The marks on both ends of the polymer are from pinching the polymer with the tweezers to guide and remove it from the die. The surface of the membranes has small grooves that run lengthwise that are from the rough surface of the die orifice.



**Figure 2.7: Extruded membranes**

### **2.1.2 Injection Molding**

The process of injection molding involves a molten shot of polymer being forcibly injected into a mold cavity. The mold cavity is allowed to cool and the part is extracted from the mold cavity to yield the final solid polymer part. The following sections explain the injection molding process developed in this study.

#### **2.1.2.1 Process Design and Set-Up**

The same machine that was used for the extrusion process is used for the injection molding process. The photograph in Figure 2.8 is of the same machine but in a different orientation and nozzle set up. The photograph shows the machine set up and ready to use in the lab.

The injection molder that was used is a hand operated machine used for hobby enthusiasts. In a production environment in the industry, the machines are much different. They operate at very high pressures and are fed by a screw that melts polymer beads and increases the pressure as it churns. Since the injection molder used in this study is hand operated, the limiting factor in injection molder is the injection pressure. Injection molding pressures in industrial applications range in the 20,000 psi range and beyond. A

high pressure is required to successfully inject small, thin parts because of the cooling effects of the mold and the viscosity of the polymer melt.

The pressure produced in the benchtop injection molder is calculated in the same fashion as in the extrusion experiment in the previous section. The only factor that changes is the force applied to the lever. It is assumed that a force of 667.2 N (150 lbf), the body weight of an average person, was applied at the end of the lever. The resulting pressure produced in the chamber is 14.15 MPa (2052 psi). This pressure is much less than the pressure produced in industrial applications.

To increase this pressure, there are a few options. A larger force must be applied to the end of the lever. The magnitude of this force may be limited due to the ability of the operator. Another option is to increase the lever length. This will increase pressure slightly, but the speed at which the operator can inject is limited due to the large stroke of the extended lever. The final option is to decrease the area of the plunger and cylinder, thus increasing the pressure inside the chamber. This is a viable option, but it was not developed during this study. However, the idea is explored further in Appendix B.

#### **2.1.2.2 Injection Mold Design and Fabrication**

An injection mold was custom designed and fabricated for use in this study. The design is depicted in Figure 2.8. The way the injection mold handles the pressures produced in the mold and the distribution and flow of the polymer melt is key to the success of the injection mold design. In the mold design pictured below, the sprue is kept short to reduce the initial pressure loss. The runner allows the plastic to quickly be distributed along the whole length of the mold. The cavity depth in this design is 0.5 mm. Considering the high viscosity of the polymer melt, the 0.5 mm depth may prove difficult

for the polymer to enter when injected. The air vents that are about 0.001 in deep are placed at the top half of the mold to allow air to evacuate as the polymer fills the cavity from the bottom up. It is nearly impossible to inject the polymer without these vent holes.

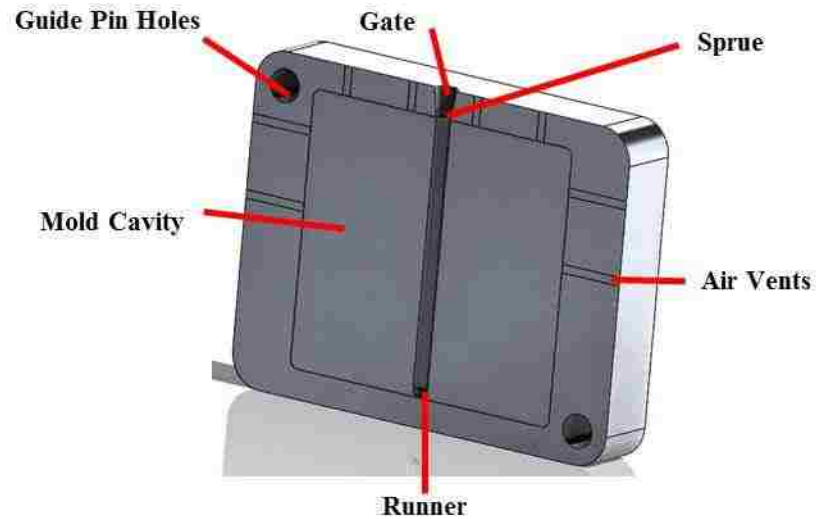


**Figure 2.8: SolidWorks rendering of the mold designed with labeled parts.**

The mold was machined out of aluminum because of its machinability and availability. In industrial applications, the mold is usually made out of steel because it is more durable through the many injection cycles in a manufacturing environment. Aluminum is acceptable to use in this application because of the small quantities of injections required. The mold was fabricated on the CNC mill, and both halves are photographed in Figure 2.9.

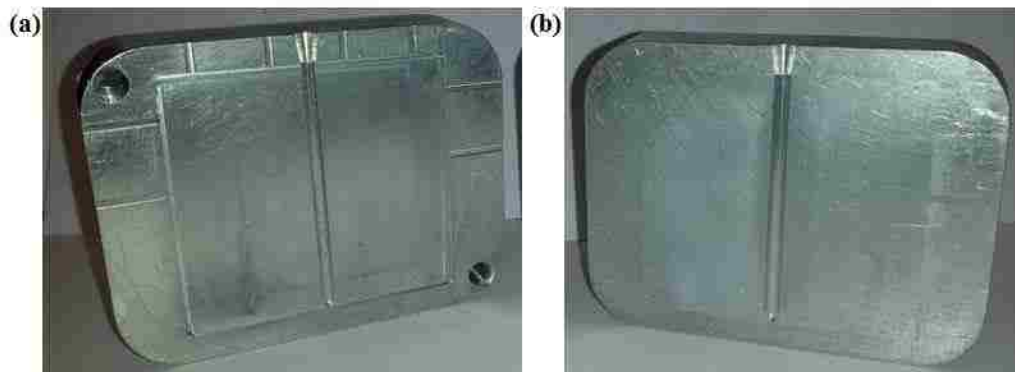


**Figure 2.9: Injection mold fabricated out of aluminum; (a) mold half containing the mold cavity, (b) opposite mold half with runner**

### **2.1.2.3 Processing Procedure**

The injection molder was preheated to 250°C. This temperature was chosen by trial and error so that the Nafion<sup>®</sup> precursor pellet melt was flowing enough to be injected into the mold. Nafion<sup>®</sup> precursor pellets were poured into the injection mold chamber. The pellets were left in the chamber for 15 minutes until they became soft and gooey. The plunger was gently pressed on the polymer melt to fill the air gap in the extruder nozzle and to compact the pellet melt. More pellets were added to the chamber at this time. The plunger was used to purge plastic out of the injection molder nozzle. Once the polymer melt flowed easily through the nozzle, the excess was scraped off, and the injection molder was ready for use.

The preheated injection mold at 275°C was aligned in the vice of the injection molder. This temperature was chosen by trial and error because it showed good results of the polymer flowing into the mold. The vice was tightened to securely hold the two mold halves together. A handle extension bar was placed over the plunger handle to apply more leverage. The handle was rapidly and forcibly pressed then released with the entire weight of the operator (about 150 lb). This action injects the polymer into the mold at a

quick rate in order to combat cooling of the polymer on the mold walls. There is a high variability with rate and force due to the fact that the injection molder machine is manually operated. This inconsistency may be seen in later property tests of injection molded membranes.

After the polymer was injection into the mold, the mold was released from the vice and was cooled under running tap water. Once the mold was cool to the touch, the mold halves were separated and the part was removed from the mold.

The process described in this section was the product of trial and error experimenting to achieve the best injection mold results with the given set-up. One must be careful not to leave the polymer melt in the heated chamber for a long time. It will start to degrade and turn the Nafion<sup>®</sup> precursor melt brown which leads to contamination in the membrane and future complications during processing.

#### **2.1.2.4 Results**

The injection molded samples are pictured in Figures 2.10(a) and (b) below. The injected Nafion<sup>®</sup> did not fill the mold cavity in its entirety. This was due to the rapid cooling of the polymer in the very small (0.5mm thick) injection cavity in the mold. It is difficult and requires a lot of pressure to perform a successful injection mold at this size. Appendix B discusses an alternative solution in the design of the injection molding chamber to increase this pressure.

The resulting membrane after injection can be seen still in the mold in Figure 2.10(a). Figure 2.10(b) is the part removed from the mold. The thickness of this membrane is 0.5 mm. The membranes produced by injection molding are very consistent throughout the whole membrane due to the constant thickness of the mold. Notice how

the polymer did not fill the entire mold. It has difficulty filling the mold that is furthest away from the gate. This is due to the lack of pressure and the polymer cooling off too quickly.

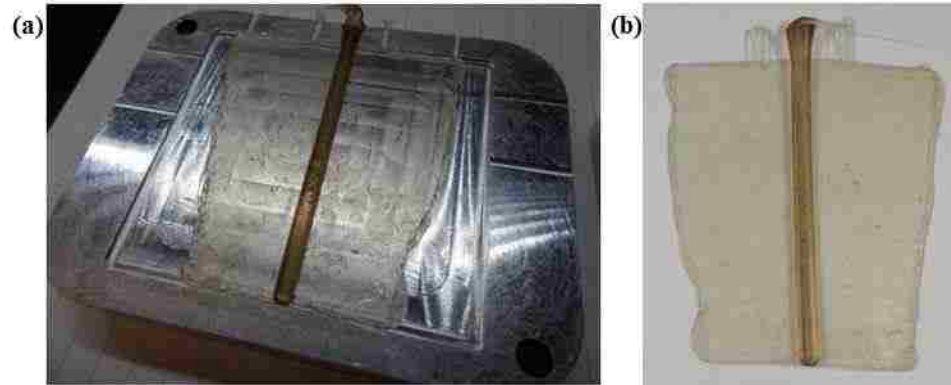


**Figure 2.10: (a) injection mold containing molded membrane right after injection, (b) molded membrane removed from mold**

### **2.1.3 Hot Pressing**

Hot pressing is the process of heating up multiple layers of membranes in a heated mold and applying pressure to fuse them together into a single membrane. This process is common to manufacture IPMC membranes of different thicknesses because of its simplicity. In the following sections, the mold design is explained, and the processing procedure is outlined. The results of this method are shown in the last section.

#### **2.1.3.1 Mold Design**

The mold design for hot pressing is very simple. The bottom half of the mold contains the spacer and the top plate. A 0.6 mm thick spacer is inserted in the bottom half to space up the top half. This determines the thickness of the material being hot pressed. Figure 2.11 shows the stainless steel mold halves. Figure 2.11(a) is the bottom half of the mold with the spacer placed into the cavity.



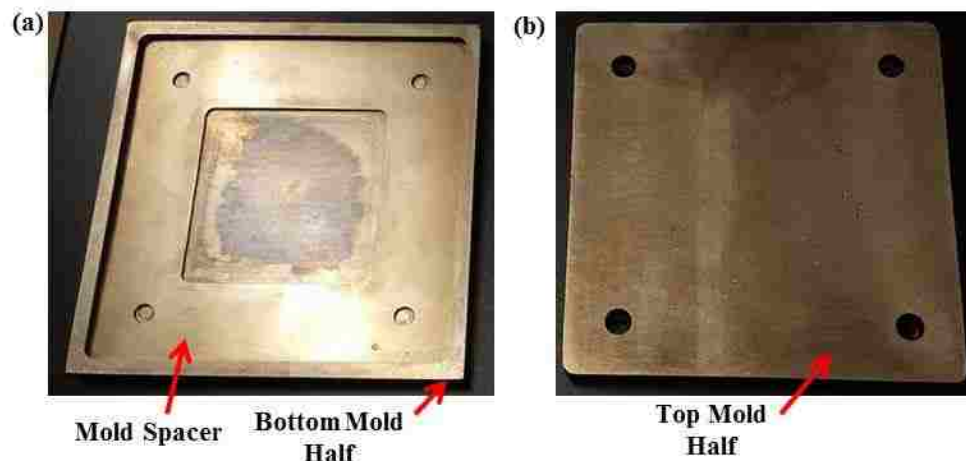


**Figure 2.11: Stainless steel hot press mold with spacer (both halves pictured)**

### 2.1.3.2 Processing Procedure

Hot pressing is a very simple process that is developed by trial and error. The press was preheated to 180°C while the Nafion<sup>®</sup> samples were prepared. This temperature was chosen based off of another research work [26]. Two pieces of Nafion<sup>®</sup> N1110 with thicknesses of 0.25 mm were cut to fit in the square section of the spacer. The membranes were cut 2 mm short on all four sides to allow the membranes to expand when pressed. Two pieces of polyimide film were cut to the same dimensions as the Nafion<sup>®</sup> membranes. The membranes were stacked on top of each other with the polyimide film on each side. The polyimide film was used so the Nafion<sup>®</sup> would not stick to the surface of the mold after it was pressed. Polyimide has a higher melting temperature. The stack of film and membranes were placed in the mold, and the mold was placed on the preheated press. The preheated press is photographed in Figure 2.12.



**Figure 2.12: Carver, Inc. (Model # 3851-0) heated press used to press the mold halves together**

The press was adjusted so that the top half of the press was touching the top mold half with minimal pressure applied. The mold was allowed to sit on the press and heat up for 20 minutes. After the 20 minutes of heating, the pressure of the press was increased to 15 metric tons. The mold was allowed to sit under pressure and heat for 10 minutes. The pressure was released and the mold was cooled under running tap water until it was cool to the touch. The mold halves were separated and the new membrane was removed from the mold. The polyimide film was peeled off of both sides to reveal a single membrane.

### **2.1.3.3 Results**

The resulting membranes are shown below. The result is of uniform thickness of 0.48 mm. The membrane has gotten a lot darker due to the heat. There are also small specks seen in the membrane from dirt particles. These dirt particles can be easily cleaned out during processing.

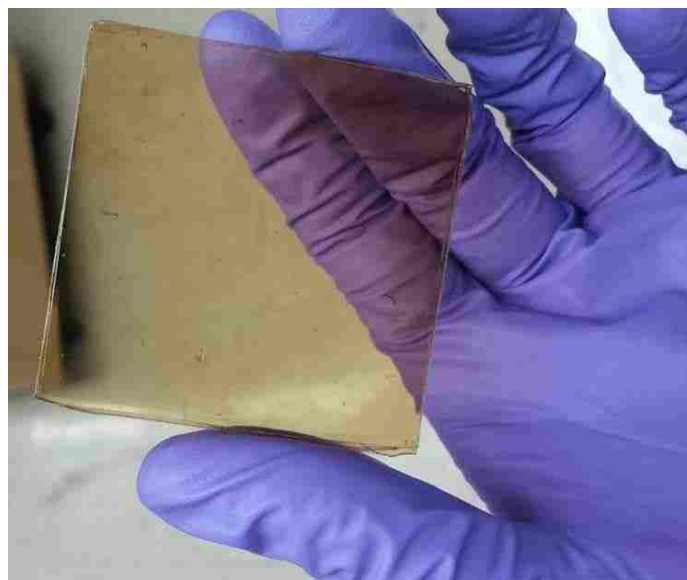


**Figure 2.13: Hot pressed membranes from Nafion<sup>®</sup> N1110. Resulting average thickness is 0.48 mm**

## **2.2 IPMC Processing**

The following sections describe the methodology of transforming the fabricated membranes into IPMCs. The precursor membranes made by injection molding and extrusion had to be activated before they were plated. The hot pressed and GEFC membranes were already in the sulfuric acid form, so they went straight into cleaning then primary plating.

### **2.2.1 Membrane Activation (Base Hydrolysis)**

In its precursor form, Nafion<sup>®</sup> is completely hydrophobic. In order for it to be used as ion exchange membrane, the membranes must be hydrolyzed to convert the SO<sub>2</sub>F functional group to its acidic SO<sub>3</sub>H form.

The membranes are hydrolyzed in a base solution using potassium hydroxide (KOH) and dimethyl sulfoxide (DMSO). Dimethyl sulfoxide is used as a swelling agent in order to increase the reactivity of the hydroxyl ion [35]. A potassium hydroxide (KOH)

and dimethyl sulfoxide (DMSO) solution is prepared. The solution is heated and stirred at 60°C. Once the solution is heated thoroughly, the samples are suspended in it. The hydrolysis process begins on the outside layer of the membrane and works its way inward. The outer layer swells allowing in more potassium and hydroxyl ions [35]. The membranes should stay in the solution for a total of about 2-3 hours to allow the entire membrane to become completely hydrolyzed. At this time, the SO<sub>2</sub>F function group was chemically altered to SO<sub>3</sub>K form.

After activation, the membranes need to go through a cleaning stage to remove impurities and to replace the potassium ion with the hydrogen ion. The membranes are soaked in a heated 3% solution of hydrogen peroxide. Then they are transferred to a heated 1M solution of sulfuric acid. Then the membranes are soaked in heated deionized water twice to ensure there is no sulfuric acid residing in the membrane. At this point, the membranes are now in its SO<sub>3</sub>H acid form. The membranes are now hydrophilic due to the acid functional group.

### **2.2.2 Primary Plating**

Primary plating is an impregnation-reduction reaction, and is performed on all the activated membranes. Before the process can begin, the surface of the membranes must be sanded in the direction perpendicular to the bending of the IPMC. Sanding the surface will allow better water uptake and platinum adhesion to the surface. The membranes then must be thoroughly cleaned using a the 3% heated hydrogen peroxide solution, 1 M heated sulfuric acid solution, and the two baths of heated deionized water.

After the membranes are cleaned, they must be impregnated with platinum. This is done by soaking the membranes in a diluted Pt(II) salt solution for four hours. After the

membranes are done soaking up the platinum atoms, a reduction reaction pulls them to the surface of the membrane. The reduction reaction consists of a sodium borohydride and ammonium hydroxide solution heated to 60°C and stirred. The membrane is then suspended in the solution for a total of 2 hours. Every half an hour 0.2 g of the sodium borohydride is added to the solution to maintain the concentration level.

After the reduction reaction takes place, the membranes are cleaned in a heated 1M sulfuric acid solution and two baths of deionized water. This whole procedure is referred to as primary plating. Primary plating is repeated 3 times.

### **2.2.3 Secondary Plating**

After primary plating, the surface resistance should be checked with a multi-meter. If the surface resistance reads less than 20Ω, secondary plating should commence.

Secondary plating is known as a chemical deposition reaction because it chemically plates the membrane by depositing platinum on the outer surface. First, a solution of platinum (II) salt and ammonium hydroxide is prepared and heated to 50°C. Once the solution is thoroughly heated, 1ml of 20% wt. hydrazine monohydrate solution and 2ml of 5% wt. hydroxylamine hydrochloride solutions are added to the Pt and ammonium heated solution. Once these chemicals are added, the membrane must be immediately submerged and suspended in the solution.

The membrane should remain in the solution for a total of 4 hours. Every half hour hydrazine monohydrate and hydroxylamine hydrochloride are replenished to the solution. After one hour, the temperature should be raised 1-2 degrees every at each chemical replenishment. The final temperature should be at 60°C. After four hours, the

membrane is cleaned in a heated 1M solution of sulfuric acid and two baths of heated deionized water.

After the secondary plating, the surface resistance should be checked with a multi-meter. If the multi-meter is less than  $20\Omega$ , then the plating process is complete. If not, the secondary plating process should be repeated. Care should be taken not to plate the membranes with too much platinum because that will make the membrane too stiff.

#### **2.2.4 Ion Exchange**

The plated membranes should be submerged in a 1M solution of lithium chloride for 24 hours to exchange the hydrogen ion with lithium. The lithium ion is used because the lithium ion transports better than the hydrogen ion [28].

#### **2.2.5 Results**

The GEFC and hot pressed membranes are photographed in Figure 2.14. The membranes were cut into 5 mm x 25 mm strips. The extrusion and injection molding samples did not survive the plating processes. Large bubbles formed in the membrane during cleaning and plating. More about this failure is explained in Appendix B.

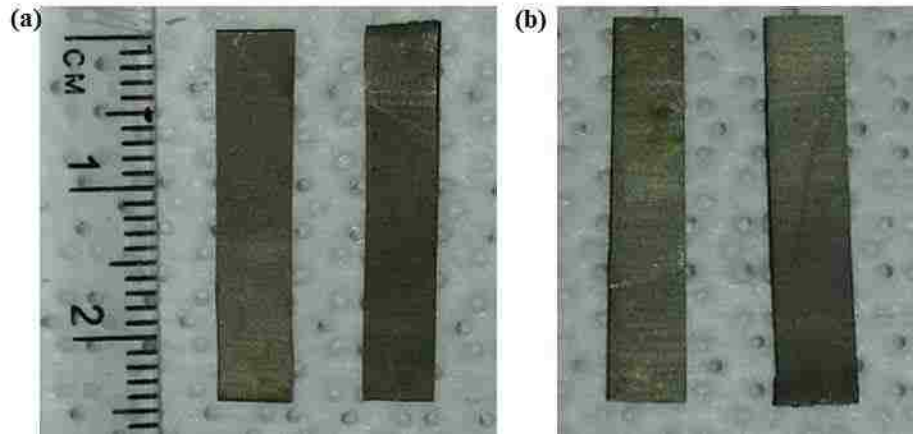


**Figure 2.14: IPMC samples cut to 5 mm x 25 mm strips. (a) hot pressed IPMC strips  
(b) GEFC IPMC strips**

## **CHAPTER 3: Characterization, Results, and Discussion**

### **3.1 Water Uptake**

Water uptake is a percentage of the amount of water that the membrane absorbed. More absorption of water means that the mobile cations will be able to transfer favorably through the membrane while pulling along water molecules. The more mobile hydrated cations there are in the membrane, the more the membrane will deform during actuation as an IPMC and a better voltage signal will be produced as a sensor. The consequence of a high water uptake percentage is that the membrane will be stiffer.

An experiment to measure the water uptake of the activated membranes was designed. The activated membranes were first prepared by sanding the surface of each membrane perpendicular to the direction that the membranes would be bending in IPMC sensing. The samples were then cut to 5 mm x 25 mm strips. Three samples of each activated, hydrated membrane were soaked in deionized water for 24 hours prior to being weighed. This was to ensure that the membrane was fully hydrated. Next, the samples were prepared for weight measurement. Before each sample was weighed, the hydrated sample was removed from its water storage container and was gently blotted with a Kim Wipe to remove any noticeable water droplets on the surface of the membrane. This was carefully done without absorbing too much of the water within the membrane. The membrane was then placed on the scale and the mass was recorded.

After the mass of the membranes were recorded in their hydrated condition, they were placed in an 80 °C oven to dry for 24 hours. Next, the dehydrated membranes were placed on the scale again and the mass of each membrane was recorded. Using the mass



of the membrane in its hydrated condition and the mass of the membrane in its dehydrated condition, the water uptake percentage was calculated using Equation 3.1.

$$\text{Water Uptake (\%)} = \frac{M_{hydrated} - M_{dehydrated}}{M_{dehydrated}} \times 100\% \quad (3.1)$$

The water uptake measurement was repeated for three different samples per membrane. These measurements were averaged to one value and the standard deviation and standard error were taken. Table 3.1 summarizes the results. The membrane with the highest water uptake percentage was the hot pressed membrane at 33.04% followed by the extruded membrane, injection molded membrane, and finally the commercial GEFC membrane. GEFC was not expected to have the smallest water uptake percentage. This could be due to not roughening the surface of the membrane enough. Before any processing is done to the GEFC membrane, the surface appears to be shiny and hard. Without sanding this surface, the membrane absorbs water at a slower rate due to the hydrophilic nano-channels in the membrane shrinking after being dried out. Since it will take longer for the membranes to reabsorb the water, not roughening the surface of the membrane enough could be causing the water uptake percentage to appear lower than reality.

**Table 3.1: Summary table for average water uptake % measurements taken of activated membranes with the % change from GEFC**

<b>Water Uptake % Measurement of Activated Membranes</b>		
<b>Fabrication Process</b>	<b>Average Water Uptake %</b>	<b>% Difference from GEFC</b>
Extruded	29.90 ± 3.46	134.72
Injection Molded	21.38 ± 4.29	67.86
Hot Pressed	33.04 ± 1.31	159.38
GEFC	12.74 ± 0.54	-

The results from Table 3.1 are depicted in the bar graph in Figure 3.1 to visually show the differences between the membranes. A standard error bar was placed on each column to show the location of expected values of water uptake percentage. With the extruded membrane having such a high error of  $\pm 3.46\%$ , the upper range of this membrane would be very close to the average range of the hot pressed membranes. This suggests that it is possible that extruded membranes will perform as well as hot pressed membranes when processed into IPMCs. This broad range in error suggests that the surface preparation of the membranes, i.e. sanding the surface, is the cause of this discrepancy. Although each membrane was sanded in the same direction and for the same duration of time, some surfaces allowed more water inside the membranes while others did not. This error is due to human error in the sample preparation. Overall, the membrane with the highest water uptake percentage is the hot pressed manufactured membrane.

The GEFC membrane has the lowest water uptake percentage. This is due to inadequate sanding of the surface of the membrane. Sanding the surface of the membrane creates a rough surface that water is better able to penetrate through. If the GEFC was left in the water for a longer duration, the results will be much higher.

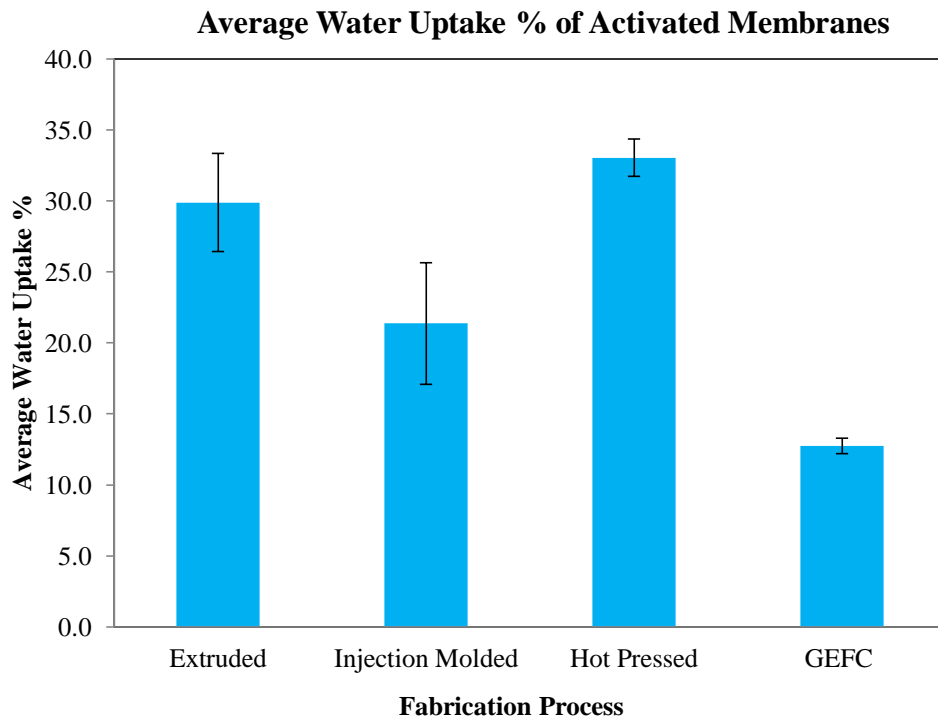


**Figure 3.1: Average measured water uptake % of all activated membranes**

### 3.2 Ion Exchange Capacity

Ion exchange capacity is a measurement of the amount of cations that reside inside the membranes. It is measured in milliequivalents per gram (meq/g). Milliequivalents are defined as the amount of substance required to combine with 1 mole of hydrogen ions. The larger the number, the better the ion exchange capacity.

To find the ion exchange capacity, a titration was performed. The activated membranes were first prepared by sanding the surface of each membrane perpendicular to the direction that the membranes would be bending in IPMC sensing. The samples were cut to 5 mm x 25 mm strips. The activated membranes were dried for 24 hours in an oven at 80 °C. Next, the mass of each membrane was recorded. Then they were soaked in 20 ml of 1M solution of sodium chloride (NaCl) for 24 hours to exchange the hydrogen

ion in the membrane with the sodium ion in the solution. After the ion exchange, the membrane should have a sodium ion attached to the functional group, and the hydrogen ion should be in the remaining solution bonded with the Cl ion as HCl and water. Since the remaining HCl solution is acidic it can be titrated with a base to find the amount of HCl in the solution. The remaining HCl solution was titrated with 0.01M sodium hydroxide (NaOH) using phenolphthalein as the indicator. The NaOH neutralizes the HCl, and the phenolphthalein indicates when the HCl is completely neutralized by changing the color of the solution from clear to light pink. The titration was done on three samples per membrane.

The results of the titration were substituted into Equation 3.2 to determine ion exchange capacity.

$$\text{Ion Exchange Capacity} = \frac{VC}{M_{\text{dehydrated}}} \quad (3.2)$$

where V is the volume of the titrant (NaOH) in mL added at the equivalent point, C is the molar concentration of the titrant, and  $M_{\text{dehydrated}}$  is the mass of the dehydrated membrane. The values calculated for ion exchange capacity were averaged and the standard deviation and standard error were also calculated. A percent change from GEFC was calculated. A summary of the results is shown in Table 3.2.

**Table 3.2: Summary of ion exchange capacity of activated membrane and % change from GEFC membrane**

<b>Ion Exchange Capacity of Activated Membranes and % Difference from GEFC</b>		
<b>Fabrication Process</b>	<b>Average IEC (meq/g)</b>	<b>% Difference</b>
<b>Extruded</b>	0.84 ± 0.23	121%
<b>Injection Molded</b>	0.87 ± 0.018	129%

<b>Hot Pressed</b>	0.93 ± 0.003	121%
<b>GEFC</b>	0.39 ± 0.021	-

Similar to the water uptake percentage results, it appears that the commercial membrane from GEFC has the lowest ion exchange capacity. Since ion exchange capacity is similar to water uptake percentage, this lower value may also be due to the surface not being properly sanded. When the membrane is dried out in the oven, the hydrophilic nano-channels in the membrane shrink, and it takes longer for the membrane to absorb water again. The membrane did not have enough time to absorb the NaCl and properly exchange the hydrogen ion which was detected during the titration.

Figure 3.2 depicts the ion exchange capacity results visually in a bar graph. GEFC is noticeably lower than the other three membranes. This may be due to the poor surface sanding that was done on the GEFC before the experiment. As in the water uptake percentage measurement, the ability for the membrane to absorb water is also diminished because it is more difficult for the water to penetrate a smoother surface than a rougher surface.

Error bars were added to Figure 3.2 to show the error in the samples. The extruded samples had the most amount of error. This is due to the inconsistency in the thickness of the sample in the extrusion process. The error bars of the injection molded and hot pressed samples are very small and cannot be seen at this scale.

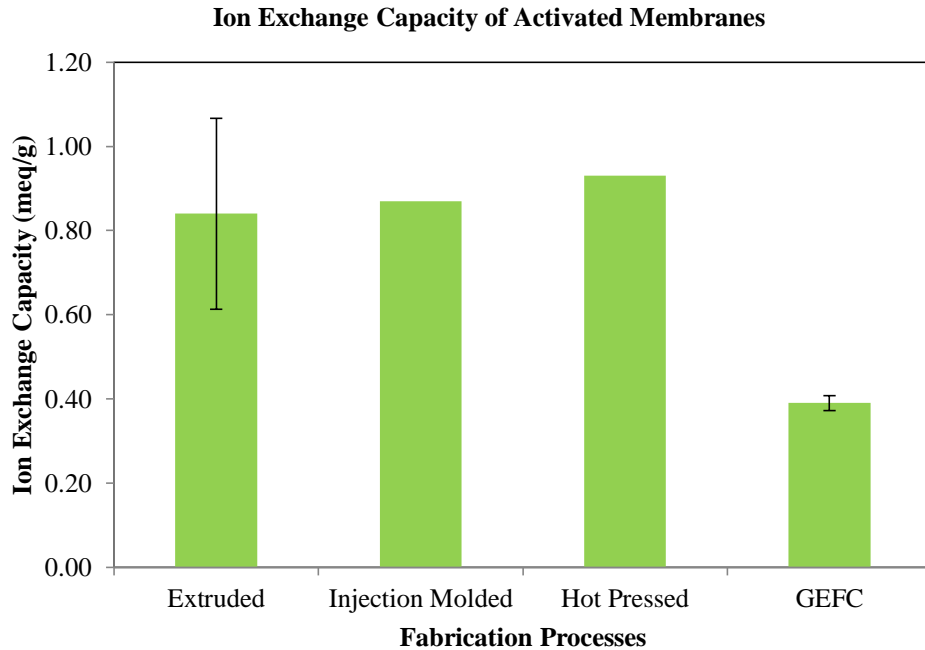


**Figure 3.2: Ion exchange capacity found from activated membranes. GEFC\* is the value taken from the GEFC website [36].**

### 3.3 Contact Angle

A contact angle measurement measures the resulting angle of a water droplet onto a surface. This tries to quantify the hydrophobicity or hydrophilicity of the surface. The contact angle is measured from the surface of the membrane to a line drawn tangent to the water droplet surface. This measurement is depicted as  $\theta$  in Figure 3.3.

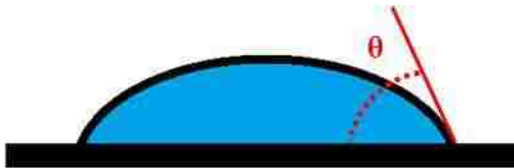


**Figure 3.3: Contact angle definition. The contact angle of a water droplet is measured from the inside of the droplet outwards.**

Hydrophobicity and hydrophilicity are classified into different degrees of wetting. A higher degree of wetting where the contact angle is less than  $90^\circ$  indicates that the

surface is more hydrophilic. A lower degree of wetting where the contact angle is greater than or equal to  $90^\circ$  indicates that the surface is more hydrophobic. Table 3.3 summarizes the degree of wetting based on the contact angle measurement.

**Table 3.3: Degree of wetting of contact angle measurements. This table was taken from Wikipedia [37].**

Contact angle	Degree of Wetting
$\theta = 0^\circ$	perfect wetting (hydrophilic)
$0^\circ < \theta < 90^\circ$	high wettability
$90^\circ \leq \theta < 180^\circ$	low wettability
$\theta = 180^\circ$	perfectly non-wetting (hydrophobic)

The OneAttension contact angle software by Attension was used to measure the contact angle of the different surfaces from a photograph taken of the droplet on the surface. The membrane was fixed on a glass slide using double sided tape. The surface was lightly wiped with isopropyl alcohol to clean off any oils and residue that might misconstrue the measurements. A tiny drop of water from the syringe was placed on the surface of the membrane and a photograph of the surface was taken. The OneAttension software analyses the photograph and outputs a contact angle for each side of the droplet. The hydrated membranes were treated the same way except they were squirted with deionized water to keep them hydrated, and then they were gently blotted to remove any large water droplets on the surface. The contact angles were averaged to obtain a single contact angle per membrane. This contact angle was used to classify the membranes into the degree of wetting. A summary of these values is found in Table 3.4.

All of the surfaces of the activated hydrated membranes exhibited high wettability with contact angles less than 90 degrees. The activated, dehydrated membranes exhibited

higher contact angles and lower wettability. However, the injection molded sample was border-line between high and low wettability with a contact angle of 88.79°. Even though both sets of membranes were activated, the hydrated membranes exhibited more wettability than the dehydrated membranes. This is due to the initial hydrophobic properties of the activated, dehydrated membranes. The measurement was immediately taken right after the drop placement on the surface. Since the measurement was taken immediately after the drop was placed onto the membrane, the constricted hydrophobic nano-channels were not captured absorbing water. If the measurement was taken a few minutes later, the membrane would have absorbed the drop and the contact angle would become less. When there is more water inside the membrane, the surface wetting properties increase.

**Table 3.4: Contact angle and degree of wetting summary table for all membranes**

<b>Contact Angle Measurement And Degree of Wetting</b>			
<b>Process Stage</b>	<b>Fabrication Method</b>	<b>Average Contact Angle (deg)</b>	<b>Degree of Wetting</b>
Pre-activated	Extruded	83.66	high
	Injection Molded	103.16	low
Activated, Hydrated	Extruded	61.29	high
	Injection Molded	73.05	high
	Hot Pressed	78.35	high
	GEFC	60.40	high
Activated, Dehydrated	Extruded	96.14	low
	Injection Molded	95.94	low
	Hot Pressed	88.79	high
	GEFC	95.40	low
IPMC	Hot Pressed	20.79	high
	GEFC	38.73	high



Figure 3.4 is a photograph of the droplet placed on the pre-activated extruded and injection molded membranes. The extruded membrane is on the left and the injection molded membrane is on the right. Table 3.5 summarizes the average contact angle of the pre-activated membranes. The injection molded contact angle is about 23.3% more than the extruded membrane meaning that the injection molded sample is more hydrophobic than the extruded sample.

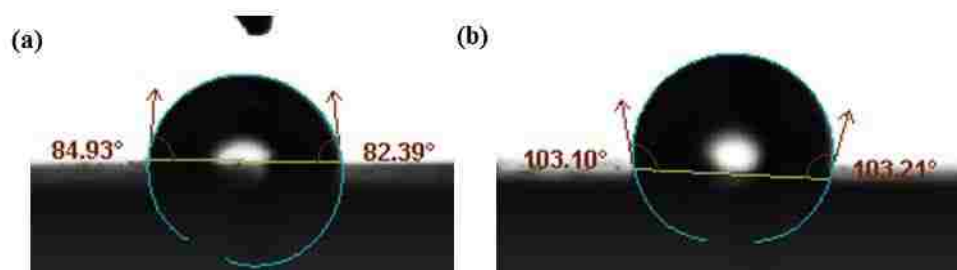


**Figure 3.4: Pre-activated membrane contact angle photograph and measurements; (a) Extruded pre-activated membrane, (b) injection molded pre-activated membrane**

**Table 3.5: Pre-activated membrane contact angle summary and comparison to extruded membrane**

Pre-Activated Membranes Average Contact Angle % Change from Extruded Membrane			
Fabrication Process	Average Contact Angle (deg)	Degree of Wetting	% Change from Extruded
Extruded	83.7	High	-
Injection Molded	103.16	Low	23.3%

Figure 3.5 is a photograph of the activated, hydrated membranes. The contact angles are all at a high wettability. Table 3.6 summarizes the contact angles of each membrane and the percent change from GEFC. The most hydrophilic of the activated,

hydrated membranes is the GEFC membrane with the extruded membrane having a contact angle of only 1.471% higher than GEFC. The least hydrophilic membrane is the hot pressed membrane with a contact angle 25.88% higher than GEFC.

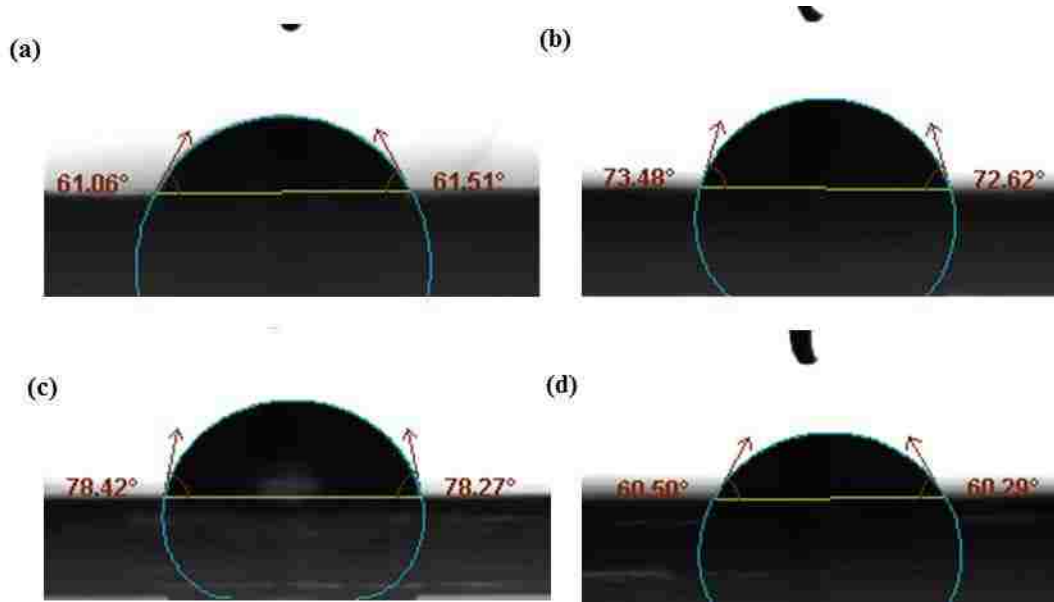


**Figure 3.5: Activated, hydrated membrane contact angle photographs and measurements; (a) extruded membrane, (b) injection molded membrane, (c) hot pressed membrane, (d) GEFC membrane**

**Table 3.6: Summary table of activated, hydrated membrane contact angles and comparison to GEFC with % difference**

Activated, Hydrated Membranes Average Contact Angle and % Change from GEFC (GEFC = 60.40°)			
Fabrication Process	Average Contact Angle (deg)	Degree of Wettability	% Change from GEFC
Extruded	61.29	High	1.471%
Injection Molded	73.05	High	18.97%
Hot Pressed	78.35	High	25.88%
GEFC	60.40	High	-

Figure 3.6 is a photograph of the water droplet and contact angle of the activated, dehydrated membranes. Table 3.7 summarizes the contact angles and shows a percent change from the GEFC membrane. Most of the membranes, except the hot pressed membrane, are only barely above 90° classifying them as low wettability. The most hydrophobic membrane is the extruded membrane by about 0.7757% higher than GEFC. The hot pressed membrane contact angle is also very close to the value of the GEFC contact angle being only about 0.56% higher than GEFC. The extruded, hot pressed, and GEFC membranes all have very similar contact angles. However, the injection molded membrane has a contact angle that is about 7.2% lower than GEFC. This officially classifies the injection molded membrane as a low wetting membrane, although it might be more reasonable to consider it a transition membrane between low and high wetting.

**Table 3.7: Summary table of activated, dehydrated membrane contact angle measurements and comparison to GEFC**

<b>Activated, Dehydrated Membranes Average Contact Angle and % Change from GEFC (GEFC = 95.40°)</b>			
<b>Fabrication Process</b>	<b>Average Contact Angle (deg)</b>	<b>Degree of Wettability</b>	<b>% Change from GEFC</b>
Extruded	96.14	Low	0.776%
Injection Molded	88.79	High	-7.183%
Hot Pressed	95.94	Low	0.559%
GEFC	95.40	Low	-

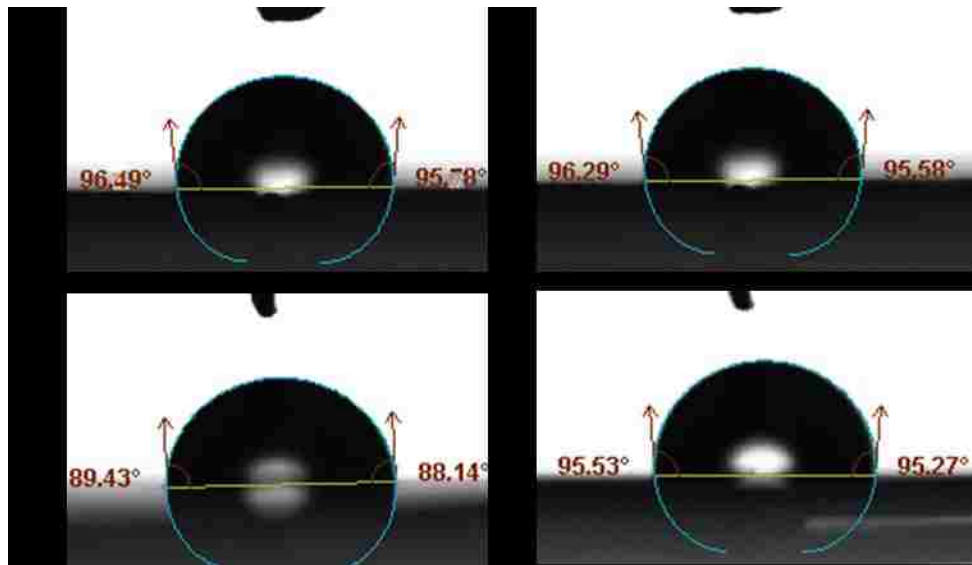


**Figure 3.6: Activated, dehydrated membrane contact angle photographs and measurements; (a) extruded membrane, (b) injection molded membrane, (c) hot pressed membrane, (d) GEFC membrane**

Figure 3.7 is a photograph of the water droplet and contact angle of the hot pressed and GEFC IPMCs. The summary of the contact angle values is shown in Table 3.8. Both of the IPMCs have a high wettability. The most hydrophilic IPMC is the hot pressed membrane with a contact angle that is 46.32% lower than the GEFC membrane. An IPMC with a more hydrophilic surface will perform better in actuation and sensing because more water can cover the surface and enter the membrane to hydrate the cations.

**Table 3.8: Summary of IPMC contact angle measurements and comparison to GEFC IPMC**

IPMC Average Contact Angle and % Difference to GEFC (GEFC = 38.73°)			
Fabrication Process	Average Contact Angle (deg)	Degree of Wettability	% Difference
Hot Pressed	20.79	high	-46.32%
GEFC	38.73	high	-

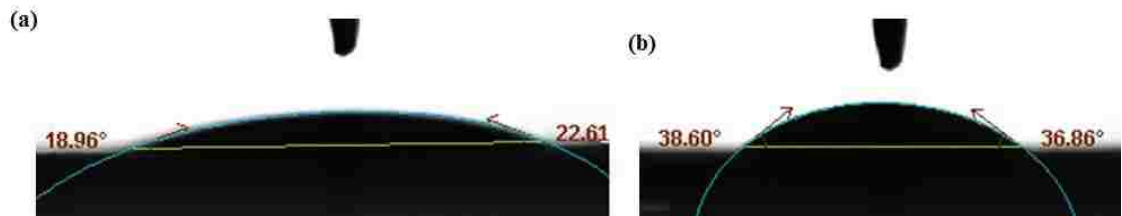


**Figure 3.7: IPMC contact angle photographs and measurements; (a) hot pressed IPMC, (b) GEFC IPMC**

Overall, the membranes were more hydrophilic in the activated, hydrated process stage than the activated, dehydrated and pre-activated processing stages. However, after the membranes have become IPMCs, they are the most hydrophilic. As IPMCs, the hot pressed sample is the most hydrophilic.

### **3.4 Thermal Degradation**

A thermogravimetric analysis (TGA) was performed to find the thermal degradation trend of the membranes. This experiment determines the thermal degradation of the membrane based on the weight change over a temperature increase. This is important to know because processing and/or operating temperatures should never come near this temperature or the polymer will start to decompose and will yield a membrane with undesirable properties.

Each sample was dried in the oven at 80°C for 24 hours to fully dehydrate the samples. A small sample (<4mg) was cut from each membrane and tested using TA Instruments TGA Q500 machine. The samples were run from 30°C to 700°C at a rate of 10°C/min with a Nitrogen gas purge flow. The resulting graphs are shown in Figures 3.8-3.10. The thermal degradation temperature was estimated for each sample using the graphs. This was done by drawing two tangent lines where the weigh percentage starts to drop and finding the intersection point. One line was aligned at the beginning of the

graph and the other was at the end of the graph. The thermal degradation temperature was taken where the two lines intersected and aligned with the x-axis which was set at 10 degree intervals giving an accuracy of  $\pm 1^\circ$ . The measurements were taken five times and were averaged to find the error of the measurement.

Figure 3.8 is the TGA graph of the pre-activated membranes. Both the extruded and the injection molded membranes resulted in a very similar thermal degradation temperature. Table 3.8 shows the thermal degradation temperatures and the % change from the extruded membrane. The injection molded thermal degradation temperature is less than 1% lower than the extruded membrane.

**Table 3.9: Summary table of thermal degradation temperature of pre-activated membranes and comparison to extruded membrane**

Pre-Activated Membranes Thermal Degradation Temperature, $T_d$ (°C) and % Change from Extruded Membrane		
Fabrication Process	$T_{d,1Avg}$ (°C)	% Change from Extruded
Extruded	$435 \pm 0.471$	-
Injection Molded	$434 \pm 0.272$	-0.153%

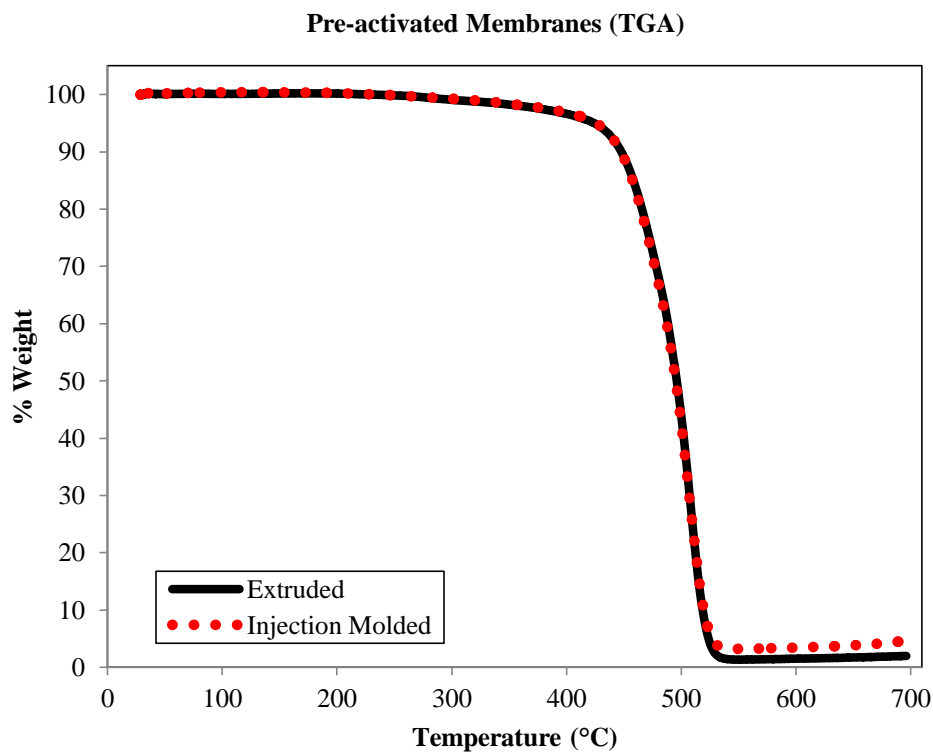


**Figure 3.8: Thermal gravimetric analysis of pre-activated membranes.**

Figure 3.9 shows the TGA results for the activated, dehydrated membranes. It appears that both GEFC and hot press membranes have two degradation temperatures. These values are recorded in Tables 3.10 and 3.11. The second thermal degradation temperatures of the hot pressed and GEFC membranes are closer to the first thermal degradation temperatures of the extruded and injection molded membranes. This could be

due to the similar molecule movement in the polymer at these temperatures. The first thermal degradation temperatures of the hot pressed and GEFC membranes are much lower than the extruded and injection molded membranes. This could be due to contaminants within the two membranes that were pressed together during the hot press manufacturing. The first thermal degradation temperature of GEFC could be attributed to the different polymer structure than Nafion<sup>®</sup>.

**Table 3.10: Summary table of activated, dehydrated membrane thermal degradation temperature and % change from GEFC membrane**

<b>Activated, Dehydrated Membranes First Thermal Degradation Temperature, T<sub>d</sub> (°C) and % Change from GEFC Membrane</b>		
<b>Fabrication Process</b>	<b>T<sub>d,1Avg</sub> (°C)</b>	<b>% Change from GEFC</b>
Extruded	441 ± 0.544	17.9%
Injection Molded	435 ± 0.272	16.5%
Hot Pressed	309 ± 0.471	-17.3%
GEFC	374 ± 0.544	-

**Table 3.11: Summary table of activated, dehydrated membrane second thermal degradation temperature and % change from GEFC membrane**

<b>Activated, Dehydrated Membranes Second Thermal Degradation Temperature, T<sub>d</sub> (°C) and % Change from GEFC Membrane</b>		
<b>Fabrication Process</b>	<b>T<sub>d,1Avg</sub> (°C)</b>	<b>% Change from GEFC</b>
Hot Pressed	428 ± 0.720	-1.76%
GEFC	435 ± 0.720	-



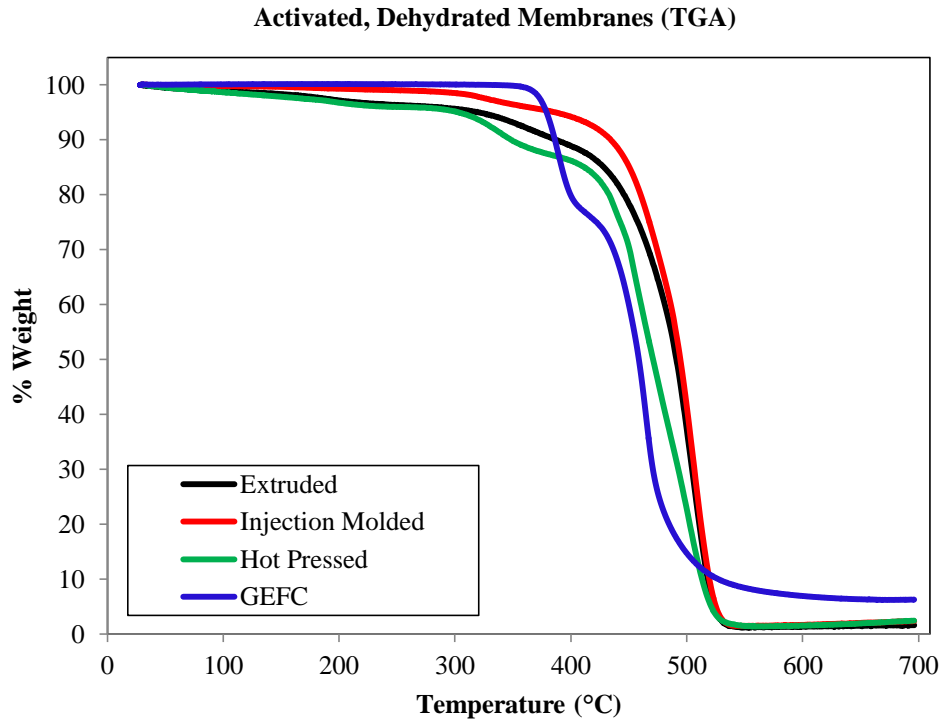


**Figure 3.9: Thermal gravimetric analysis of activated, dehydrated membranes**

Figure 3.10 shows the TGA results from IPMCs made from hot pressed and GEFC membranes. There is only one thermal degradation temperature for these two membranes which is fairly similar. The temperatures are summarized in Table 3.12. The thermal degradation temperature for the hot pressed membrane is only 1.18% higher than GEFC. Once plated, the hot pressed and GEFC IPMCs have similar thermal degradation temperatures.

**Table 3.12: Summary of thermal degradation temperature of IPMCs and % difference to GEFC IPMC**

IPMCs Thermal Degradation Temperature, T <sub>d</sub> (°C) and % Difference to GEFC IPMC		
Fabrication Process	T <sub>d,1Avg</sub> (°C)	% Difference
Hot Pressed	458 ± 0.471	1.18%
GEFC	453 ± 0.544	-

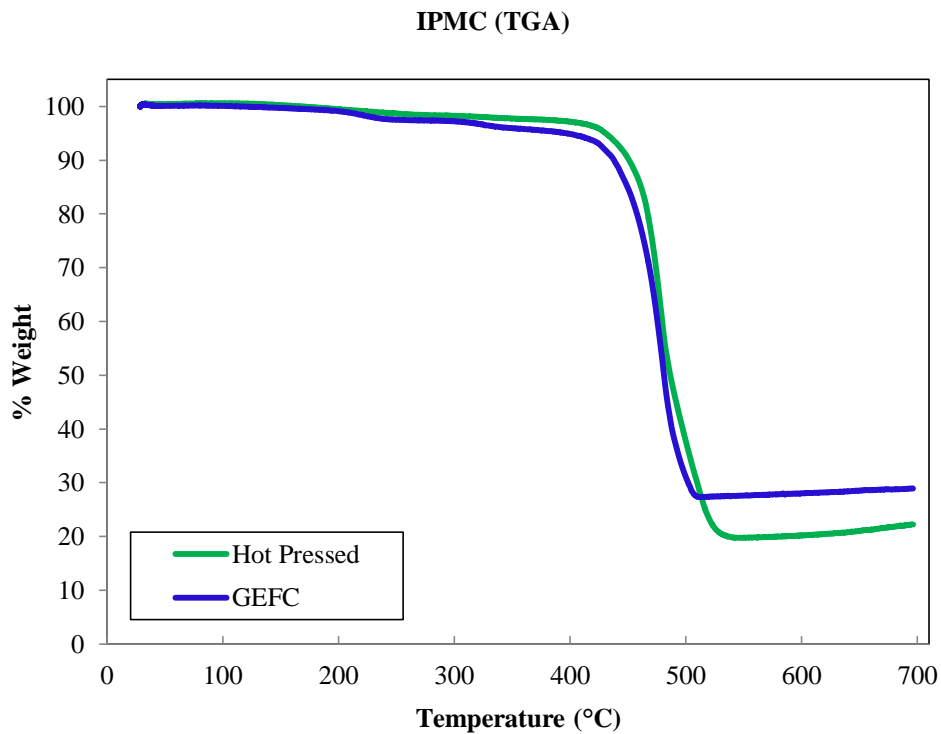


**Figure 3.10: Thermal gravimetric analysis of IPMCs**

### 3.5 Tensile Properties

The objective of doing the tensile test was to find the modulus of elasticity and observe the viscoelastic characteristics of the samples. The samples were cut into dog bone shapes as defined by ASTM D638 [38]. The dimensions of the dog bone shape are shown in Figure 3.11(a).  $W_G$  is the width of the gauge section,  $L_G$  is the gauge length,  $R$

is the radius of curvature between the gauge and clamping sections,  $L_T$  is the total length,  $W_T$  is the total width of the clamp section, and  $t$  is the thickness of the membrane. The cut samples, shown in Figure 3.11(b), from left to right are the extruded, injection molded, hot pressed, and GEFC activated, dehydrated membranes. The injection molded sample seen second from the left is slightly smaller than the rest of the samples. This is due to the slightly smaller injection mold size. Due to the space restrictions of the mold vice, the injection mold dimensions were limited which explains the shorter sample. The tensile friction grips were still able to properly grip the sample at the same location as the other tensile samples. ASTM D638 was used as a basic guide for calculating stress, strain, and modulus of elasticity.

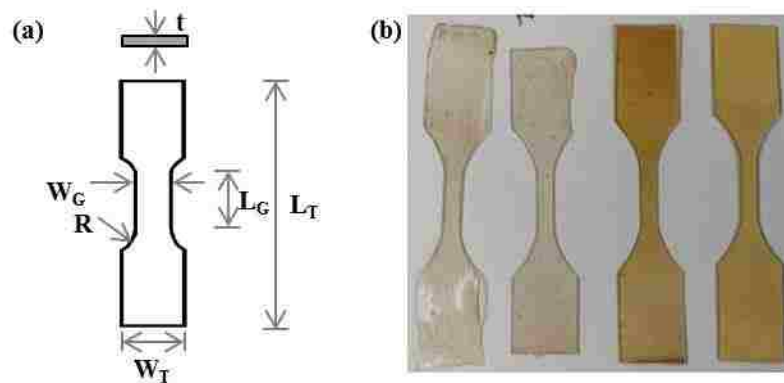


**Figure 3.11: (a) Tensile sample with dimensions:  $t = 0.38 \text{ mm} - 0.79 \text{ mm}$ ,  $W_G = 2.5 \text{ mm}$ ,  $R = 15 \text{ mm}$ ,  $W_T = 10 \text{ mm}$ ,  $L_G = 10 \text{ mm}$ ,  $L_T = 60 \text{ mm}$ ; (b) all activated, dehydrated tensile samples cut from tensile die. Membranes from left to right: extruded, injection molded, hot pressed, and GEFC. Note that the injection molded sample is shorter than the other three samples. This is due to the slightly smaller injection molding size.**

The specimens were fixture in the Instron 5565 universal testing machine. The fixtures are friction clamps as shown in Figure 3.12 below. The sample was put in the fixture and was aligned as straight as possible. The sample was tensioned to take out the initial slack. The strain rate for the tests was 20 mm/min. The tensile test was carried out

for each sample. The test could only be completed once due to high material cost and low availability.

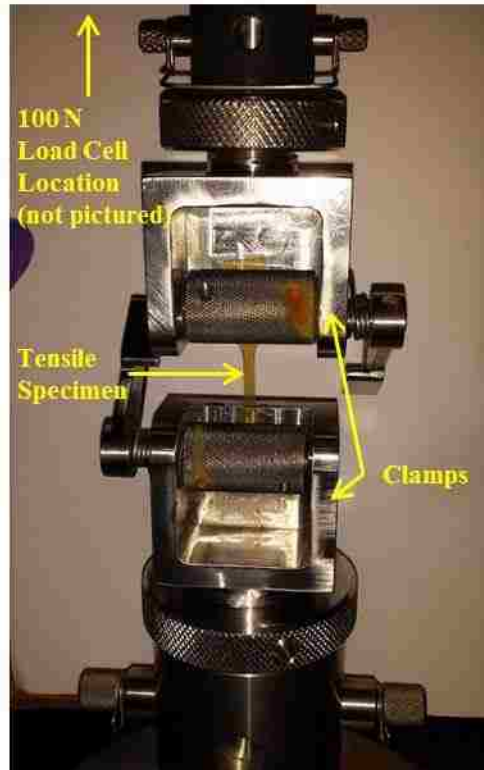


**Figure 3.12: Tensile fixture with tensile specimen clamped in and ready to start the test. The load cell is a 100 N load cell and is not pictured in this photograph.**

The tensile stress and strain were calculated using Equations 3.3 and 3.4 respectively.

$$\sigma_t = \frac{F_I}{A_o} \quad (3.3)$$

$$\epsilon_t = \frac{D_I}{L_G} \quad (3.4)$$

where  $\sigma_t$  is the tensile stress,  $F_I$  is the applied force recorded from the Instron,  $A_o$  is the initial cross-sectional area of the gauge section,  $\epsilon_t$  is the tensile strain,  $D_I$  is the displacement recorded by the Instron, and  $L_G$  is the gauge length of the specimen. The

displacement measurement is measured by motors that track the displacement of the machine.

The modulus of elasticity is determined for each sample. This was measured by taking the slope of the tangent line to the initial straight line of each curve as per ASTM D638. This was calculated in Excel by determining the slope between two adjacent points and averaging them.

Figures 3.14-3.17 show the results of the tensile tests. The data is plotted in a stress-strain plot. From these graphs, the modulus of elasticity was calculated from the initial slope of the stress-strain curves for each membrane up to 1% strain. The results of these measurements are summarized in Tables 3.13-3.16. The membranes in the pre-activated state seen in Figure 3.14 and summarized in Table 3.13 have the lowest modulus of elasticity and the highest strain values. The pre-activated membranes stretched to roughly 1,000% -1,200% of their original size.

The pre-activated membranes stiffened up during the activation process and gave a higher modulus of elasticity in the activated, hydrated and activated, dehydrated state. However, the stiffest membrane in both the activated, hydrated and dehydrated groups was the GEFC membrane by over 50% for all membranes. The next stiffest membrane was the hot pressed membrane. The injection molded and extruded membranes were the most flexible in all cases, and they resulted in values that were generally close to each other. These results are summarized in Tables 3.14 and 3.15.

The modulus of elasticity of the GEFC and hot pressed IPMC was very similar to each other. This can be seen in Figure 3.17 and summarized in Table 3.16. The modulus of elasticity for the GEFC membrane decreased after being plated as seen by the high

modulus of elasticity of the activated, dehydrated and hydrated GEFC membrane. The modulus of elasticity of the hot pressed IPMC decreased after being processed into an IPMC. The IPMCs also stretched the least unlike the other membranes.

Figures 3.14-3.17 also show the mechanical behavior of the polymer membrane. As the strain increases, the stress increases also. Although this can be seen in all of the stress-strain graphs, it is more prevalent in the activated, dehydrated membranes where the stress increases more dramatically as strain is increased.

Overall, GEFC was the stiffest membrane throughout each process. Hot pressed was the second stiffest. Injection molded and extruded were always similar to each other, and the least stiff of all.

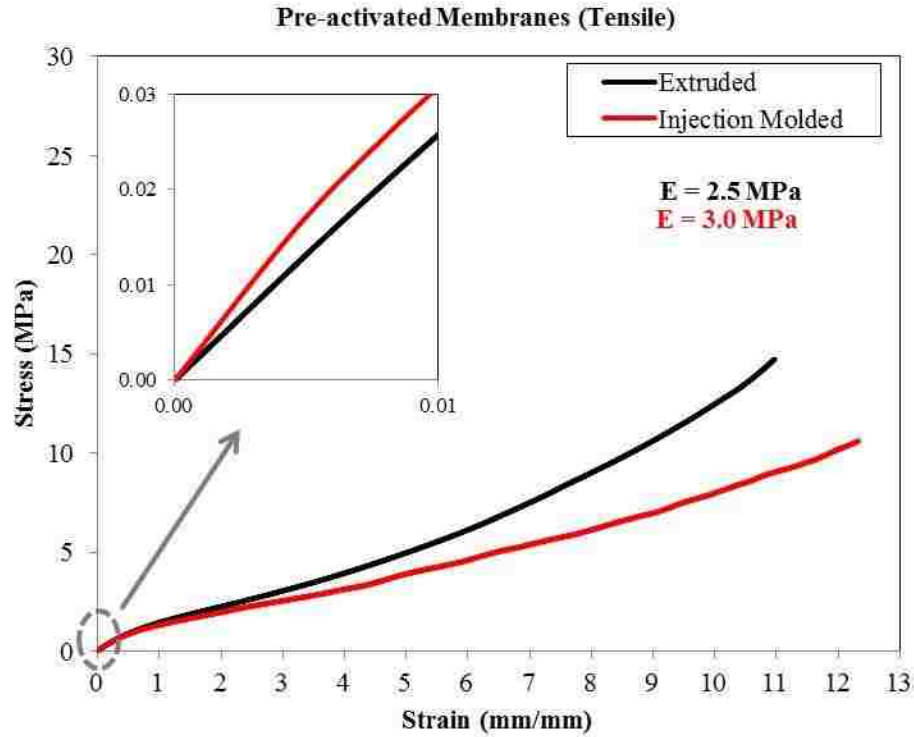


**Figure 3.13: Pre-activated membrane stress-strain curve with a zoomed section of the initial curve**

**Table 3.13: Modulus of elasticity of pre-activated membranes and % change from extruded membrane**

<b>Pre-Activated Membranes Modulus of Elasticity Extruded and Injection Molded % Change from Extruded Membrane</b>		
<b>Fabrication Process</b>	<b>Modulus of Elasticity (MPa)</b>	<b>% Difference</b>
Extruded	2.5	20.0%
Injection Molded	3.0	

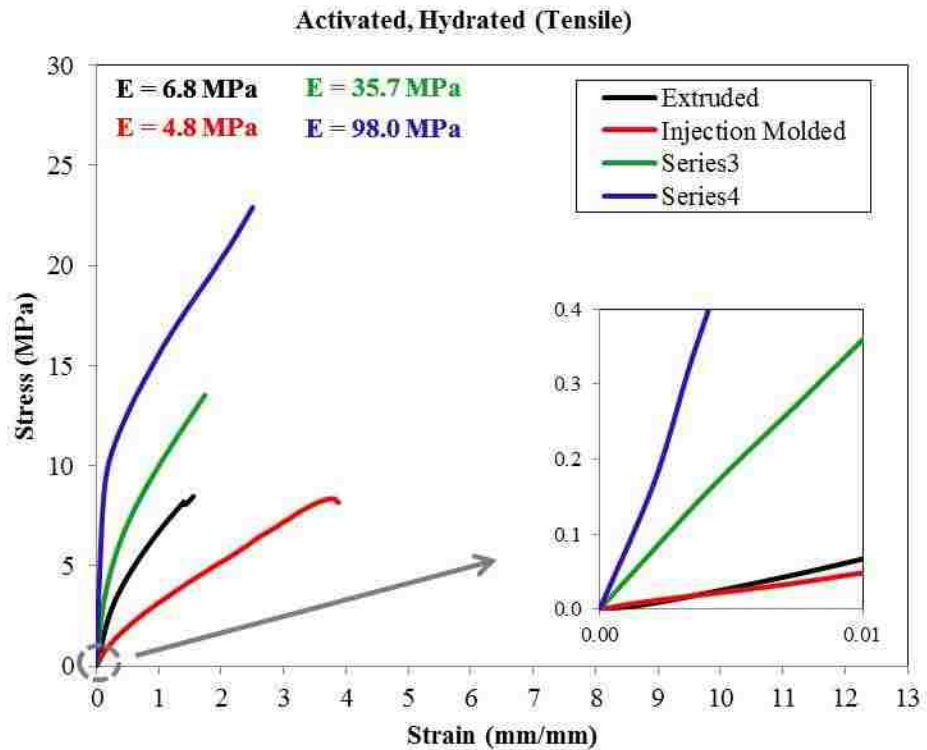


**Figure 3.14: Activated, hydrated membrane stress-strain curve with a zoomed section of the initial curve**

**Table 3.14: Summary of modulus of elasticity of activated, hydrated membrane and % change from GEFC membrane**

<b>Activated, Hydrated Membranes Modulus of Elasticity and % Change from GEFC</b>		
<b>Fabrication Process</b>	<b>Modulus of Elasticity (MPa)</b>	<b>% Error</b>
Extruded	6.8	-93%
Injection Molded	4.8	-95%
Hot Pressed	35.7	-64%
GEFC	98.0	-



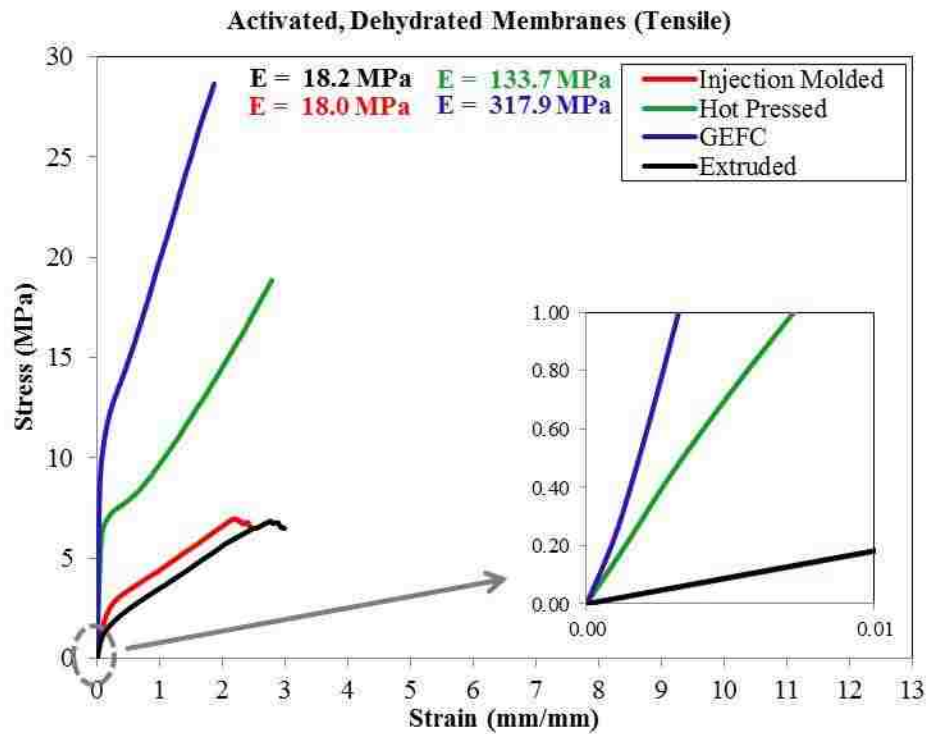


**Figure 3.15: Activated, dehydrated membrane stress-strain curve with a zoomed section of the initial curve**

**Table 3.15: Summary of modulus of elasticity of activated, dehydrated membrane and % change from GEFC membrane**

<b>Activated, Dehydrated Membranes Modulus of Elascicity and % Change from GEFC</b>		
<b>Fabrication Process</b>	<b>Average Modulus of Elasticity (MPa)</b>	<b>% Error</b>
Extruded	14.5	-93%
Injection Molded	18.3	-91%
Hot Pressed	100.0	-50%
GEFC	200.0	-

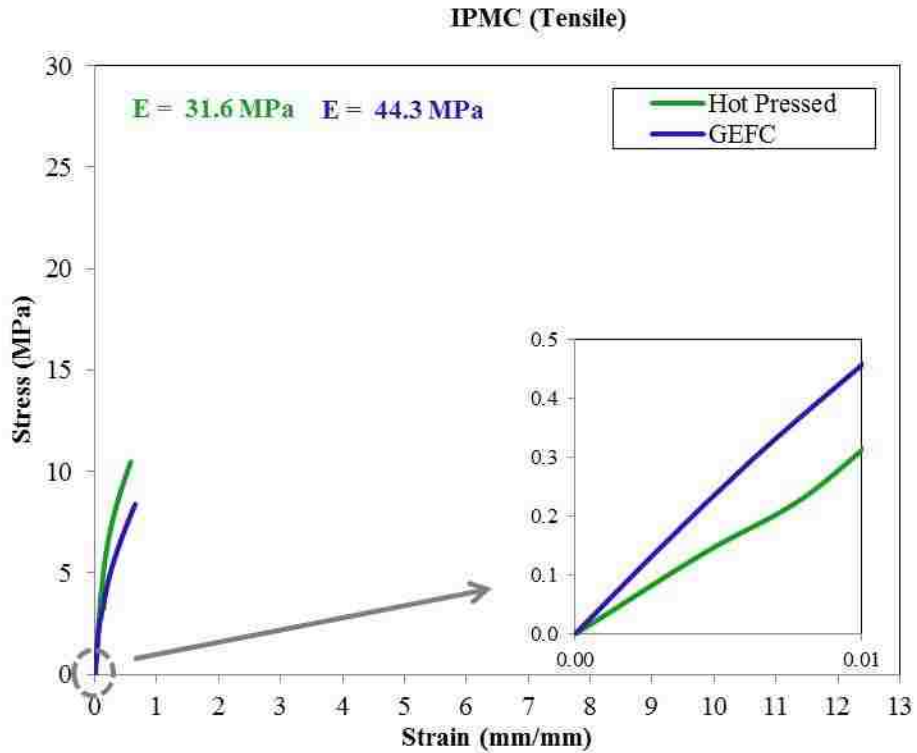


**Figure 3.16: Hot pressed and GEFC IPMC stress-strain curve with a zoomed section of the initial curve. Extruded and injection molded are not pictured because they were not able to be processed into IPMCs**

**Table 3.16: Summary of modulus of elasticity of IPMC and % change from GEFC membrane**

<b>Hot Pressed IPMC Modulus of Elasticity and % Change from GEFC</b>		
<b>Fabrication Process</b>	<b>Average Modulus of Elasticity (MPa)</b>	<b>% Error</b>
Hot Pressed	31.6	-29%
GEFC	44.3	-

### 3.6 Dynamic Mechanical Analysis

A dynamic mechanical analysis using the Pyris Diamond DMA was done on each membrane after each processing stage. A dynamic mechanical analysis (DMA) is important to understand the viscoelastic properties of the material. The samples were set up in tension, and they were oscillated at different frequencies (1 Hz, 2 Hz, 5 Hz, 10 Hz). A sinusoidal force is applied to the material resulting in a displacement output. In a viscoelastic material, the displacement output lags behind the force input resulting in a phase angle shift. The machine calculates the storage modulus, loss modulus, and the tangent of the phase angle, which is the ratio of the loss to storage modulus. These properties are plotted at each frequency for each sample to show the change in the properties as frequency increases.

The storage modulus is the in-phase component of the elastic response of the sample at the different frequencies. This is not the same as the Young's modulus. The loss modulus is the out of phase component of the viscous response of the material under different frequencies. The ratio between the loss and storage modulus is the tangent of the phase angle. This measurement is also known as damping and is the measure of the dissipation of energy of the material.

Figures 3.17-3.28 show the storage modulus, loss modulus, and damping of each membrane in their different processing stage. For the majority of the membranes, the higher the frequency, the stiffer the material is. This can be seen by the increase in values of the Storage modulus. There is also an increase in value for the loss modulus and damping as the frequency is increased for the majority of membranes. This means that the membranes become stiffer and more viscous with higher frequencies.

### 3.6.1 Pre-activated Membrane Results

Figures 3.17-3.19 show how the pre-activated membranes become less elastic and more viscous as the frequency increases. Table 3.17, the summary table for the pre-activated membranes, gives actual numbers of this trend. The increase in storage modulus, loss modulus, and damping is gradual as if approaching an asymptote as the frequency increases. The injection molded membrane a higher storage modulus and loss modulus than the extruded membrane. However, it has less damping than the extruded membrane.

**Table 3.17: Summary table of DMA results of pre-activated membranes and percent change from extruded membrane**

<b>Storage Modulus, E' of Pre-activated Membranes and % Difference from Extruded Membrane</b>			
<b>Frequency</b>	<b>Storage Modulus, E' (MPa)</b>		<b>% Difference</b>
	<b>Extruded</b>	<b>Injection Molded</b>	
1	7.59	8.93	18%
2	9.07	10.65	17%
5	12.06	14.05	16%
10	15.54	17.89	15%
<b>Loss Modulus, E'' of Pre-activated Membranes and % Difference from Extruded Membrane</b>			
<b>Frequency</b>	<b>Loss Modulus, E'' (MPa)</b>		<b>% Difference</b>
	<b>Extruded</b>	<b>Injection Molded</b>	
1	3.76	4.03	7%
2	5.29	5.64	7%
5	8.42	8.94	6%
10	12.02	12.64	5%
<b>Damping, tan(<math>\delta</math>) of Pre-activated Membranes and % Difference from Extruded Membrane</b>			
<b>Frequency</b>	<b>Damping, tan(<math>\delta</math>)</b>		<b>% Difference</b>
	<b>Extruded</b>	<b>Injection Molded</b>	
1	0.50	0.45	-9%
2	0.58	0.53	-9%
5	0.70	0.64	-9%
10	0.77	0.71	-9%

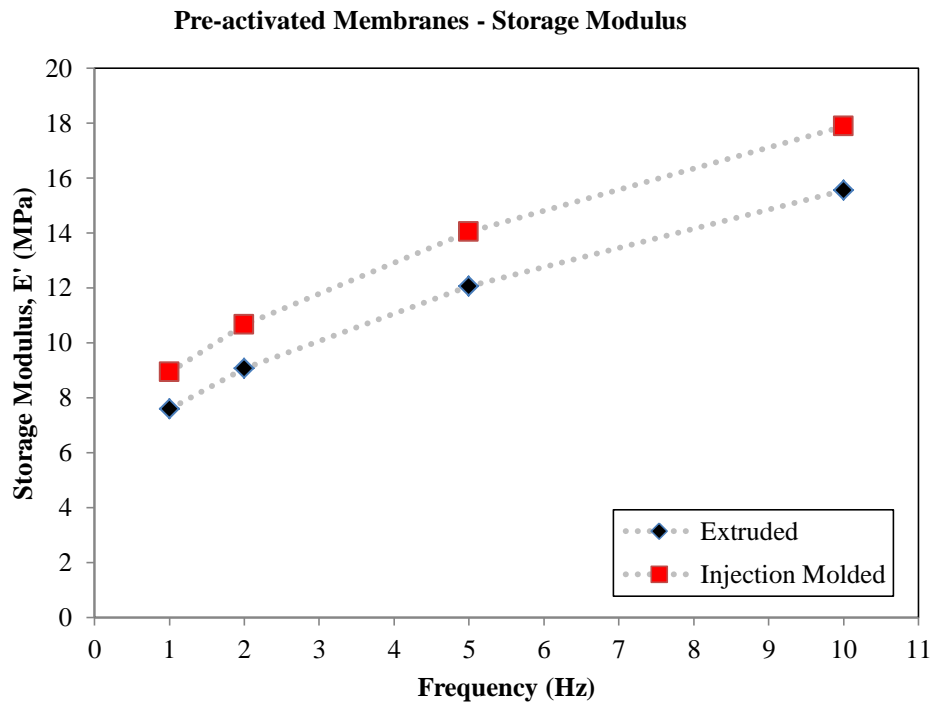


**Figure 3.17: Pre-activated membrane - storage modulus,  $E'$**

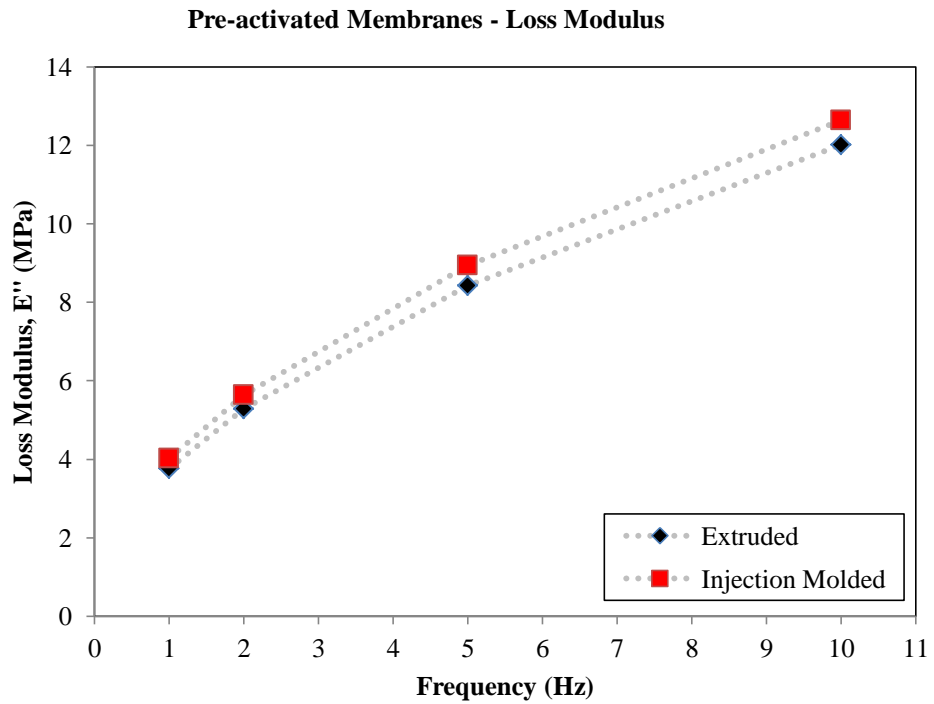


**Figure 3.18: Pre-activated membranes - loss modulus,  $E''$**

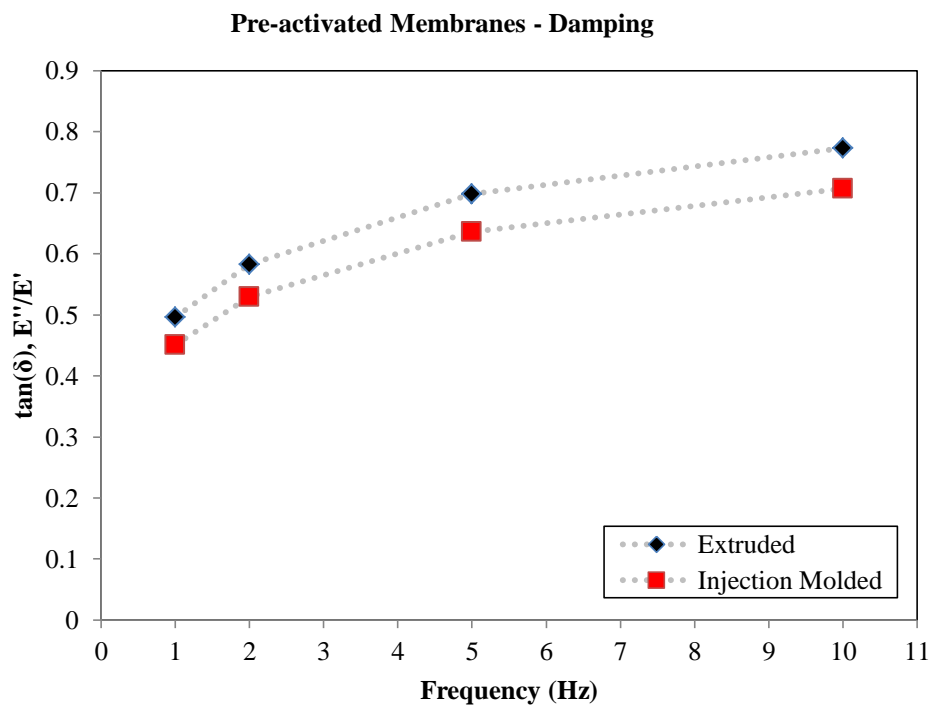


**Figure 3.19: Pre-activated membranes - damping,  $\tan(\delta)$**

### 3.6.2 Activated, Dehydrated Membrane Results

Table 3.18 summarizes the DMA results for the activated, hydrated membrane. Figures 3.20-3.22 are plots of this information in order to see the trend of the data. Overall, the storage modulus, loss modulus, and damping increase in value in the dry, activated state. The storage modulus of these membranes shown in Figure 3.20 exhibits the same trend as the pre-activated membranes. It is gradually increasing as the frequency increases. However, the loss modulus of the GEFC seen in Figure 3.21 and hot pressed membranes decrease as the frequency increases. This is also seen in the damping as well in Figure 3.22. As the frequency increases, the GEFC and hot pressed membranes are less viscous and have smaller damping than the extruded and injection molded membranes where the viscous and damping effects increase as the frequency increases.

As seen in Figure 3.20, the GEFC membrane has the highest storage modulus compared to the other membranes with the injection molded and extruded membranes at the lowest storage modulus. The GEFC is the least elastic membrane, and the injection molded and extruded membranes being the most elastic. Looking at Figure 3.21, GEFC is generally more viscous than the other membranes at lower frequencies. The extruded membrane makes a drastic jump to being the most viscous at the highest frequency. The injection molded membrane also increases as the frequency is increased surpassing the hot pressed membrane with the hot pressed membrane being the least viscous at the higher frequencies.

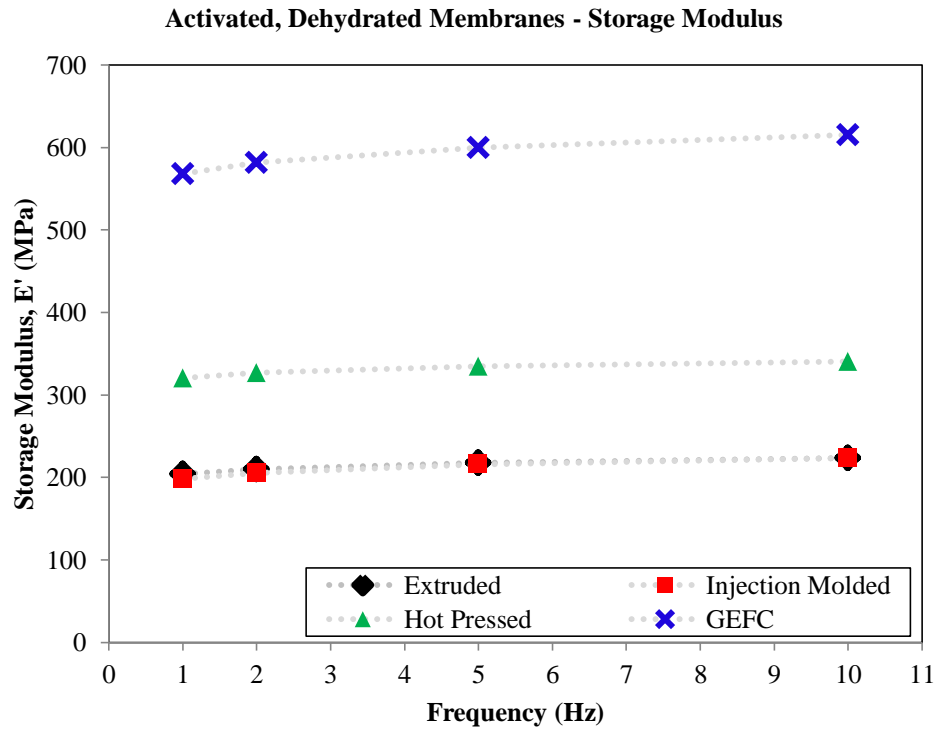
The extruded membrane makes this large jump in loss modulus to become the most viscous membrane at 10 Hz because of the polymer chain alignment. During the manufacturing process of the extruded membrane, the polymer chains are allowed to align in the direction of extrusion. When the polymer is pulled enough, the chains start to resist motion.

Figure 3.21 shows the damping of the membrane. The extruded membrane has the most damping characteristics and the hot pressed has the least. This is also due to the polymer chain alignment of the membrane as mentioned before. When the polymer chains are pulled they want to resist motion which dissipates energy at the higher frequencies.

**Table 3.18: Summary of DMA results of activated, dehydrated membranes and percent change from GEFC membrane**

<b>Storage Modulus, E' of Activated, Dehydrated Membranes and % Difference from GEFC Membrane</b>							
<b>Freq. (Hz)</b>	<b>Storage Modulus (MPa)</b>				<b>% Difference Hot Pressed &amp; GEFC</b>	<b>% Difference Injection Molded &amp; GEFC</b>	<b>% Difference Extruded &amp; GEFC</b>
	<b>Extruded</b>	<b>Injection Molded</b>	<b>Hot Pressed</b>	<b>GEFC</b>			
1	204.1	198.4	320.3	568.2	-64%	-65%	-44%
2	209.9	205.5	326.8	581.5	-64%	-65%	-44%
5	217.6	215.7	334.7	599.9	-64%	-64%	-44%
10	223.8	223.6	340.5	615.0	-64%	-64%	-45%
<b>Loss Modulus, E'' of Activated, Dehydrated Membranes and % Difference from GEFC Membrane</b>							
<b>Freq. (Hz)</b>	<b>Loss Modulus (MPa)</b>				<b>% Difference Hot Pressed &amp; GEFC</b>	<b>% Difference Injection Molded &amp; GEFC</b>	<b>% Difference Extruded &amp; GEFC</b>
	<b>Extruded</b>	<b>Injection Molded</b>	<b>Hot Pressed</b>	<b>GEFC</b>			
1	14.68	16.17	16.68	38.64	-62%	-58%	-57%
2	15.05	16.82	16.32	40.04	-62%	-58%	-59%
5	15.84	17.94	15.85	42.63	-63%	-58%	-63%
10	16.76	19.07	15.54	45.20	-63%	-58%	-66%
<b>Damping, tan(δ) of Activated, Dehydrated Membranes and % Difference from GEFC Membrane</b>							
<b>Freq. (Hz)</b>	<b>Damping tan(δ)</b>				<b>% Difference Hot Pressed &amp; GEFC</b>	<b>% Difference Injection Molded &amp; GEFC</b>	<b>% Difference Extruded &amp; GEFC</b>
	<b>Extruded</b>	<b>Injection Molded</b>	<b>Hot Pressed</b>	<b>GEFC</b>			
1	0.072	0.082	0.052	0.068	6%	20%	-23%
2	0.072	0.082	0.050	0.069	4%	19%	-28%
5	0.073	0.083	0.047	0.071	2%	17%	-33%
10	0.075	0.085	0.046	0.074	2%	16%	-38%





**Figure 3.20: Activated, dehydrated membrane – storage modulus, E'**

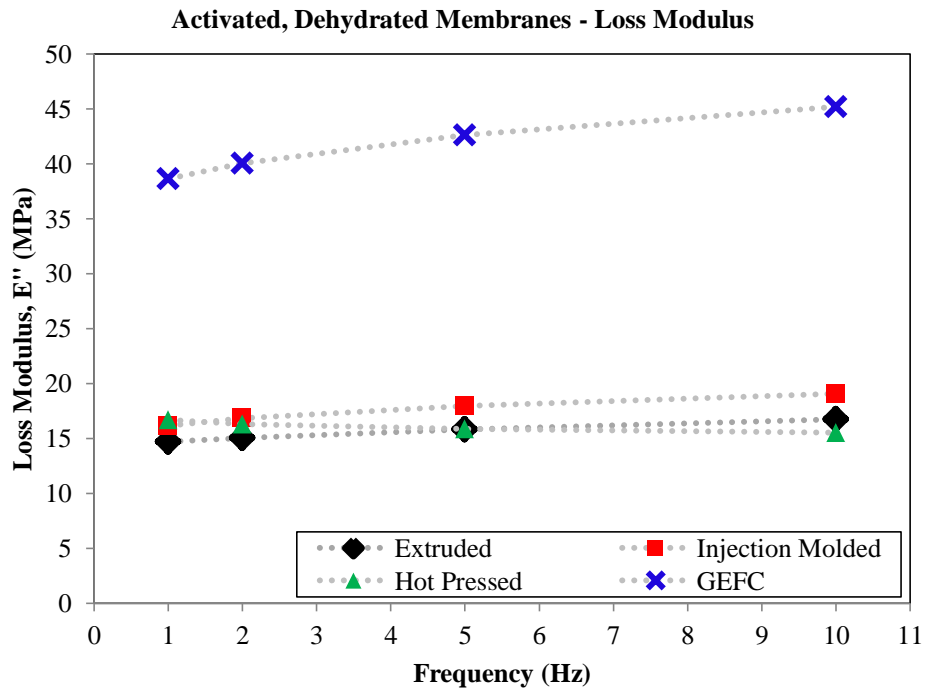


**Figure 3.21: Activated, dehydrated - loss modulus, E''**

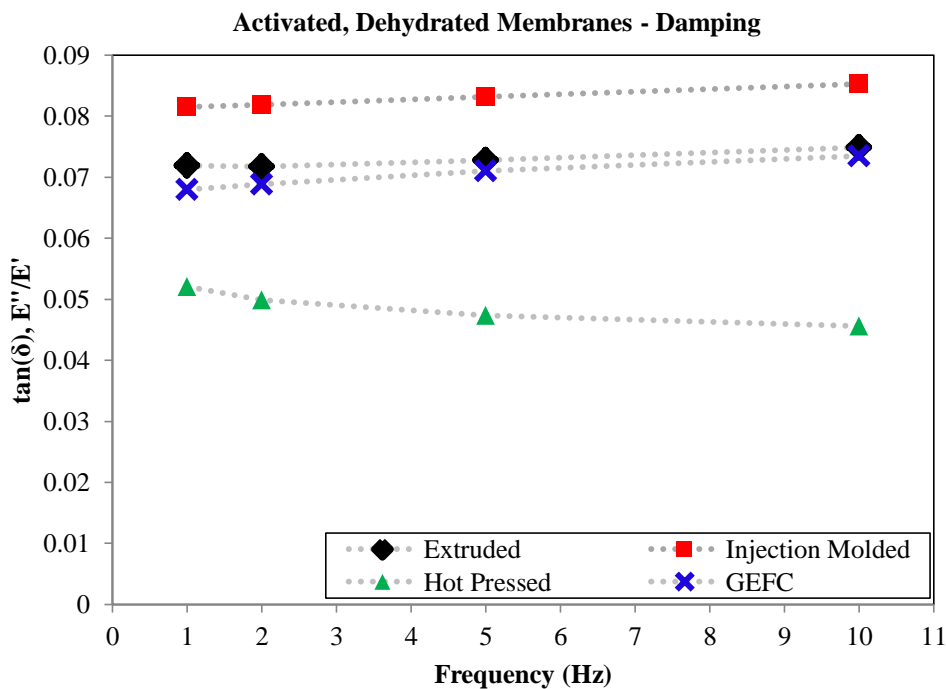


**Figure 3.22: Activated, dehydrated - damping, tan(δ)**

### 3.6.3 Activated, Hydrated Membrane Results

Figures 3.23-3.25 are plots of the storage modulus, loss modulus, and damping of the activated, hydrated membranes. Table 3.19 is the summary table of these results. Overall, the activated hydrated membranes show the same trends as the activated, dehydrated membranes. The only difference is that the numerical values of each property decreased. When hydrated, the membranes lose their stiffness and viscous characteristics. They also become less able to dissipate energy from applied forces. When the plots of the activated, hydrated membranes and the activated, dehydrated membranes are compared, they look almost identical qualitatively.

**Table 3.19: Summary of DMA results of activated, hydrated membranes and percent change from GEFC membrane**

<b>Storage Modulus, E' of Activated, Hydrated Membranes and % Difference from GEFC Membrane</b>							
<b>Freq. (Hz)</b>	<b>Storage Modulus (MPa)</b>				<b>% Difference Hot Pressed &amp; GEFC</b>	<b>% Difference Injection Molded &amp; GEFC</b>	<b>% Difference Extruded &amp; GEFC</b>
	<b>Extruded</b>	<b>Injection Molded</b>	<b>Hot Pressed</b>	<b>GEFC</b>			
1	44.01	38.54	91.54	231.90	-81%	-83%	-61%
2	47.55	41.04	93.25	237.80	-80%	-83%	-61%
5	53.29	44.04	94.96	248.10	-79%	-82%	-62%
10	59.38	47.57	96.96	254.40	-77%	-81%	-62%
<b>Loss Modulus, E'' of Activated, Hydrated Membranes and % Difference from GEFC Membrane</b>							
<b>Freq. (Hz)</b>	<b>Loss Modulus (MPa)</b>				<b>% Difference Hot Pressed &amp; GEFC</b>	<b>% Difference Injection Molded &amp; GEFC</b>	<b>% Difference Extruded &amp; GEFC</b>
	<b>Extruded</b>	<b>Injection Molded</b>	<b>Hot Pressed</b>	<b>GEFC</b>			
1	8.08	4.32	4.87	18.63	-57%	-77%	-74%
2	10.15	5.18	4.77	18.00	-44%	-71%	-74%
5	14.12	6.78	4.81	17.75	-20%	-62%	-73%
10	18.29	8.56	5.05	17.60	4%	-51%	-71%
<b>Damping, tan(δ) of Activated, Hydrated Membranes and % Difference from GEFC Membrane</b>							
<b>Freq. (Hz)</b>	<b>Damping tan(δ)</b>				<b>% Difference Hot Pressed &amp; GEFC</b>	<b>% Difference Injection Molded &amp; GEFC</b>	<b>% Difference Extruded &amp; GEFC</b>
	<b>Extruded</b>	<b>Injection Molded</b>	<b>Hot Pressed</b>	<b>GEFC</b>			
1	0.183	0.112	0.053	0.080	129%	40%	-34%
2	0.214	0.126	0.051	0.075	183%	67%	-32%
5	0.265	0.153	0.051	0.071	272%	115%	-29%
10	0.308	0.179	0.052	0.069	347%	159%	-25%

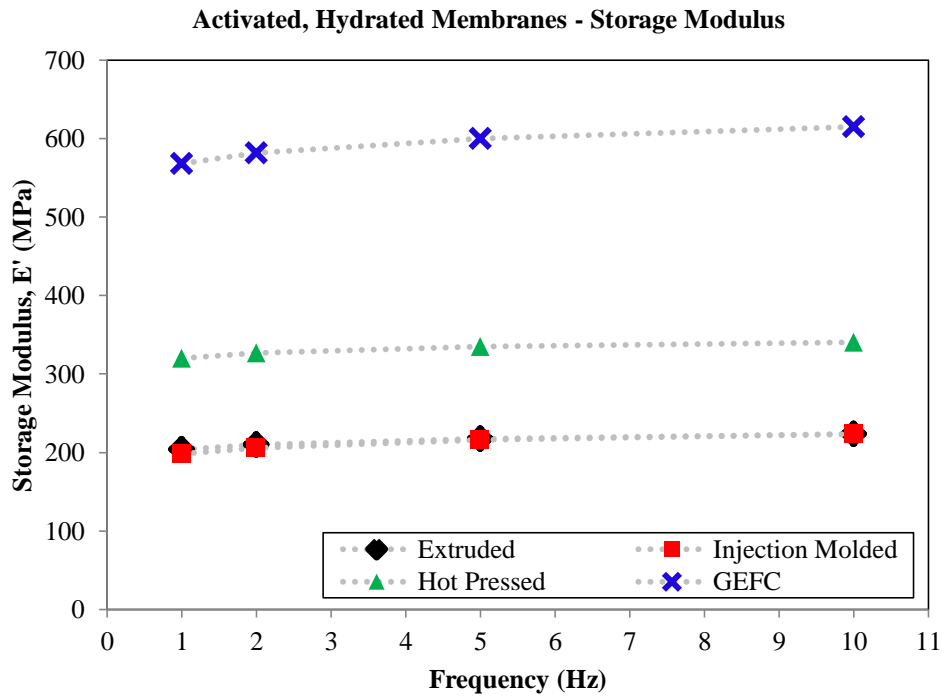


**Figure 3.23: Activated, hydrated membrane - storage modulus, E'**

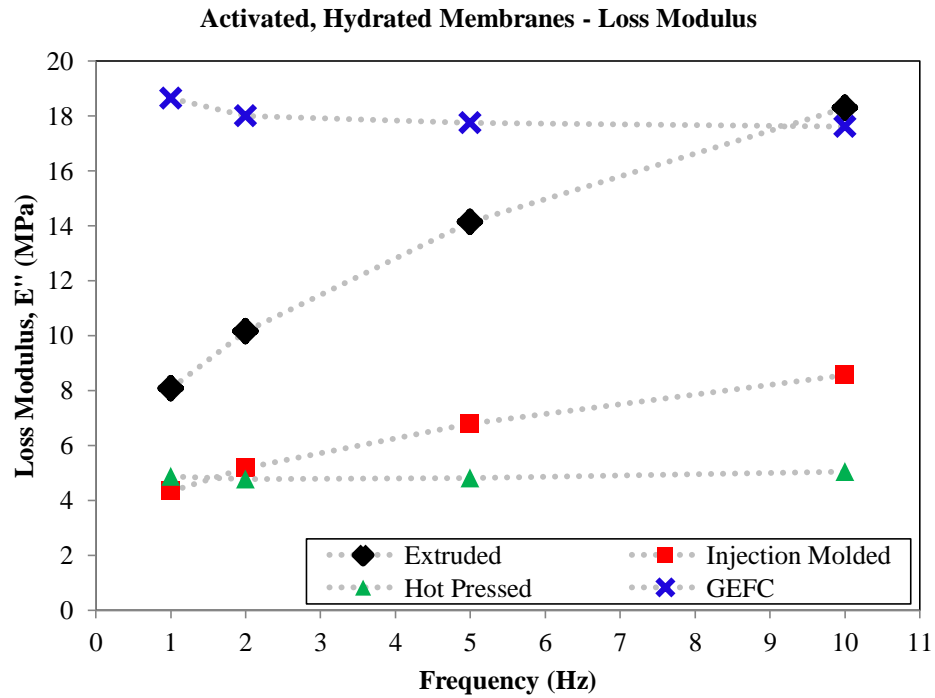


**Figure 3.24: Activated, hydrated membranes - loss modulus, E''**

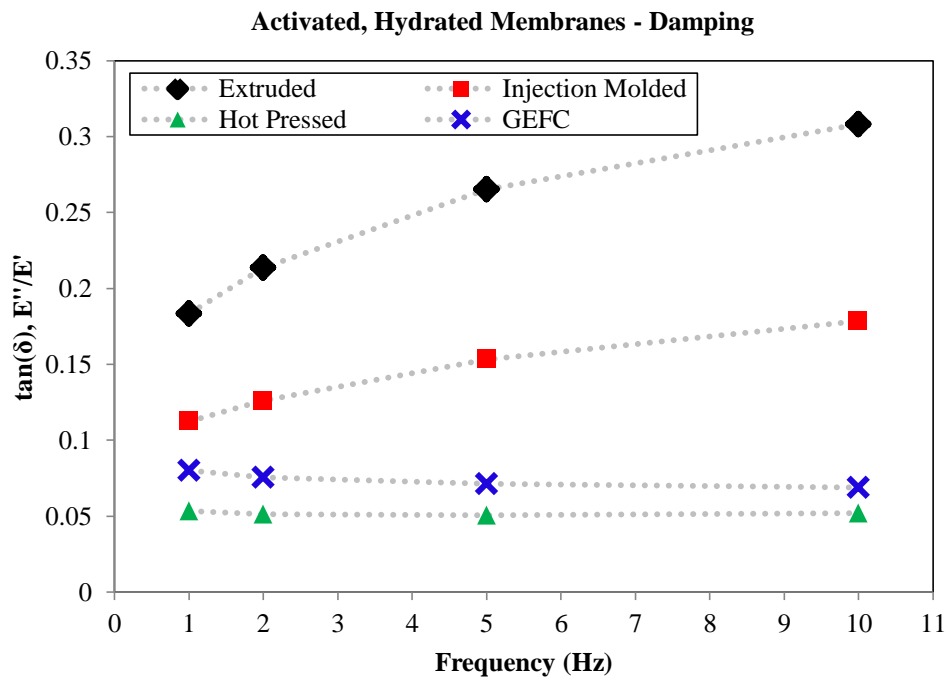


**Figure 3.25: Activated, hydrated membranes - damping,  $\tan(\delta)$**

### 3.6.4 Hot Pressed and GEFC IPMC Results

Figures 3.26-3.28 show the plots of the storage modulus, loss modulus, and damping of the hot pressed and GEFC IPMCs. Table 3.20 summarizes these results. Overall, the loss modulus, storage modulus, and damping increase gradually as the frequency is increased. The hot pressed IPMC has a higher storage and loss modulus than the GEFC membrane. However, the GEFC IPMC has higher damping values than the hot pressed IPMC.

**Table 3.20: Hot Pressed and GEFC IPMC DMA results summary and % Change from GEFC IPMC**

<b>Storage Modulus, E' of IPMCs and % Difference from GEFC Membrane</b>			
<b>Frequency</b>	<b>Storage Modulus (MPa)</b>		<b>% Difference Hot Press &amp; GEFC</b>
	<b>Hot Pressed</b>	<b>GEFC</b>	
1	149.70	131.20	14%
2	151.50	133.00	14%
5	154.20	135.20	14%
10	157.00	137.00	15%
<b>Loss Modulus, E'' of IPMCs and % Difference from GEFC Membrane</b>			
<b>Frequency</b>	<b>Loss Modulus (MPa)</b>		<b>% Difference Extruded &amp; GEFC</b>
	<b>Hot Pressed</b>	<b>GEFC</b>	
1	7.16	6.80	5%
2	7.29	7.04	4%
5	7.74	7.50	3%
10	8.30	8.03	3%
<b>Damping, tan(<math>\delta</math>) of IPMCs and % Difference from GEFC Membrane</b>			
<b>Frequency</b>	<b>Damping tan(<math>\delta</math>)</b>		<b>% Difference Extruded &amp; GEFC</b>
	<b>Hot Pressed</b>	<b>GEFC</b>	
1	0.05	0.05	-8%
2	0.05	0.05	-9%
5	0.05	0.06	-9%
10	0.05	0.06	-10%

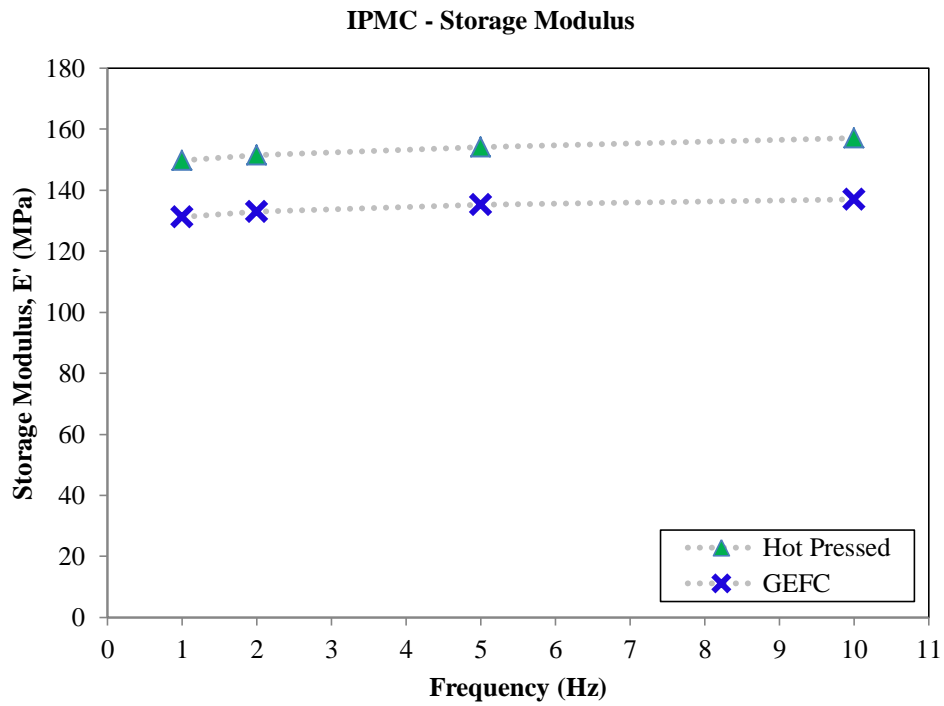


**Figure 3.26: IPMC - storage modulus,  $E'$**

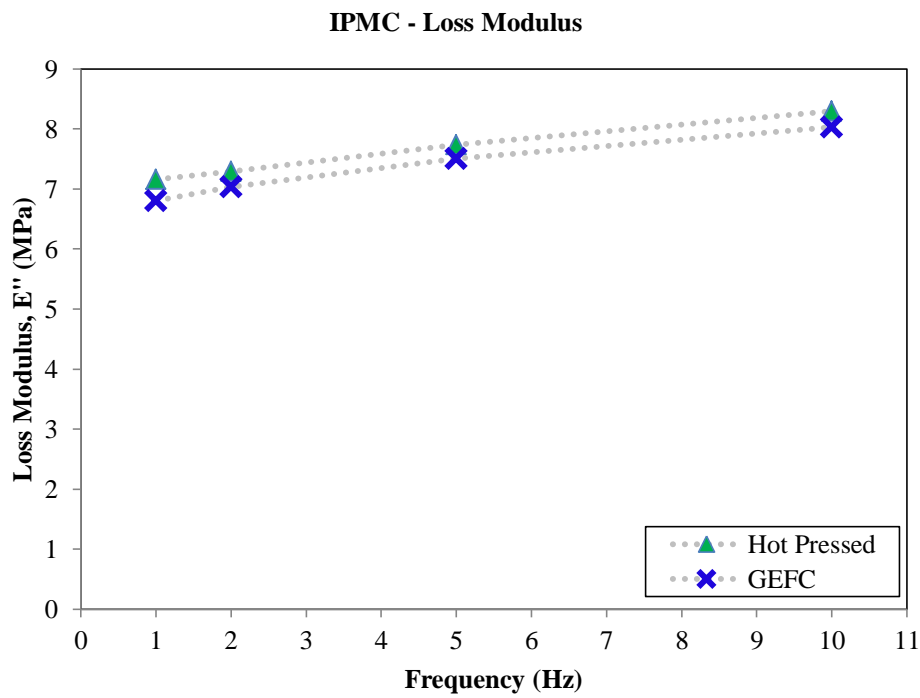


**Figure 3.27: IPMC - loss modulus,  $E''$**

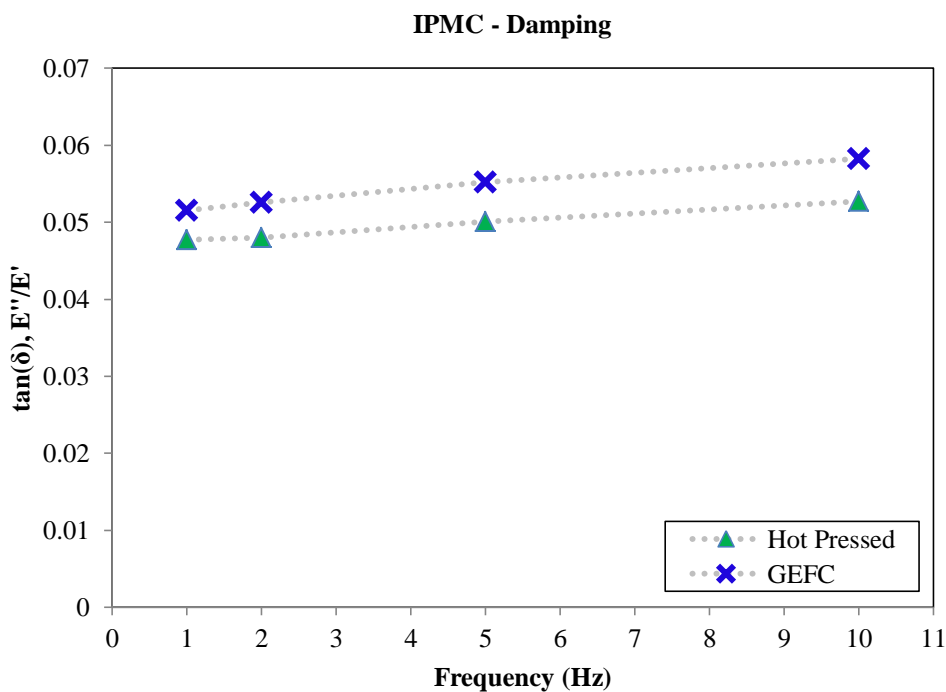


**Figure 3.28: IPMC - damping,  $\tan(\delta)$**

### 3.7 Surface and Cross-sectional Quality

Membrane quality was assessed by examining the visual qualities of the surface and the cross-section of each membrane using the optical microscope. One photo was at 100X magnification and a close up was taken around 1,000X magnification of the surface of the membranes as well as the cross-section. The surface quality was examined and was based on the smoothness of the surface. Bubbles were also looked at in surface view of the membrane. Any noticeable roughness patterns were noted. The cross-section view as also looked at and assessed. The resulting photographs are shown in Figures 3.29 and 3.30 below.

Both the GEFC and the hot pressed IPMCs show scratches in the electrode surface. These scratches are from sanding the membrane before plating them. The scratches appear closer together on the GEFC IPMC while the scratches on the hot



pressed IPMC are further apart and more random. The surface of the hot pressed IPMC in Figure 3.29(c) shows signs of small cracking in the direction perpendicular to the scratches. This will affect the surface conductivity measurement. On the 1,000X magnification of the surface of the IPMCs shown in Figure 3.29(b) and (d), the scratches on the GEFC surface appear to be deeper than the scratches on the hot pressed surface.

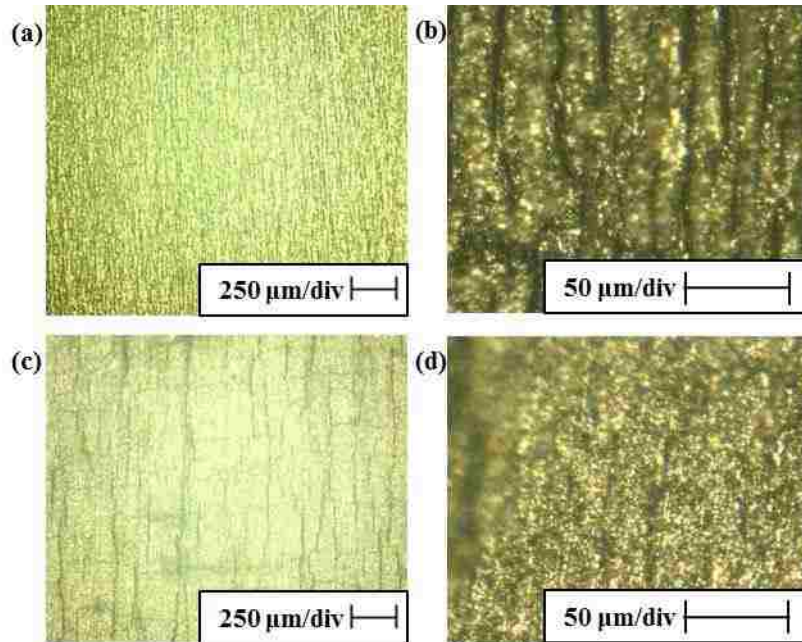


**Figure 3.29: Optical microscope photographs of the surfaces of IPMCs; (a) GEFC at 100X, (b) GEFC at 1,000X, (c) hot pressed at 100X, (d) hot pressed at 1,000X**

Figure 3.30 shows the surface and the cross-section of the activated, hydrated membranes. The hot pressed and GEFC membrane surfaces in Figure 3.30(e) and (g) are more uniform than the surface of the injection molded and extruded membrane in Figure 3.30(a) and (c). This is due to the manufacturing process of the extruded and injection molded membranes. Since the hot pressed membrane is pressed against a smooth surface, it will have a smooth surface after it is processed. The injection molded sample appears to

look very uneven and goopy. Even though it was injected into a mold with a smooth surface, the membrane still has a rough texture.

The cross-sections of the hot pressed and GEFC in Figure 3.30(f) and (h) are more consistent in their texture than the extruded and injection molded in Figure 3.30 (b) and (d). The thickness of the cross-section of the extruded membrane is not uniform. This was to be expected for the extruded membrane because of die swell and inconsistent extrudate drawing. Both the extruded and injection molded cross-sections appear to have layers. This is due to the cooling of the membrane in the manufacturing process. Both the injection molded and extruded membrane cool from the outside in and the polymer consequentially forms in layers.

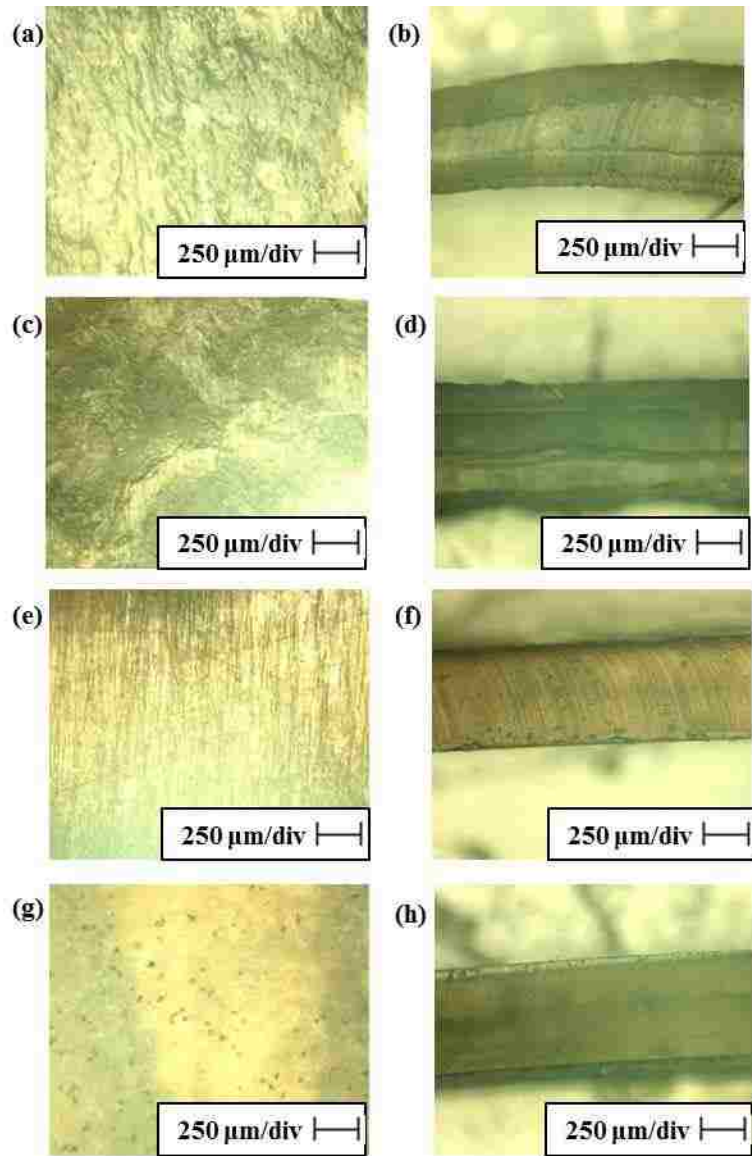


**Figure 3.30: Optical microscope photographs of the surface and cross-section of activated, dehydrated membranes all at 100X; (a) extruded surface, (b) extruded cross-section, (c) injection molded surface, (d) injection molded cross-section, (e) hot pressed surface, (f) hot pressed cross-section, (g) GEFC surface, (h) GEFC cross-section**

### **3.8 Platinum Layer Thickness**

Primary plating was repeated three times and secondary plating was done only once on the GEFC and hot pressed membranes. One of the measures of the success of the plating is the thickness of the layer platinum on the surface of the membrane. To measure the thickness of the platinum layer, the SEM was used because it provides good contrasting photos to clearly see the location of the boundary of the membrane and platinum layer. The samples were prepped first. They were submerged in liquid nitrogen and then the samples were snapped in half by hand in order to get a clean break. If a blade is used to cut the samples, the platinum will become damaged and a good reading will not be possible. The thickness of the platinum layers were measured at five different locations and averaged. The resulting values are summarized in the Table 3.21. The platinum layer thickness measurements are accurate within 1 micron. The photographs of the cross-section of the hot pressed and GEFC IPMC are shown in Figure 3.31. The platinum layer on the GEFC membrane was slightly thicker than the platinum on the hot pressed membrane.

To get a better idea of how much platinum is deposited on the surface, the thickness of the unplated activated, dehydrated membrane was measured. The ratio of the membrane to the thickness of the platinum layer will show a percentage of how much platinum there was deposited on the surface. A summary of these percentages can be seen in Table 3.21. More platinum deposited on the surface along with surface quality means the more conductive the sample will be; however, a thicker layer of platinum will make the membrane more resistive to bending, and it will be stiffer. Both membranes have similar percentage of platinum deposited on the surface of the membrane.

**Table 3.21: Summary of the measured platinum layer thicknesses and the percentage of platinum to membrane**

Platinum Layer Thickness ( $\mu\text{m}$ ) and % Platinum			
Sample	Pt Layer Thickness ( $\mu\text{m}$ )	Average Membrane Thickness ( $\mu\text{m}$ )	% Pt
Hot Pressed	$5.7 \pm 0.23$	530	2.2%
GEFC	$6.3 \pm 1.8$	480	2.6%

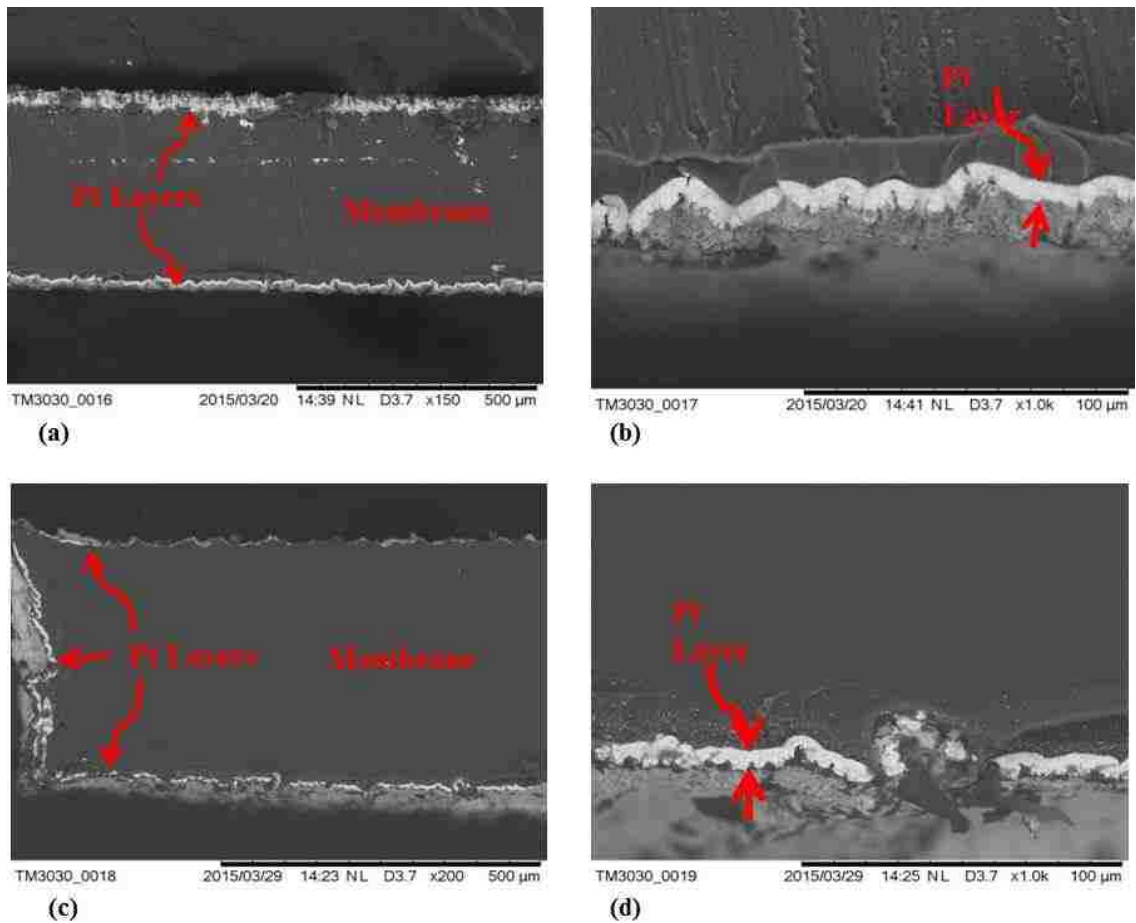


**Figure 3.31: SEM photographs of the cross-section of IPMCs showing the platinum layer; (a) GEFC cross-section at 150X, (b) GEFC cross-section at 1000X, (c) hot-pressed cross-section at 200X, (d) hot-pressed cross-section at 1000X**

### 3.9 Surface Electrode Resistance

The resistance of the surface of the IPMC is measured after the samples are cut into 5 mm x 25 mm strips. Measurements were taken on both sides of the IPMC. The resistance of the samples was measured by how much resistance the sample produced while probing the sample with two probes, one at each of the ends with 25 mm of space between the probes. The measurements were repeated five times each side of the sample. The measurements were averaged on each side of the sample. The resulting measurements are shown in the Table 3.22. A visual representation of this data can be seen in the bar graph in Figure 3.32.

The GEFC membrane had lower surface resistance than the hot pressed membrane for both sides of the membrane. This could be due to the surface sanding of the membrane before the membrane was processed into an IPMC. It could also be due to discrepancies within the processing procedure as well.

For both membranes, one side appears to have a higher resistance than the other side. This is seen more drastically in the hot pressed membrane. This discrepancy between the sides of the IPMC could also be from inconsistency when prepping the surface. This difference in the surface resistance of each side of the membrane might be seen during the IPMC performance tests.

There is also a very large error seen in the back side of the hot pressed membrane. This could be due to the large cracks on the surface of the hot pressed membrane. At each point where the surface resistance was measured with the probes of the multi-meter could be drastically different than the previous spot because of the different size cracks.

**Table 3.22: Surface resistance measurement of each side of the membrane and percent change from GEFC membrane**

Surface Resistance Per Side of Membrane and % Change from GEFC Membrane			
Side of Membrane	GEFC ( $\Omega$ )	Hot Pressed ( $\Omega$ )	% Change
Front	$6.6 \pm 0.8$	$18.5 \pm 5.9$	95%
Back	$4.0 \pm 0.4$	$8.7 \pm 2.3$	74%

**Surface Resistance Per Side of GEFC and Hot Pressed IPMCs**

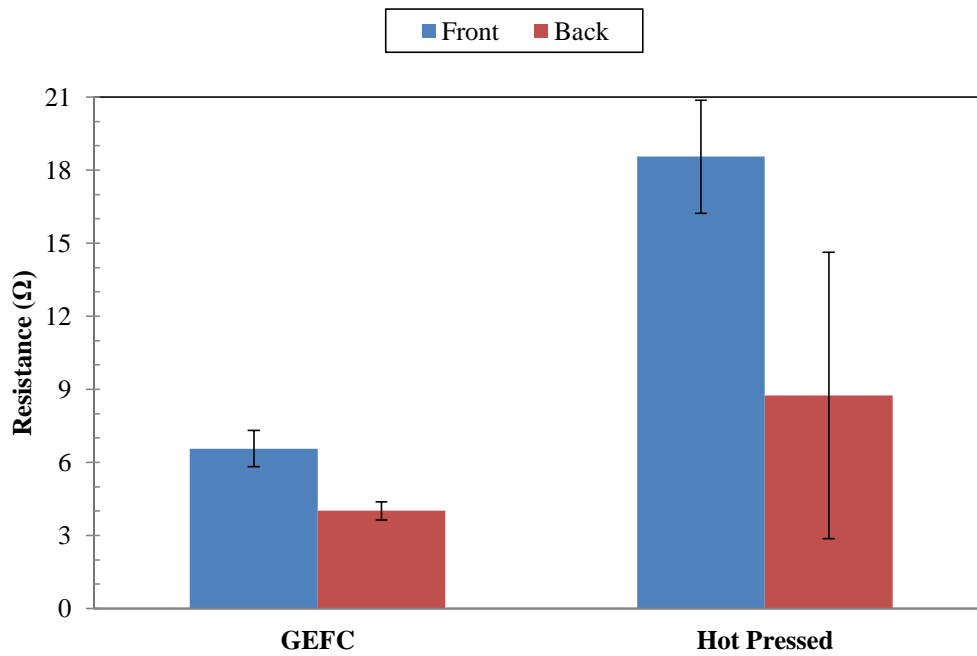


**Figure 3.32: Surface resistance bar graph of the GEFC and hot pressed IPMCs. Each bar represents the front and back sides of the membrane.**

## **CHAPTER 4: IPMC Performance Sensor Test**

The IPMC samples were prepared for testing as sensors. The samples were cut to 10mm x 25 mm strips. One end of the sample was clamped gently in the electrode contacts. 5 mm of the end of the sample was clamped. The other end was fixture to the clamp with the shaker. Again, 5 mm of the sample was clamped. The free length of the sample was 15 mm. The sample was submerged in deionized water during the test. The shaker was programmed to give an amplitude of 3 mm peak to peak for all of the samples. The samples were run at 1 Hz, 5 Hz, and 10 Hz. A displacement laser sensor kept track of the displacement at the tip while the voltage at the clamp was sensed by the circuit and put into LabView. The data was processed using Origin Lab 9.0. A smoothing function was used to reduce sample noise.

A photograph of the experimental set-up is shown in Figure 3.34 below. The equipment that was used is labeled in the figure. The shaker is an electrodynamic shaker (VR-5200) which oscillates the tip of the IPMC. The displacement of the tip is sensed by a laser displacement sensor (optoNCDT-1401, Micro-Epsilon). The voltage produced by the IPMC is measured at the electrode contact clamp, the signal output is amplified by a custom amplifier circuit, and the signal data is recorded using LabVIEW with National Instruments USB-6008.



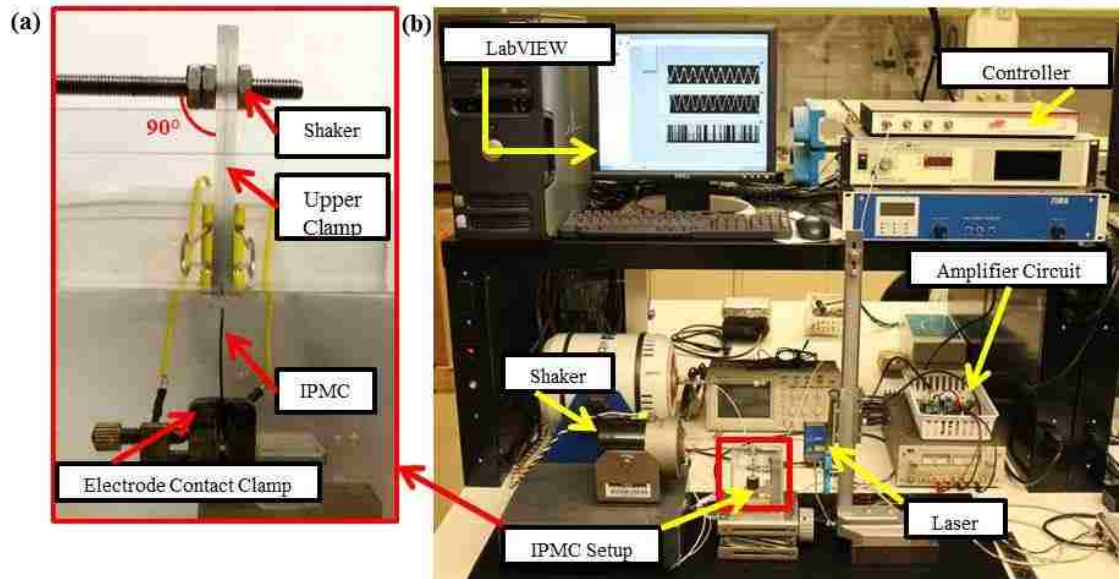


**Figure 4.1: Experimental set up for IPMC sensor; (a) IPMC clamped in electrode contact clamp and shaker submerged in deionized water, (b) complete experimental set-up of IPMC sensor test**

Figures 4.2 – 4.7 show the voltage and displacement plots of the GEFC and hot pressed membranes tested as sensors. Figures 4.2 – 4.4 are the GEFC sensor results, and Figures 4.5 – 4.7 are the hot pressed IPMC sensor results. The GEFC IPMC voltage signal is very noisy at lower frequencies. At lower frequencies the voltage signal produced is less than the signal produced at higher frequencies.

The signal at lower frequencies is also very noisy compared to the signal produced at higher frequencies. This is due to the cation migration inside the membrane. At lower frequencies the cations are allowed more time to move towards the location where the anions are concentrated. The voltage measured is the difference in charge between the cations and anions. Since there is more time for the cations to travel towards the anions, the cations are able to affect the signal more so than at higher frequencies. Since the cation motion is chaotic inside the membrane, a noisy signal is produced. Overall, at low frequencies, the cations are the dominant factor affecting the signal.

At higher frequencies, the cations play a less significant role. The anions are now the dominant force. At higher frequencies, the cations are able to travel less distance through the membrane. The cations still want to travel towards the anions; however, they do not travel very far at high frequencies. Since they barely move within the membrane, there are less cations to cancel the charge of the anions. The anions are now the main contributor to the signal. Since they are fixed to the polymer chains, they move with the membrane as it bends. Their motion is less chaotic which produces a strong signal with little noise. This can be seen in Figure 4.3 and 4.7 with both the GEFC and hot pressed membranes oscillating at 10 Hz.

There is a phase shift that occurs with both the GEFC and hot pressed IPMC. The voltage signal for both the GEFC and hot pressed membranes appear to be more linear than sinusoidal. The voltage signal (red dots) seems to lead the displacement signal (black dots) for the GEFC test at 1 Hz, 5 Hz, and 10 Hz (Figures 4.2-4.4 respectively). The time interval between the peaks of the voltage and displacement signal is about 0.25 s, 0.020 s, and 0.0030 s for 1 Hz, 5 Hz, and 10 Hz tests respectively.

The hot pressed IPMC also has a phase shift where the time interval between the peaks of the voltage and displacement signal is 0 s, -0.040 s, and 0.0025 s for the 1 Hz, 5 Hz, and 10 Hz tests respectively. The time interval for the 5 Hz test is negative because the voltage signal lags behind the displacement signal where the voltage signal is leading the displacement signal for the positive time intervals. There does not seem to be a signal delay between voltage and displacement for the hot pressed membrane at 1 Hz.

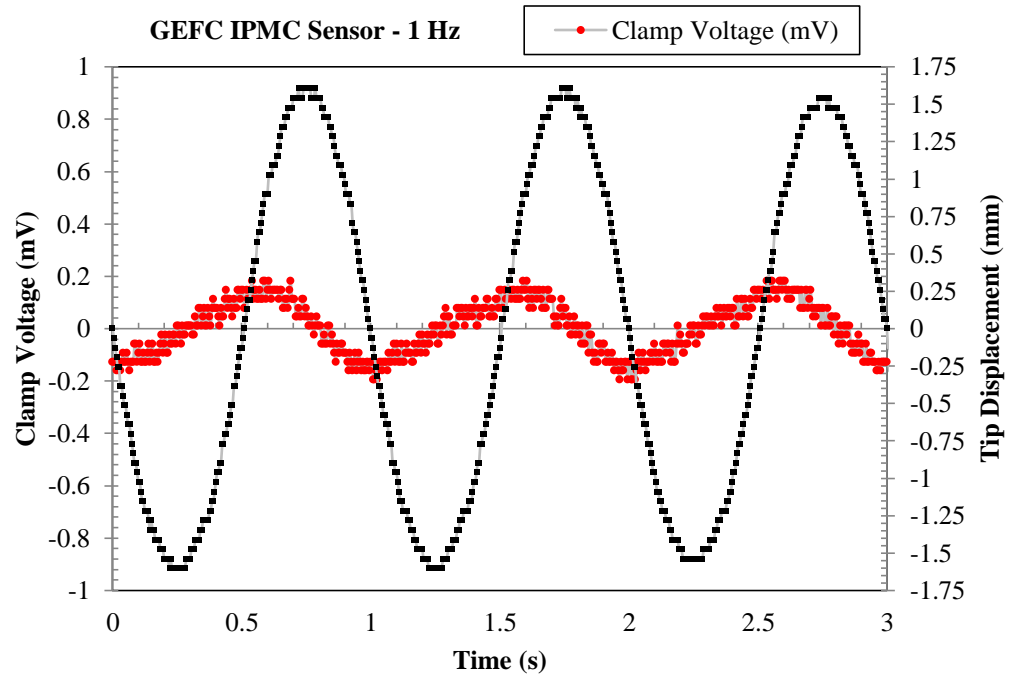
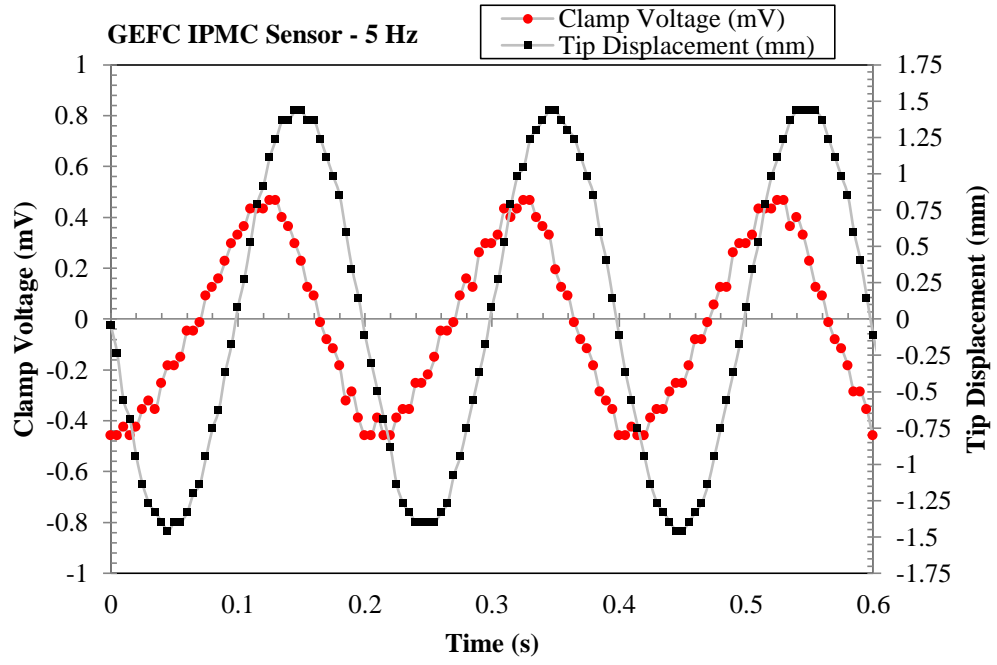
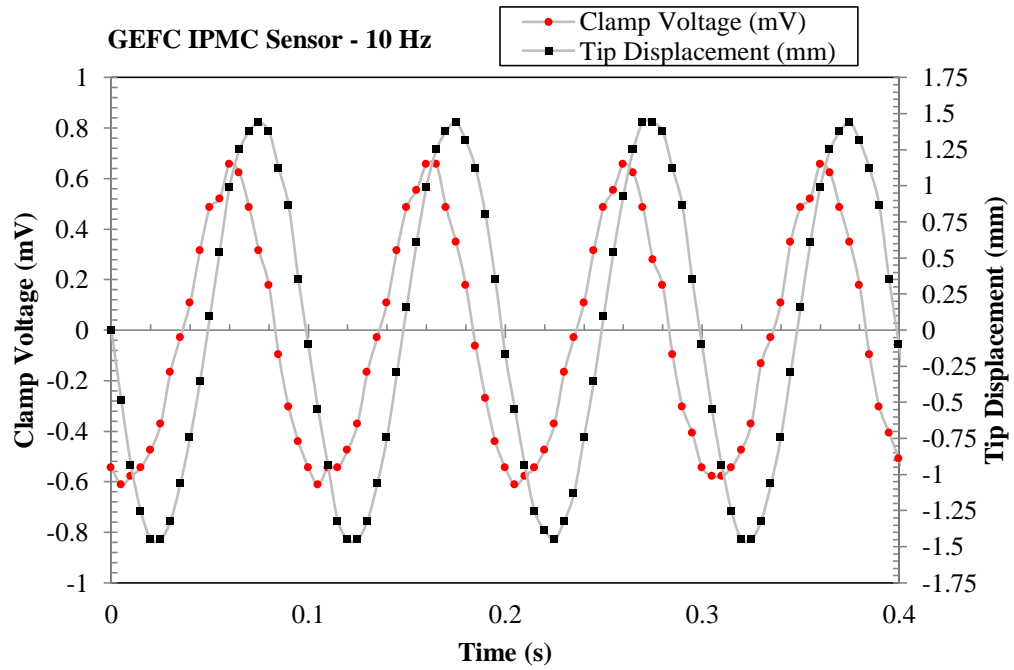


Figure 4.2: GEFC IPMC sensor data at 1 Hz and 3 mm peak to peak displacement



**Figure 4.3: GEFC IPMC sensor data at 5 Hz and 3 mm peak to peak displacement**



**Figure 4.4: GEFC IPMC sensor data at 10 Hz and 3 mm peak to peak displacement**

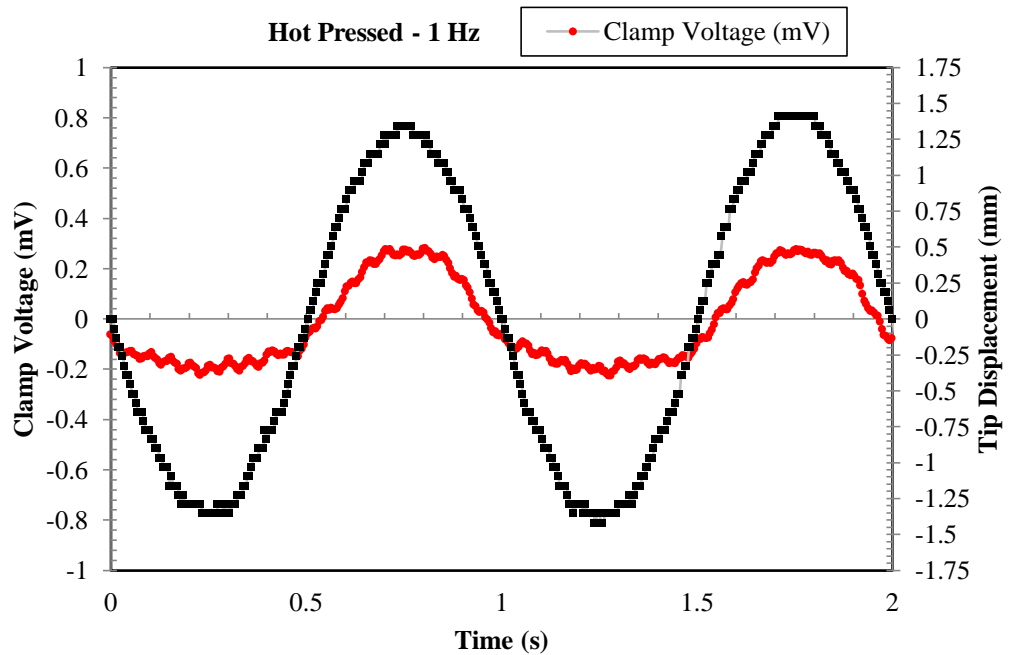


**Figure 4.5: Hot pressed IPMC sensor data at 1 Hz and 3 mm peak to peak displacement**

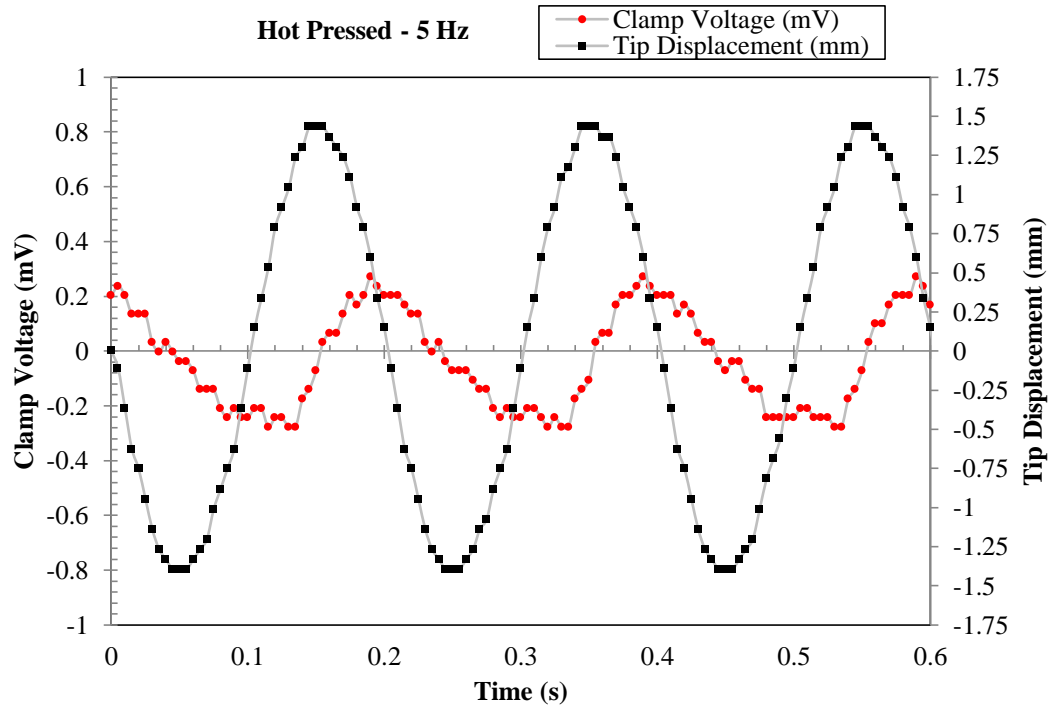


Figure 4.6: Hot pressed IPMC sensor data at 5 Hz and 3 mm peak to peak displacement

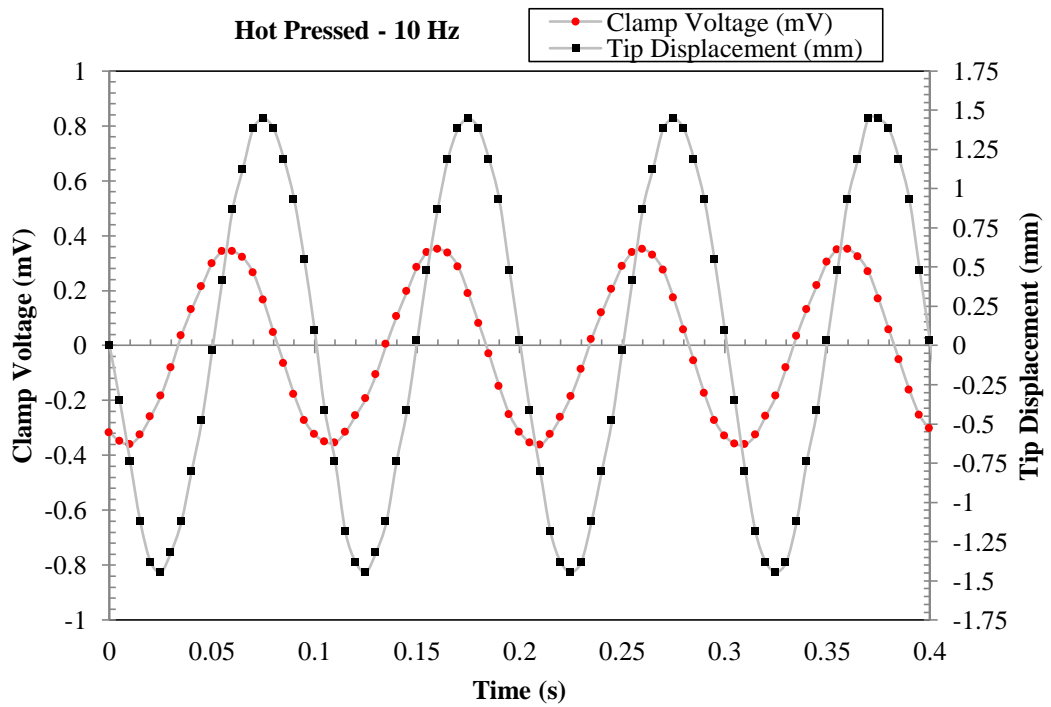


Figure 4.7: Hot pressed IPMC sensor data at 10 Hz and 3 mm peak to peak displacement

Table 3.23 summarizes the maximum voltage of the hot pressed and GEFC IPMCs. The more voltage the sensor produces, the better the sensor is at performing. The voltages are absolute values. Although the signal was more erratic, the maximum value of the voltage of the hot pressed IPMC is 64% higher than the GEFC IPMC at 1 Hz. However, as the frequency increased to 5 Hz and 10 Hz, the GEFC IPMC had higher maximum values of voltage than the hot pressed membrane. At higher frequencies, the GEFC IPMC is the better performing IPMC sensor.

**Table 4.1: Summary of the average absolute value of the maximum voltage and % change from the GEFC IPMC**

<b>Average Absolute Value of Maximum Voltage (mV) and % Change of Hot Pressed to GEFC</b>			
<b>Frequency (Hz)</b>	<b>Max Voltage (mV)</b>		<b>% Change</b>
	<b>Hot Pressed</b>	<b>GEFC</b>	
1	0.29	0.18	64%
5	0.31	0.46	-33%
10	0.36	0.60	-40%



## CHAPTER 5: Conclusion and Recommendations for Future Study

Multiple options for fabricating Nafion<sup>®</sup> membranes for use in IPMC sensor applications were demonstrated in this project: extrusion, injection molding, and hot pressing. A commercial membrane from GEFC was also used to compare with the custom fabricated membranes. GEFC and hot pressed membranes were able to be processed into IPMCs while the extruded and injection molded membranes failed during the reduction reaction. Extruded and injection molded membranes were able to be manufactured and activated to the hydrogen cation form, so tests were able to be done on these membranes up until this step. It is feasible to fabricate Nafion<sup>®</sup> membranes through injection molding, extrusion, and hot pressing. However, more work to increase the pressure of the injection molder and to automate the extrusion drawing process would improve the processes.

Multiple tests were done on the extruded, injection molded, hot pressed, and GEFC membranes to examine their properties throughout the different stages of IPMC processing. The first stage is the pre-activated membrane made from the Nafion<sup>®</sup> precursor pellet. Only the extruded and injection molded membranes were made from the precursor pellet. The next stage is the activated membrane with the hydrogen cation where the membrane can be dehydrated or hydrated. All membranes were able to reach this stage with the hot pressed and GEFC membranes already residing in this stage. The last stage is the final IPMC form where the membrane is hydrated and chemically plated with platinum. Only the hot pressed and GEFC membranes were able to reach this stage.

Throughout the different processing stages, the stiffness of the membranes were affected. The stiffest membrane was the GEFC membrane in its dehydrated activated

form. The hot pressed membrane was the second stiffest membrane in the tensile tests and dynamic mechanical analysis. The least stiff membranes were the extruded and injection molded membranes. These membranes usually were very similar in stiffness. This pattern was seen throughout the tensile tests as well as the dynamic mechanical analysis.

The hot pressed and GEFC membranes were processed into IPMCs and were tested as sensors. Overall, the GEFC IPMC gave a stronger voltage output while the hot pressed IPMC was weaker. Both signals had noise at the lower frequencies caused by the cation dominance during low frequencies.

Overall, the hot pressed and GEFC membranes are able to be used as IPMC sensors currently while the extruded and injection molded membranes still need more development within the manufacturing process.

## **5.1 Recommendation for Future Work**

More development in the extrusion and injection molding membrane manufacturing processes is needed to be able to use these membranes as IPMC sensors. The extrusion process needs to be automated to reduce the large variances in cross-sectional thicknesses. The membranes should be cooled as soon as they leave the extruder die. This will prevent the formation of cooling layers in the membrane. Any non-uniformity within the membrane is a potential failure in the reduction process.

The injection molding process needs modifications as well. More pressure is needed to inject the viscous Nafion<sup>®</sup> melt into the small cavity of the mold. More injection pressure will fill the mold quicker and will minimize the cooling layer formation. The more uniform the membrane, the more likely it will survive the reduction

reaction in primary plating because the platinum particles will be able to reach the surface of the membrane without any layers blocking the path.

Most importantly, a more cost effective method to characterize the membranes should be developed. More samples need to be tested to provide a better understanding of whether these properties are repeatable and are reliable. Since the material is expensive, more attention to the property testing should be paid in order to maximize sample usage and minimize wasted samples.

The test that used the most samples was the tensile test. Because of cost and the limited sample availability, the tensile test was only performed with one sample. The DMA tests were also performed with one sample for the same reasons. To show the problem with using only one sample, Table 5.1 was constructed to show the discrepancy between values of the storage modulus taken at 1 Hz from the DMA and the elastic modulus measured from the stress-strain curve from the tensile test.

Table 5.1 shows the storage moduli of each sample were significantly higher than the elastic moduli. This could be due error introduced in the experimental setup, i.e. specimen alignment within the tensile machine. However, this discrepancy is primarily due to relying on the displacement outputted by the tensile machine to calculate strain. In the strain calculation, it is assumed that the displacement is only occurring within the gauge length. When in reality, the displacement could be occurring at the larger cross-sectional area in the dog bone tabs at the end of each sample. This could give a higher strain rate than what is actually occurring within the gauge section, as well as a higher elastic modulus.

It is recommended that the future researcher use a laser extensometer to measure the displacement of the gauge section of each sample. It is also recommended that the next research make a custom jig to align each sample straight and consistently.

**Table 5.1: Storage modulus vs. elastic modulus and a % difference calculation**

<b>Storage Modulus (DMA) vs. Modulus of Elasticity (Tensile Test) with Respect to Process Stage</b>				
<b>Process Stage</b>	<b>Fabrication Process</b>	<b>Storage Modulus, DMA (MPa)</b>	<b>Modulus of Elasticity Tensile (MPa)</b>	<b>% Difference</b>
Pre-activated	Extruded	7.8	2.5	103%
	Injection Molded	8.9	3.0	99%
Activated, Hydrated	Extruded	44.0	6.8	146%
	Injection Molded	38.5	4.8	156%
	Hot Pressed	91.5	35.7	88%
	GEFC	231.9	98.0	81%
Activated, Dehydrated	Extruded	204.1	18.2	167%
	Injection Molded	198.4	18.0	167%
	Hot Pressed	320.3	133.7	82%
	GEFC	568.2	317.9	56%
IPMC	Hot Pressed	149.7	31.6	130%
	GEFC	131.2	44.3	99%

This thesis was able to determine whether these custom manufacturing processes are even feasible for IPMC membrane fabrication. Although there can be some room for improvement within processes and testing procedures, this study gives a good starting point for the researcher interested in developing their own membranes without having to rely on the limited commercial product.

## **APPENDIX A: Error Discussion for the Tensile Tests**

Since there was only one sample tested in the tensile testing, there is an error in the results that must be considered. Normally, as stated by ASTM D790, there must be at least six samples tested to gain an understanding of the behavior of the specimen. Since material cost and availability was strictly limited for this experiment, only one sample was tested to conserve the material for other tests.

The modulus of elasticity was calculated for the first initial linear section of each sample was calculated by dividing the stress by the strain. This calculation was performed for data points until 1% strain (0.10 mm/mm). This resulted in about 10-15 data points to analyze. The calculated values of modulus of elasticity were averaged to get the final modulus of elasticity of the material. The standard deviation of these values was also taken. Using the standard deviation, the standard error was also calculated for the averaged modulus of elasticity. This was the expected range of modulus of elasticity for the material.

Table A.1 summarizes the average modulus of elasticity of all the membranes in each different process stage. The standard deviation and the standard error are shown for all samples. These two numbers were calculated using the method described above. Except for the injection molded samples, the standard deviation seemed to get larger with the increasing stiffness of the material giving a higher standard error. This could be due to the steep initial slope of the elastic region of the samples. When the modulus of elasticity is calculated, the steep slope changes throughout the data points selected resulting in a higher standard deviation and standard error.

**Table A.1: Summary of the modulus of elasticity with respect to process stage**

<b>Tensile Test Modulus of Elasticity with Respect to Process Stage</b>				
<b>Process Stage</b>	<b>Fabrication Process</b>	<b>Average Modulus of Elasticity (MPa)</b>	<b>Standard Deviation (MPa)</b>	<b>Standard Error (MPa)</b>
Pre-activated	Extruded	2.4	0.1	0.02
	Injection Molded	3.0	0.1	0.02
Activated, Hydrated	Extruded	6.8	2.3	0.4
	Injection Molded	4.8	0.3	0.05
	Hot Pressed	35.7	2.9	0.5
	GEFC	98.0	11.8	1.6
Activated, Dehydrated	Extruded	18.2	1.9	0.3
	Injection Molded	18.0	0.2	0.1
	Hot Pressed	133.7	18.2	2.9
	GEFC	317.9	67.2	8.9
IPMC	Hot Pressed	31.6	5.8	1.1
	GEFC	44.3	3.8	0.7

## **APPENDIX B: Extrusion and Injection Molding Challenges**

The extrusion and injection molded samples were not successfully plated with platinum to produce a functioning IPMC. The problems arose at first during the cleaning process after activation. When the membranes were placed in the heated hydrogen peroxide solution, they began to bubble profusely, more than normal. After about 20 minutes in the solution, the membranes had gas bubbles in them. Some bubbles were small at about 2 mm in diameter where other membranes were rather large, about 20 mm in diameter.

The first response to these bubbles was that the membranes had specs of contamination in them causing the hydrogen peroxide to react with these dirt particles resulting in a gas bubble formation. These specs of contamination were thought to be from the initial manufacturing process of the membrane. Since the injection molder was outfitted to both injection mold and extrude, dirt in the injection chamber was thought to be the cause of the contaminated membranes.

Both the injection chamber and the plunger were cleaned thoroughly between both the extrusion and the injection molding process. The stainless steel chamber was cleaned using a wire brush to clean debris out and to polish the chamber. The plunger was cleaned with a Scotch Brite pad. Once cleaned, both the injection chamber and plunger were wiped with ethanol and were allowed to dry. The nozzle was also cleaned with a wire brush, flushed with ethanol, and was allowed to dry.

Once all the parts of the machine that touches the polymer were cleaned, they were assembled, and the machine was heated up to processing temperature to allow all the components to thoroughly dry. Clean Nafion<sup>®</sup> precursor pellets were placed within

the injection chamber, and the manufacturing commenced. New pellets were used to make these membranes to reduce the risk of contamination caused by reusing the once melted Nafion<sup>®</sup>. Based on experience during this experiment, it is recommended that the Nafion<sup>®</sup> precursor pellets are used only once. If the Nafion<sup>®</sup> is reused after melting it once, the polymer starts to degrade and the risk for contamination of the membrane due to small burnt particles is greater.

The resulting membranes appeared much cleaner. They were clearer and had less specs. However, there were still some specs present, but not as much as when the machine was not cleaned. The machine must be cleaned after each processing use or after the polymer has been sitting at processing temperature for a long time. The polymer starts to break down and appear dark brown in color. There were also a lot of specs present in the membranes.

After activating the new membranes, they were cleaned in the heated hydrogen peroxide solution and a couple of baths in deionized water. They survived the cleaning with no bubbles present. Paying careful attention to the cleanliness of the manufacturing process to prevent contamination seemed to have been successful. However, more bubbles reappeared during the first half of the primary plating process.

About an hour into the reduction reaction, the first step in the primary plating process, large bubbles reappeared in both the extruded and injection molded membranes. The injection molded samples had larger bubbles in them than the extruded membranes. The injection molded membranes formed gas pockets that filled almost the whole sample causing the membrane to float. The extruded samples had smaller round bubbles. These bubbles can be seen in Figure B.1.





**Figure B.1: (a) Injection molded samples with air pockets, (b) injection molded sample inside air pocket, (c) extruded samples with air pockets, (d) close up of extruded samples**

More investigation was done to find out why these bubbles occurred during the plating process. The surface of these samples was examined using the optical microscope. Figure B.2 shows the photographs of the surface of the samples. The samples do not appear to have any obvious grain marks from sanding even though these membranes were sanded before they were plated. Both surfaces look pitted with small indentations. These small holes on the surface of the membrane are caused by the manufacturing processes of the membrane. When the heated Nafion<sup>®</sup> is cooled during the extrusion or injection process, parts of the surface seem to cave in on itself due to inconsistencies in the polymer causing the small indentations on the surface of the membrane.

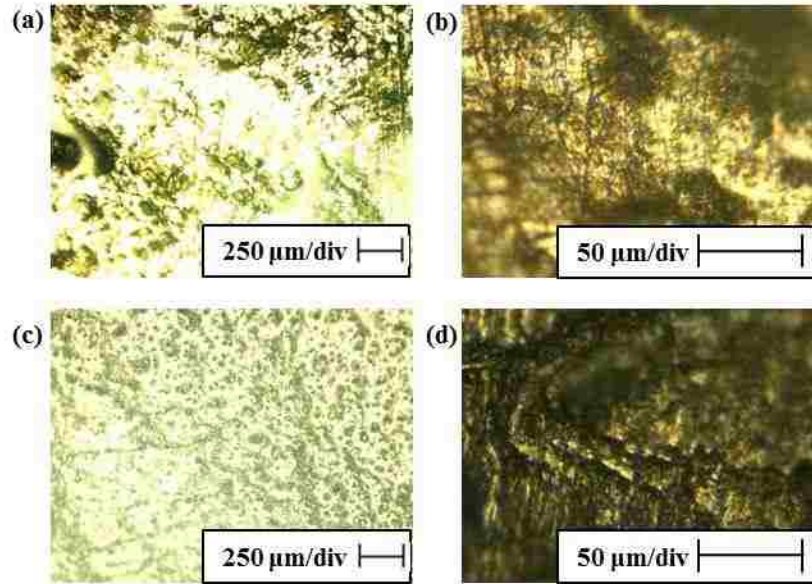


**Figure B.2: (a) Plated surface of extruded sample at 100X, (b) plated surface of extruded sample at 1000X, (c) plated surface of injection molded sample at 100X, (d) plated surface of injection molded sample at 1000X**

The cooling process during the manufacturing process of both the extrusion and injection molding manufacturing processes is also suspected to make the membrane more prone to gas bubble formation. Figure B.3 below is a photograph of the cross-section of the injection molded and extruded samples right after the bubbles formed during primary plating.

The injection molded membrane appears to have been formed in layers. The layers are more pronounced in the injection molded sample because of the cooling process in the mold during manufacturing. Even though the mold is preheated to help the viscous flow of the polymer traverse the mold, the polymer still cools from the outside in causing obvious boundaries to form during each cooling phase. Each time the layers build up, the polymer is forced through a smaller opening causing harsh boundaries to form.

The extruded membrane forms bubble in a similar way. The extrudate is cooled by the ambient air surrounding it as it exits the die. This causes the polymer to cool from

the outside in just like in the injection molded sample except. Since the extrudate leaves the die slowly and with a pressure held constant for a long time, the polymer cools more evenly and at a slower rate causing less obvious layers to form in the polymer.

During the impregnation of platinum in the membrane, it is suspected that these layers in both of the membranes cause the platinum to be unevenly distributed throughout the membrane. When the reduction reaction occurs, these boundaries stop platinum from being pulled to the surface of the membrane. The reaction now sits at these boundary layers in the membrane causing gas to be released into the membrane itself. The membrane contains this gas causing the bubble formations.

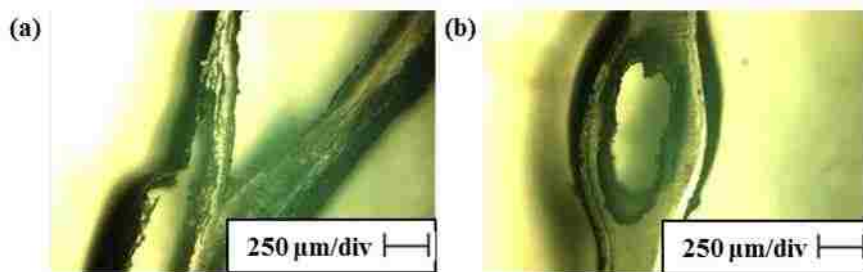


**Figure B.3: (a) injection molded sample cross-section at bubble location, (b) extruded sample cross-section at bubble location**

To combat these negative results, the manufacturing process of both the extrusion and injection molding must be redesigned. The injection molding process requires more pressure to injection the polymer quickly into the mold to reduce the thick cooling layers from forming. More pressure can be achieved by reducing the diameter of the plunger and the injection chamber. To reduce the bubble formation in the extruded membrane, it is recommended that the extrudate should be cooled rapidly after exiting the die. This can be done by setting up a rig where the extrudate passes through cool water after it is extruded.

Another investigation of the hydrolysis procedure to activate the membranes must also be considered. The injection molded and extruded membranes in this thesis were hydrolyzed for 3 hours. This may not be enough time for the KOH and DMSO to reach the entire thickness of the membrane.

## REFERENCES

- [1] V. Palmre, D. Pugal, K. J. Kim, K. K. Leang, K. Asaka, and A. Aabloo, “Nanohorn electrodes for ionic polymer-metal composite artificial muscles,” *Sci. Rep.*, vol. 4, p. 6176, Jan. 2014.
- [2] M. Shahinpoor and K. J. Kim, “Ionic polymer – metal composites: I . Fundamentals,” *Smart Mater. Struct.*, vol. 10, pp. 819–833, 2001.
- [3] C. Jo, D. Pugal, I. K. Oh, K. J. Kim, and K. Asaka, “Recent advances in ionic polymer-metal composite actuators and their modeling and applications,” *Prog. Polym. Sci.*, vol. 38, no. 7, pp. 1037–1066, 2013.
- [4] J. Park, “Ionic Polymer-Metal Composites (IPMCs) with Various Ion Exchange Membranes and Their Potential Use in IPMC Applications,” University of Nevada, Reno, 2012.
- [5] K. Fukushima, S. Takizawa, K. Hinokuma, A. Nishimoto, and K. Noda, “Ion-Dissociative Functional Compound, Method for Production thereof, Ionic Conductor, and Electrochemical Device,” 2011.
- [6] S.-M. Kim and K. J. Kim, “Palladium buffer-layered high performance ionic polymer–metal composites,” *Smart Materials and Structures*, vol. 17, no. 3. p. 035011, 2008.
- [7] C. K. Chung, P. K. Fung, Y. Z. Hong, M. S. Ju, C. C. K. Lin, and T. C. Wu, “A novel fabrication of ionic polymer-metal composites (IPMC) actuator with silver nano-powders,” *Sensors Actuators B Chem.*, vol. 117, no. 2, pp. 367–375, Oct. 2006.
- [8] V. Palmre, E. Lust, A. Jänes, M. Koel, A.-L. Peikolainen, J. Torop, U. Johanson, and A. Aabloo, “Electroactive polymer actuators with carbon aerogel electrodes,” *J. Mater. Chem.*, vol. 21, no. 8, p. 2577, 2011.

- [9] F. Kaasik, J. Torop, I. Must, E. Soolo, I. Põldsalu, A.-L. Peikolainen, V. Palmre, and A. Aabloo, "Ionic EAP transducers with amorphouse nanoporous carbon electrodes," in *Proceedings of SPIE - The International Society for Optical Engineering*, 2012, vol. 8340, p. 83400V–83400V–8.
- [10] R. Tiwari and E. Garcia, "The state of understanding of ionic polymer metal composite architecture: a review," *Smart Mater. Struct.*, vol. 20, no. 8, p. 083001, Aug. 2011.
- [11] L. Shen, Y. Cha, A. Shams, and M. Porfiri, "Fabrication and buckling analysis of ionic polymer metal composite pipes," *Smart Mater. Struct.*, vol. 22, no. 10, p. 105032, Oct. 2013.
- [12] Y. Wang, H. Chen, Y. Wang, J. Liu, and D. Li, "Manufacturing Process for Patterned IPMC Actuator with Millimeter Thickness," pp. 235–239, 2013.
- [13] H. Lei, W. Li, and X. Tan, "Microfabrication of IPMC cilia for bio-inspired flow sensing," vol. 8340, p. 83401A–83401A–9, 2012.
- [14] I. Dominik, J. Kwaśniewski, and F. Kaszuba, "Application of the Ionic Polymer-Metal Composite Sensor Array Indisplacement Measurement," *Key Eng. Mater.*, vol. 605, pp. 396–399, 2014.
- [15] J. Zhong, D. L. S. Hung, G. Zhu, and X. Tan, "Cycle-to-cycle response of ionic polymer-metal composite materials subject to pulsing flow-induced stimulus," *IEEE/ASME Int. Conf. Adv. Intell. Mechatronics, AIM*, pp. 432–437, 2012.
- [16] D. J. Griffiths, "Development of Ionic Polymer Metallic Composites as Sensors," Virginia Polytechnic Institute and State University, 2008.
- [17] B. Andò, S. Baglio, A. Beninato, S. Graziani, F. Pagano, and E. Umama, "A seismic sensor based on IPMC combined with ferrofluids," *IEEE Trans. Instrum. Meas.*, vol. 62, no. 5, pp. 1292–1298, 2013.

- [18] DuPont, “DuPont Nafion Membranes and Dispersions,” 2015. [Online]. Available: [http://www2.dupont.com/FuelCells/en\\_US/products/nafion.html](http://www2.dupont.com/FuelCells/en_US/products/nafion.html). [Accessed: 04-Apr-2015].
- [19] Ion Power, “NAFION R-1100 and R-1000 Precursor Beads.” [Online]. Available: [http://www.ion-power.com/res/Nafion\\_and\\_XL\\_MEA/R1000\\_R1100\\_Bulletin\\_May2013.pdf](http://www.ion-power.com/res/Nafion_and_XL_MEA/R1000_R1100_Bulletin_May2013.pdf). [Accessed: 12-Apr-2015].
- [20] Ion Power, “Nafion Products Listing,” *Ion Power, Inc Nafion Products*, 2013. [Online]. Available: <http://www.ion-power.com/nafionproducts.html>. [Accessed: 01-Jan-2015].
- [21] R. . Silva, M. De Francesco, and a Pozio, “Solution-cast Nafion® ionomer membranes: preparation and characterization,” *Electrochim. Acta*, vol. 49, no. 19, pp. 3211–3219, Aug. 2004.
- [22] G. Gebel, P. Aldebert, and M. Pineri, “Structure and Related Properties of Solution-Cast Perfluorosulfonated Ionomer Films,” *Macromolecules*, vol. 20, pp. 1425–1428, 1987.
- [23] K. Kim and M. Shahinpoor, “Development of three-dimensional polymeric artificial muscles,” in *SPIE’s 8th ...*, 2001.
- [24] K. Kim, “A novel method of manufacturing three-dimensional ionic polymer–metal composites (IPMCs) biomimetic sensors, actuators and artificial muscles,” *Polymer (Guildf)*., vol. 43, no. 3, pp. 797–802, Feb. 2002.
- [25] R. B. Moore, K. M. Cable, and T. L. Croley, “Barriers to flow in semicrystalline ionomers. A procedure for preparing melt-processed perfluorosulfonate ionomer films and membranes,” *J. Memb. Sci.*, vol. 75, no. 1–2, pp. 7–14, Dec. 1992.
- [26] S. J. Lee, M. J. Han, S. J. Kim, J. Y. Jho, H. Y. Lee, and Y. H. Kim, “A new fabrication method for IPMC actuators and application to artificial fingers,” *Smart Mater. Struct.*, vol. 15, no. 5, pp. 1217–1224, 2006.

- [27] C. Bonomo, M. Bottino, P. Brunetto, G. Di Pasquale, L. Fortuna, S. Graziani, and a Pollicino, “Tridimensional ionic polymer metal composites: optimization of the manufacturing techniques,” *Smart Mater. Struct.*, vol. 19, no. 5, p. 055002, 2010.
- [28] T. Stalbaum, S. E. Nelson, V. Palmre, and K. J. Kim, “Multi degree of freedom IPMC sensor,” vol. 9056, p. 90562J, 2014.
- [29] S. Ruiz, B. Mead, V. Palmre, K. J. Kim, and W. Yim, “Corrigendum: A cylindrical ionic polymer-metal composite-based robotic catheter platform: modeling, design and control (2015 Smart Mater. Struct. 24 015007),” *Smart Mater. Struct.*, vol. 24, no. 4, p. 049501, 2015.
- [30] Y. Bar-Cohen, X. Bao, S. Sherrit, and S.-S. Lih, “Characterization of the Electromechanical Properties of Ionomeric Polymer-Metal Composite (IPMC),” *Proc. 2002 SPIE Smart Struct. Mater. Symp. EAPAD Conf.*, pp. 286–293, 2002.
- [31] H. Lei and X. Tan, “Fabrication and characterization of a two-dimensional IPMC sensor,” vol. 8687, pp. 868707–868707–12, 2013.
- [32] I.-S. Park, S.-M. Kim, and K. J. Kim, “Mechanical and thermal behavior of ionic polymer–metal composites: effects of electroded metals,” *Smart Mater. Struct.*, vol. 16, no. 4, pp. 1090–1097, 2007.
- [33] J. Park, V. Palmre, T. Hwang, K. Kim, W. Yim, and C. Bae, “Electromechanical performance and other characteristics of IPMCs fabricated with various commercially available ion exchange membranes,” *Smart Mater. Struct.*, vol. 23, no. 7, 2014.
- [34] M. P. Groover, *Fundamentals of Modern Manufacturing Materials, Processes, and Systems*. Upper Saddle River: Prentice Hall, 1996.
- [35] J. A. Elliott, P. J. James, T. J. McMaster, J. M. Newton, A. M. S. Elliott, S. Hanna, and M. J. Miles, “Hydrolysis of the Nafion® precursor studied by X-ray scattering and in-situ atomic force microscopy,” no. 022, pp. 1–11, 2001.



- [36] GEFC, “Materials.” [Online]. Available: <http://gefc.com/products/materials/>. [Accessed: 01-Jan-2015].
- [37] Wikipedia, “Wetting,” *Wikipedia The Free Encyclopedia*, 2015. [Online]. Available: <http://en.wikipedia.org/wiki/Wetting>. [Accessed: 01-Jan-2015].
- [38] ASTM International, “ASTM D638 Standard test method for tensile properties of plastics,” vol. 08. 2003.

## CURRICULUM VITAE

### SHELBY E NELSON

Phone: (702) 292-2495  
shelby.e.nelson@gmail.com

7409 Enchanted Hills Ct.  
Las Vegas, NV 89129

### EDUCATION

---

- MS University of Nevada, Las Vegas, Mechanical Engineering** August  
Thesis: "Feasibility Study of Custom Manufacturing Methods 2015  
of Ionic Polymer-Metal Composite Sensors"  
Advisor: Kwang J. Kim  
  
3.85/4.00 GPA
- BS University of Nevada, Las Vegas, Mechanical Engineering** May 2013  
Graduated Magna Cum Laude  
Minored in Mathematics  
Department Honors  
Thesis: "Supersonic Turbine Cascade Studies Using  
Computational Fluid Dynamic and Water Table  
Experiments"  
Advisor: Yitung Chen  
  
3.69/4.00 GPA

### HONORS AND AWARDS

---

- Dean's List** 2008-2013
- Phi Kappa Phi Honor Society** 2012-Present
- Tau Beta Pi Engineering Honor Society** 2011-Present
- University Turbine Systems Research Fellowship** 2012

### RESEARCH AND ENGINEERING EXPERIENCE

---

- University of Nevada, Las Vegas, Las Vegas, NV** 2013-2015  
**Graduate Research Assistant**, Active Materials and Smart Living Lab
- Perform research in the manufacturing methods of ionic polymer-metal composites

- Use lab equipment for material characterizations
- Operate and maintain injection molders and desktop CNC mill

**Society of Automotive Engineers (SAE), UNLV Student Chapter,** 2011-2015  
Las Vegas, NV

**President, Mini-Baja Off-road Vehicle**

- Project Goal: design/fabricate a single seat off-road vehicle to be raced in the SAE International collegiate competition
- Write funding proposals to obtain industry sponsorships, manage project deadlines and club business
- CNC various parts, TIG weld frame and suspension components, teach new students machine shop practices

**Industrial Inkjet, Las Vegas, NV** 2011-2012

**Engineering Assistant**

- Produce print samples on various media for both domestic and international customers, maintain print sample lab
- Actively communicate with customers during the print sample process, summarize results in company job reports

## **PUBLICATIONS**

---

Stalbaum, T., Nelson, S. E., Palmre, V., & Kim, K. J. (2014). Multi degree of freedom IPMC sensor.